

SVFLUX

**1D/2D/3D SATURATED / UNSATURATED
FINITE ELEMENT GROUNDWATER SEEPAGE MODELING**

Theory Manual

Written by:
The Bentley Systems Team

Last Updated: Wednesday, August 28, 2019

Bentley Systems Incorporated

COPYRIGHT NOTICE

Copyright © 2019, Bentley Systems, Incorporated. All Rights Reserved.

Including software, file formats, and audiovisual displays; may only be used pursuant to applicable software license agreement; contains confidential and proprietary information of Bentley Systems, Incorporated and/or third parties which is protected by copyright and trade secret law and may not be provided or otherwise made available without proper authorization.

TRADEMARK NOTICE

Bentley, "B" Bentley logo, SoilVision.com, SoilVision logo, and SOILVISION, SVSLOPE, SVOFFICE, SVOFFICE 5/SVENVIRO, SVOFFICE 5/GT, SVOFFICE 5/WR, SVSOILS, SVFLUX, SVSOLID, SVCHEM, SVAIR, SVHEAT, SVSEISMIC and SVDESIGNER are either registered or unregistered trademarks or service marks of Bentley Systems, Incorporated. All other marks are the property of their respective owners.

1	INTRODUCTION – SVENVIRO/GT	6
2	FUNDAMENTALS OF SEEPAGE THEORY – SVENVIRO/GT.....	7
2.1	CONSERVATION OF MASS – SVENVIRO/GT	8
2.1.1	<i>Changes in Volume of Stored Water – SVENVIRO/GT.....</i>	8
2.2	FLOW LAWS – SVENVIRO/GT	9
2.2.1	<i>Flow of Liquid Water – SVENVIRO/GT</i>	9
2.2.2	<i>Anisotropic Flow of Liquid Water – SVENVIRO/GT.....</i>	10
2.2.3	<i>Flow of Water Vapor – SVENVIRO</i>	11
2.2.4	<i>Aquifer transmissivity and storativity - SVENVIRO.....</i>	12
3	PDE'S FOR SEEPAGE ANALYSIS – SVENVIRO/GT.....	13
3.1	ONE-DIMENSIONAL SEEPAGE – SVENVIRO/GT	13
3.1.1	<i>1D Seepage – SVENVIRO/GT.....</i>	13
3.2	TWO-DIMENSIONAL SEEPAGE – SVENVIRO/GT	13
3.2.1	<i>2D Seepage – SVENVIRO/GT.....</i>	13
3.3	PLAN SEEPAGE - SVENVIRO	14
3.4	AXIS-SYMMETRIC SEEPAGE - SVENVIRO	14
3.5	THREE-DIMENSIONAL SEEPAGE – SVENVIRO/GT	15
3.5.1	<i>3D Seepage – SVENVIRO/GT.....</i>	15
3.6	H-BASED VERSUS MIXED FORMULATION – SVENVIRO/GT	16
3.6.1	<i>H-Based Formulation – SVENVIRO/GT.....</i>	16
3.6.2	<i>H-Based Formulation (Comprehensive) - SVENVIRO.....</i>	16
3.6.3	<i>Mixed Formulation - SVENVIRO.....</i>	16
3.6.4	<i>Density-Dependent Formulation - SVENVIRO</i>	17
4	BOUNDARY CONDITIONS IN SEEPAGE – SVENVIRO/GT	19
4.1	NATURAL BOUNDARY CONDITION – SVENVIRO/GT	19
4.1.1	<i>Differences Between Actual and Applied Boundary Flux – SVENVIRO/GT</i>	19
4.2	ESSENTIAL BOUNDARY CONDITION – SVENVIRO/GT	20
4.2.1	<i>Review Boundary Condition (Drain) – SVENVIRO/GT.....</i>	20
4.2.2	<i>Upstream Head and Flow Boundary Conditions – SVENVIRO/GT</i>	21
4.2.3	<i>Upstream Head Review Boundary Conditions – SVENVIRO/GT</i>	21
4.3	GEOMEMBRANE WITH CONTACT RESISTANCE - SVENVIRO	22
4.4	INITIAL WATER TABLE – SVENVIRO/GT	24
5	WELLS AND TUNNELS – SINK/SOURCE METHOD – SVENVIRO/GT.....	25
5.1	INTRODUCTION - SVENVIRO.....	25
5.2	EQUATIONS – SVENVIRO/GT.....	25
5.3	GEOMETRY - SVENVIRO	26
5.4	SETTING THE INFLUENCE DISTANCE - SVENVIRO	27
5.5	BOUNDARY CONDITIONS – SVENVIRO/GT	27
5.5.1	<i>Rate - SVENVIRO.....</i>	27
5.5.2	<i>Head - SVENVIRO.....</i>	27
5.5.3	<i>Head - GT.....</i>	28
5.5.4	<i>Review (Wells) - SVENVIRO.....</i>	28
5.5.5	<i>Review (Wells and Tunnels) - GT.....</i>	28
5.5.6	<i>Review (Tunnels) - SVENVIRO.....</i>	28
5.6	PARAMETERS - SVENVIRO	28
5.7	REMARKS - SVENVIRO	29
6	FLUX SECTIONS – SVENVIRO/GT	30
6.1	FLUX SECTION THEORY CALCULATION – SVENVIRO/GT.....	30
7	MATERIAL PROPERTIES – SVENVIRO/GT.....	33
7.1	SOIL-WATER CHARACTERISTIC CURVE – SVENVIRO/GT	33
7.1.1	<i>Fredlund and Xing (1994) Equation – SVENVIRO/GT</i>	33
7.1.2	<i>Fredlund (2000) Bimodal Equation – SVENVIRO/GT.....</i>	33
7.1.3	<i>Fredlund 2-Point Estimation – SVENVIRO/GT.....</i>	34
7.1.4	<i>Van Genuchten (1980) Equation – SVENVIRO/GT.....</i>	34

7.1.5	Van Genuchten (1980) and Mualem (1976) Equation – SVENVIRO/GT	35
7.1.6	Vereecken, Maes, Feyen and Darius (1989) Estimation Method – SVENVIRO/GT	35
7.1.7	Gardner (1958) Equation – SVENVIRO/GT	36
7.1.8	Brooks and Corey (1964) Equation – SVENVIRO/GT	36
7.1.9	Zapata Estimation (2000) – SVENVIRO/GT	37
7.2	HYDRAULIC CONDUCTIVITY FIT METHODS – SVENVIRO/GT	37
7.2.1	Gardner's (1958) Equation – SVENVIRO/GT	37
7.3	HYDRAULIC CONDUCTIVITY ESTIMATION – SVENVIRO/GT	39
7.3.1	Brooks and Corey Estimation – SVENVIRO/GT	39
7.3.2	Modified Campbell (1973) Estimation – SVENVIRO/GT	40
7.3.3	Fredlund, Xing and Huang (1994) Estimation – SVENVIRO/GT	41
7.3.4	Van Genuchten (1980) and Mualem (1976) Estimation – SVENVIRO/GT	41
7.3.5	Van Genuchten (1980) Estimation – SVENVIRO/GT	42
7.3.6	Leong and Rahardjo (1997) Estimation – SVENVIRO/GT	43
8	SOIL ATMOSPHERE MODELING – SVENVIRO	44
8.1	ATMOSPHERIC FLUX BALANCE – SVENVIRO	44
8.2	INFILTRATION AND RUNOFF WITHOUT CONSIDERATION OF EVAPORATION – SVENVIRO	45
8.2.1	Estimated Runoff Correction – SVENVIRO	45
8.2.2	Pressure Head Calculated Runoff Correction – SVENVIRO	46
8.2.3	Gradient Calculated Runoff Correction – SVENVIRO	46
8.3	SNOW ACCUMULATION AND MELT – SVENVIRO	47
8.3.1	Temperature-index based snow melt – SVENVIRO	48
8.3.2	Snow depth – SVENVIRO	48
8.3.2.1	New snow density – Anderson approach (1976)	48
8.3.2.2	Density varying with the age of old snow	49
8.3.3	Infiltration boundary condition with snow cover	49
8.4	EVAPORATION – SVENVIRO	50
8.4.1	Potential Evaporation – SVENVIRO	50
8.4.2	Actual Evaporation – SVENVIRO	51
8.4.3	Case 1 Solution: "Limiting-Function" for AE/PE SVFLUX Model – SVENVIRO	52
8.4.3.1	Mass Flow Governing Equation	52
8.4.3.2	Initial soil water contents	53
8.4.3.3	Boundary condition for moisture flow	53
8.4.3.4	Actual Evaporation	53
8.4.3.5	Determining vapor pressure values throughout each day	54
8.4.4	Case 2 Solution: Wilson-Penman (1994) SVFLUX Model – SVENVIRO	57
8.4.4.1	Governing Equations	57
8.4.4.2	Initial soil water content profile	57
8.4.4.3	Initial soil surface temperature	57
8.4.4.4	Boundary condition for moisture flow	57
8.4.4.5	Actual Evaporation	58
8.4.4.6	Determining Vapor Pressure Values throughout each Day	58
8.4.5	Case 3 Solution: "Experimental-Based" for AE/PE SVFLUX Model – SVENVIRO	58
8.4.5.1	Governing Equation	59
8.4.5.2	Initial water content conditions	59
8.4.5.3	Boundary condition for moisture flow	59
8.4.5.4	Determine an empirical expression for the ratio of actual evaporation, AE, to potential evaporation, PE	59
8.4.6	Case 4 Solution: Coupled Moisture and Heat Modeling (SVFLUX & SVHEAT Using "Wilson-Penman (1994)" for AE – SVENVIRO	61
8.4.6.1	Moisture flow governing equation	61
8.4.6.2	Heat flow equation	61
8.4.6.3	Initial water content conditions	62
8.4.6.4	Initial temperature conditions	63
8.4.6.5	Thermal boundary condition at soil surface	63
8.4.6.6	Boundary condition for moisture flow	63
8.4.6.7	Actual Evaporative, AE	63
8.4.6.8	Calculation Procedure	63
8.4.7	Case 5 Solution: SVFLUX and SVHEAT Coupled Using the Wilson-Fredlund-Barbour "Limiting Equation" – SVENVIRO	64
8.4.7.1	Moisture flow governing equation	64
8.4.7.2	Heat flow equation:	64
8.4.7.3	Initial water content conditions	64
8.4.7.4	Initial temperature conditions	64
8.4.7.5	Thermal boundary condition at soil surface	64

8.4.7.6	Boundary condition for moisture flow	65
8.4.7.7	Actual evaporation	65
8.4.7.8	Potential Evaporative	66
8.4.8	<i>Case 6 Solution: Coupled Moisture and Heat Modeling (SVFLUX & SVHEAT) by Using the Empirical "Experimental-Based" for AE/PE – SVENVIRO</i>	66
8.4.8.1	Moisture flow governing equation	67
8.4.8.2	Heat flow equation:	67
8.4.8.3	Initial water content conditions	67
8.4.8.4	Initial temperature conditions	67
8.4.8.5	Thermal boundary condition at soil surface	67
8.4.8.6	Moisture flow boundary condition at soil surface	67
8.4.8.7	Actual evaporation, AE	67
8.4.8.8	Determine Potential Evaporation PE	68
8.5	TRANSPIRATION – SVENVIRO	68
8.6	OSMOTIC CRUST EFFECT ON ACTUAL EVAPORATION – SVENVIRO	71
8.7	PHYSICAL CRUST EFFECT ON ACTUAL EVAPORATION – SVENVIRO	72
9	STREAM TRACES – SVENVIRO/GT	74
10	PARTICLE TRACKING – SVENVIRO/GT	75
11	SPATIAL VARIABILITY - SVENVIRO	76
11.1	2D SPATIAL VARIABILITY - SVENVIRO	76
11.1.1	General - SVENVIRO	76
11.1.2	Covariance Function - SVENVIRO	76
11.1.3	Parameters - SVENVIRO	79
11.1.4	Random Field - SVENVIRO	80
12	NUMERICAL IMPLEMENTATION – SVENVIRO	81
12.1	EQUATION ANALYZER	81
12.2	MESH GENERATION	81
12.3	MESH REFINEMENT	81
12.4	INTERPOLATION ORDER	81
12.5	TIME STEPPING	81
12.5.1	Time Integration	82
12.5.2	Time Step Control	83
13	NUMERICAL IMPLEMENTATION – GT	85
13.1	INTERPOLATION ORDER	85
13.2	TIME STEPPING	85
13.2.1	Time Integration	85
13.2.2	Convergence Criteria	86
13.2.3	Time-Step Control	86
14	REFERENCES	87

1 INTRODUCTION - SVENVIRO/GT

Groundwater flow problems in geotechnical and geo-environmental engineering involve the solution of a partial differential equation referred to as a PDE. The PDE must be solved for all “finite elements” which when combined form a “continuum” (or the geometry of the problem). The theory of groundwater flow expressed in mathematical form embraces the physical behavior of the material (e.g., constitutive laws) and the conservative laws of physics (i.e., conservation of energy). The physical behavior of many materials, (particularly unsaturated soils), is nonlinear and as a consequence, the PDE becomes nonlinear in character. It is well known that the solution of nonlinear PDEs can present a challenge for numerical modeling.

The purpose of the theory manual is to provide the user with details regarding the theoretical formulation of the PDE as well as the numerical method used in the solution. The intent of the theory manual is not to provide an exhaustive summary of all theories associated with groundwater flow. Rather, the intent is to clearly describe details of the theory used in the SVFLUX software.

The SVFLUX finite element software can utilize two different solvers. Theory applicable to the SVENVIRO (FlexPDE) and GT (SVCORE) solvers are presented in this manual.

- SVENVIRO Suite – utilizes the FlexPDE solver
- GT Suite – utilizes the SVCORE solver

Section headings in this manual are tagged with their applicability to each solver. The tags [SVENVIRO/GT], [SVENVIRO], or [GT] will appear in the header to indicate a section that applies to both solvers, FlexPDE only, or SVCORE only, respectively.

These generic finite element solvers solve the partial differential equation for groundwater flow. The solver algorithm has implemented cutting-edge numerical solution techniques that can accommodate linear and highly nonlinear PDEs. The solution technique utilizes adaptive time steps algorithm and automatic mathematically designed mesh generation. The FlexPDE solver offers automatic mesh refinement. The application of these advanced numerical techniques is particularly valuable in solving highly nonlinear and complex problems. Most commonly it is the unsaturated soil portion of the soil continuum that brings in nonlinear soil behavior. The advanced solvers make it possible to obtain converged and accurate solutions for many problems that were previously unsolvable.

The primary attributes of the solution process are as follows:

- Fully automatic mesh generation,
- Fully automatic mesh refinement based on various model variables for SVENVIRO or manual mesh refinement for GT,
- Integrated climatic calculation of actual evaporation rates using the Wilson-Penman formulation as well as the Fredlund-Wilson-Penman formulation - SVENVIRO,
- Handling of seepage face boundary conditions,
- Fully implicit approach in the solver, which provides for a robust solution of difficult models with convergence issues,
- Fluid mass-balance tracking,
- SVENVIRO: 3, 6, or 10-noded triangles as elements for 2D analysis and 4, 10, or 20-noded tetrahedrons in 3D elements,
- GT: 3-noded triangle and 4-noded quadrilateral elements for 2D analysis and 4-noded tetrahedron elements for 3D analysis,
- Adaptive time stepping – SVENVIRO/GT
- Automatic generation and control of time steps,
- Newton-Raphson convergence iteration schemes,
- Use matrix preconditioning in conjugate-gradient solutions - SVENVIRO. The default preconditioner is the diagonal-block inverse matrix, and
- Rigorous calculation of runoff - SVENVIRO.

2 FUNDAMENTALS OF SEEPAGE THEORY - SVENVIRO/GT

The following section presents the fundamentals of the seepage theory implemented in SVFLUX. An overview of the PDE's used by SVFLUX for the analysis of saturated/unsaturated seepage is presented. Several phenomena are considered, including liquid water flow and water vapor flow. The seepage theory is developed based on Darcian flow law, Fick's flow law, and the conservation of mass. The theory presented below is a general outline of the theory needed to solve most seepage problems.

Continuum mechanics principles and partial differential equations (PDEs) have been traditionally used for modeling seepage in saturated/unsaturated soil systems. The partial differential equations governing seepage may involve transient coupled soil-atmosphere processes with nonlinear and heterogeneous soil properties along with nonlinear boundary conditions. Relatively simple steady-state saturated confined flow can also be addressed.

Seepage can be modeled as follows within the context of continuum mechanics principles:

- Identify the physical processes of concern associated with the problem at hand,
- Establish the "continuum variables" acting upon a representative elemental volume (REV) of the medium,
- Develop field equations governing the physical processes of concern by making the assumption that the medium can be considered as a continuum from a macroscopic standpoint (i.e., considering a REV of soil) while using measurable soil properties:
 - Apply conservation laws,
 - Apply verified constitutive laws, and
 - Develop a final system of well-posed determinate partial differential equations.
- Establish initial, internal, and boundary conditions for the problem, and
- Provide a mathematical solution for the PDE or system of PDEs.

A series of assumptions form the backdrop for the derivation of the partial differential equations governing seepage. The following set of assumptions can be considered generally valid:

- Soil phases can be described using a continuum mechanics approach,
- Pore-air and all of its constituents (including water vapor) behave as ideal gases,
- Local thermodynamic equilibrium between the liquid water and water vapor phases exists at all times at any point in the soil, and
- Atmospheric pressure gradients are negligible.

The four assumptions described above may become inadequate under certain situations. For instance, the compressibility of water may have a significant effect in an analysis of regional groundwater systems (i.e., large domains). Therefore, SVFLUX provides the capability of taking the compressibility of water into account as part of aquifer storativity (Freeze *et al.* 1979).

2.1 CONSERVATION OF MASS - SVENVIRO/GT

The conservation of mass of water in a referential element is used to derive the governing equation for saturated/unsaturated seepage. A continuum mechanics framework is used, resulting in the derivation of a differential calculus equation to represent seepage. The assumption is made that the variables involved are continuous and valid from a macroscopic, phenomenological standpoint.

A differential equation for the conservation of mass of water can be derived by considering a REV of soil (Figure 1). The continuity equation can be applied by taking into consideration the flow rates in and out of the REV and equating the difference to the rate of change of mass (or heat) to storage within the REV with time. The following differential equation is obtained by considering three-dimensional flow conditions using the Cartesian coordinate system:

$$-\frac{\partial q_x^w}{\partial x} - \frac{\partial q_y^w}{\partial y} - \frac{\partial q_z^w}{\partial z} = \frac{1}{V_o} \frac{\partial M_w}{\partial t} \quad [1]$$

where:

- q_i^w = total water flow rate in the i -direction across a unit area of the soil, $\text{kg}/\text{m}^2\text{-s}$; $q_i^w = \rho_w v_i^w$, $\text{kg}/\text{m}^2\text{-s}$,
- ρ_w = density of water, $1000 \text{ kg}/\text{m}^3$,
- v_i^w = water and air flow rate in the i -direction across a unit area of the soil, m/s ,
- V_o = referential volume, $V_o = d_x d_y d_z$, m^3 ,
- M_w = mass of water within the representative elemental volume, kg , and
- t = time, s .

The total water flow rate, v^w , also known as specific discharge, is a macroscopic measure of the rate of flow through soils. A measure of the "average actual flow velocity" for a saturated soil can be obtained by dividing v^w by the soil porosity ($n = V_v/V$). The total water flow rate, v^w , can occur as liquid water and/or water vapor flow.

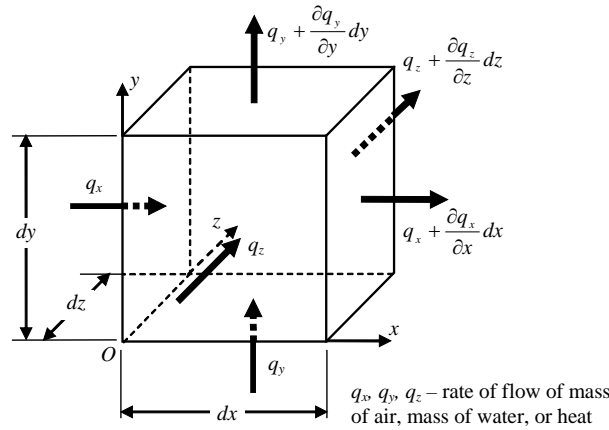


Figure 1 Soil representative elemental volume and fluxes at the element faces

2.1.1 Changes in Volume of Stored Water – SVENVIRO/GT

The constitutive relationship for the amount of water stored in the soil pores is usually written in terms of the volume of water referenced to the overall total volume. The change in volume of water stored in the soil pores can be expressed as a coefficient of water storage, m_2^w , as follows:

$$\frac{dV_w}{V_o} = m_2^w d(u_a - u_w) \quad [2]$$

where:

- $m_2^w = \frac{d(V_w/V_o)}{d(u_a - u_w)} = \frac{e}{1+e} \frac{dS}{d(u_a - u_w)}$
- V_w/V_o = volumetric water content,
- e = void ratio,

S = degree of saturation, and
 $(u_a - u_w)$ = matric suction.

The above equation is based on the assumption that changes in the volume of pore-water stored in the soil are a function of soil suction and are independent of changes in total stress. The soil property, m_2^w , is obtained by taking the derivative of the soil-water characteristic curve, swcc, (i.e., the slope), as shown in Figure 2.

Using the derivative of the SWCC provides a smooth transition between saturated and unsaturated conditions, provided that appropriate coefficients of water storage are used. As the soil saturates, the effects of changes in soil suction and changes in effective stresses (in a saturated soil) become equal (i.e., $m_2^w = m_v$). Consequently, for saturated conditions, changes in water volume can be referenced to changes in void ratio. Usually, the value of m_v is considerably lower than the maximum value of m_2^w , which occurs as the soil desaturates.

Numerical difficulties can arise from the use of extremely low values of m_2^w . This is a possible source of convergence problems when modeling ground surface infiltration problems. In order to alleviate convergent difficulties, the value of m_v must be slightly (but not excessively) raised as illustrated in Figure 2.

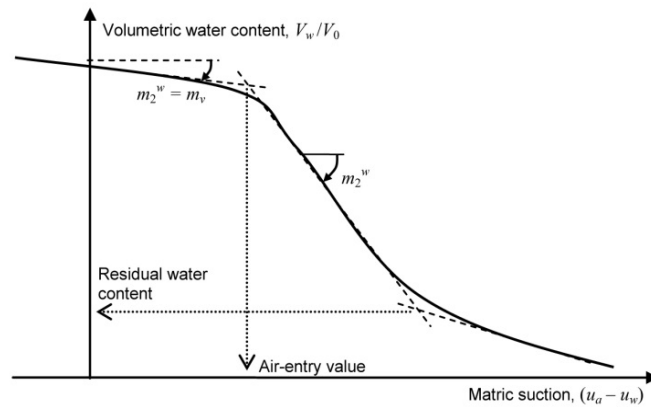


Figure 2 Soil-water characteristic curve showing the water storage characterization at low suction values.

2.2 FLOW LAWS - SVENVIRO/GT

Table 1 presents an overview of flow laws traditionally used for modeling saturated/unsaturated soil flow. The flow laws establish relationships between measures of flow and driving potentials. Driving potentials can be established based on spatial gradients of the energy stored per unit volume (Bear, 1972). There are several flow equations that have a similar form, but have distinct potentials and different material properties. The flow laws presented in Table 1 have well established equations that have been experimentally verified.

Table 1 Overview of types of flow within an unsaturated soil and the corresponding mechanisms, driving potentials, and flow laws

Flow mechanism (1)	Driving Potential (2)	Flow Law (3)
Liquid water	Hydraulic head, h (m)	Darcy's law
Water vapor diffusion	Mass concentration of vapor per unit volume of soil, C_v (kg/m ³)	Modified Fick's law

Pore-air and pore-water have both miscible and immiscible mixture characteristics. Water can flow as liquid water or as water vapor diffusing through the free air-phase. SVFLUX takes into account both liquid and vapor flow. Both flow mechanisms are essential in the modeling of certain water flow conditions. For instance, evaporation requires the consideration of the phase change from liquid to vapor water and the flow of water vapor (Wilson et al., 1994).

2.2.1 Flow of Liquid Water – SVENVIRO/GT

The rate of flow of liquid water in a saturated/unsaturated soil can be described using a generalization of Darcy's Law (Bear, 1972), where the driving mechanism is the total hydraulic head gradient. The hydraulic conductivity is assumed to mainly vary with matric suction in the soil. The generalized Darcy's law can be written as follows:

$$v_{wx} = -k_{wx}(\psi) \frac{\partial h}{\partial x}; \quad v_{wy} = -k_{wy}(\psi) \frac{\partial h}{\partial y}; \quad v_{wz} = -k_{wz}(\psi) \frac{\partial h}{\partial z} \quad [3]$$

where:

v_{wi} = liquid pore-water flow rate in the i -direction across a unit area of the soil due to hydraulic head gradients, m/s,

$k_{wi}(\psi)$	= hydraulic conductivity in the i -direction, m/s . For unsaturated soil, it is the function of soil suction.
ψ	= soil suction, kPa , which is equal to matric suction, $u_a - u_w$, plus osmotic suction, π .
h	= hydraulic head, m , which is equal to $\frac{u_w}{\gamma_w} + y$
u_w	= pore-water pressure, kPa ,
u_a	= pore-air (gauge) pressure, kPa ,
γ_w	= unit weight of water, kN/m^3 , and
y	= elevation, m .

The hydraulic conductivity function, $k_w(\psi)$ provides the relationship between the hydraulic conductivity and the soil suction. The hydraulic conductivity function can also be written in terms of volumetric water content. As a soil dries, there is less and less water present in the soil. Since water will flow only where there is water present, the hydraulic conductivity decreases accordingly as the volumetric water content decreases. This behavior is represented in SVFLUX by entering a hydraulic conductivity function for each soil. In the following context, the $k_{wi}(\psi)$ is simplified as k_w .

The use of a continuous k_w function provides a smooth transition between saturated and unsaturated soil conditions. For saturated conditions, k_{wsat} is generally considered a constant and equal to the saturated hydraulic conductivity.

The hydraulic conductivity function can be obtained experimentally using laboratory tests or field tests. The hydraulic conductivity function can also be estimated using the saturated hydraulic conductivity and the soil-water characteristic curve (Fredlund and Xing, 1994). SVFLUX provides several options for estimating the hydraulic conductivity function.

2.2.2 Anisotropic Flow of Liquid Water – SVENVIRO/GT

Natural deposition of soil layers often results in angled layering. The angled layering results in dominant water flow in a direction parallel to the direction of the layering. This observed phenomenon can be simulated in SVFLUX by specifying anisotropic angled behavior in either 2D or 3D.

Figure 3 illustrates how angled anisotropy is considered in SVFLUX. The angle origin, reference orientation, is in the horizontal direction and the angle increases counter-clockwise.

A mathematical transformation must be performed to translate rotated anisotropic permeability parameters on to the coordinate system used to solve the problem. The general form of the conductivity matrix in two-dimensional problems is as follows (Bear, 1972):

$$\begin{Bmatrix} v_{wx} \\ v_{wy} \end{Bmatrix} = \begin{bmatrix} -k_{wxx} & -k_{wxy} \\ -k_{wyx} & -k_{wyy} \end{bmatrix} \begin{Bmatrix} \frac{\partial h}{\partial x} \\ \frac{\partial h}{\partial y} \end{Bmatrix} \quad [4]$$

where:

$$\begin{aligned} k_{wxx} &= \frac{k_{w1} + k_{w2}}{2} + \frac{k_{w1} - k_{w2}}{2} \cos 2\alpha \\ k_{wyy} &= \frac{k_{w1} + k_{w2}}{2} - \frac{k_{w1} - k_{w2}}{2} \cos 2\alpha \\ k_{wxy} &= \frac{k_{w1} - k_{w2}}{2} \sin 2\alpha \end{aligned}$$

k_{w1} and k_{w2} are the values of hydraulic conductivity at the principal directions of anisotropy. These values can have constant values for saturated conditions or can vary according to water content in unsaturated soil conditions. The angle α defines the principal directions of anisotropy (Figure 3).

The transformation in 3D is slightly more complex than in 2D. Three angles are required to describe the hydraulic conductivity transformation. The theory for the hydraulic conductivity transformations is not presented in this manual.

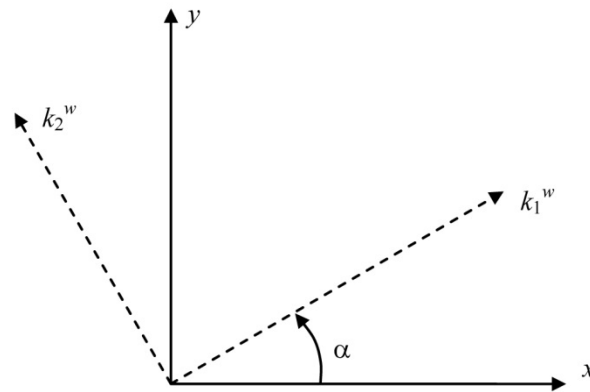


Figure 3 Principal directions of anisotropy in two-dimensions

2.2.3 Flow of Water Vapor – SVENVIRO

The flow rate of water vapor due to gradients in vapor pressure (or concentration) can be described using a modified form of Fick's law (Philip and de Vries, 1957; Dakshanamurthy and Fredlund, 1981). SVFLUX assumes thermodynamic equilibrium in order to express vapor pressure gradients in terms of negative pore-water pressure gradients:

$$v_{vx} = -\frac{k_{vd}}{\gamma_w} \frac{\partial u_w}{\partial x}; \quad v_{vy} = -\frac{k_{vd}}{\gamma_w} \frac{\partial u_w}{\partial y}; \quad v_{vz} = -\frac{k_{vd}}{\gamma_w} \frac{\partial u_w}{\partial z} \quad [5]$$

where:

u_w = pore-water pressure, kPa,
 k_{vd} = pore-water vapor conductivity by vapor diffusion within the air phase,

where $k_{vd} = \gamma_w \frac{W_v p_v}{\rho_w R(T+273.15)} \frac{D_v^*}{\rho_w}$ (m/s)

W_v = molecular weight of water vapor, 18.016 kg/kmol,

p_v = partial pressure of water vapor, kPa,

R = universal gas constant, 8.314 J/(mol-K),

T = temperature, °C,

D_v^* = vapor diffusivity through the soil, where $D_v^* = \frac{(1-S)nD_v W_v}{R(T+273.15)}$ (kg-m/kN/s)

D_v = molecular diffusivity of vapor through soil, m²/s.

The soil properties D_v and D_v^* can be directly measured or reasonably well estimated by using the value of molecular diffusivity of vapor through air and combining that value with a tortuosity factor.

SVFLUX computes the molecular diffusivity of vapor through air using the equation proposed by Kimball *et al.*, (1976), which is $2.3 \times 10^{-5} (1 + T/273.15)^{1.75}$ m²/s. Ebrahimi-B *et al.*, (2004) presents a summary of tortuosity coefficient functions proposed in the literature and shows that most existing functions result in similar values for the ranges of soil suction where vapor flow predominates over liquid flow. More details about the modeling of vapor flow can be found in Fredlund and Gitirana Jr., (2005).

Figure 4 illustrates typical shapes for the water vapor conductivity and hydraulic conductivity functions. Smooth transitions are obtained through the use of physically meaningful soil property functions. The water flow properties must reproduce a smooth transition between completely dry, unsaturated, and saturated conditions.

A dry soil has a negligible hydraulic conductivity and most water flow takes place as vapor flow. As soil suction decreases hydraulic conductivity increases and eventually may become higher than the water vapor conductivity. Further decrease in soil suction results in increasingly higher hydraulic conductivity and negligible vapor flow. As the soil comes close to being fully saturated, the hydraulic conductivity suction becomes equal to the saturated hydraulic conductivity.

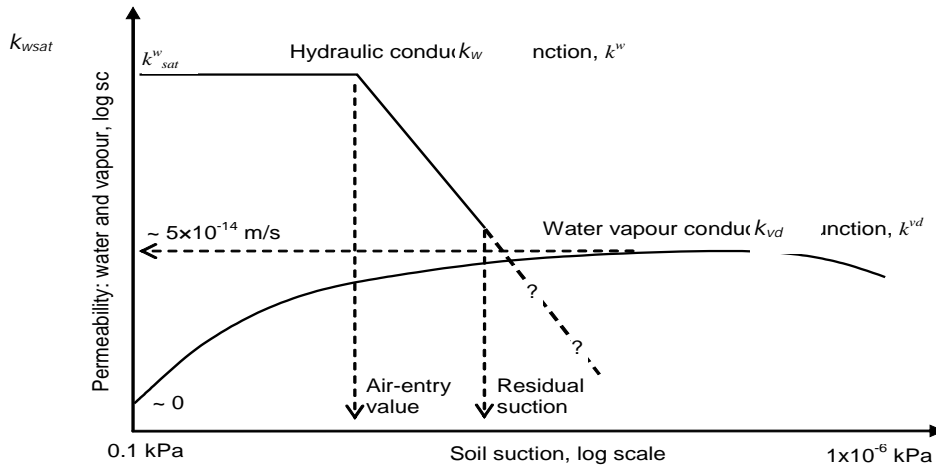


Figure 4 Conductivity functions for the water phase: liquid water and water vapor

2.2.4 Aquifer transmissivity and storativity - SVENVIRO

The storativity or storage coefficient, S is defined as:

$$S = S_s b \quad [6]$$

where:

- S_s = specific storage, and
- b = confined aquifer thickness.

The specific storage is defined as:

$$S_s = \rho_w g (\alpha + \eta \beta) \quad [7]$$

where:

- ρ_w = density of water,
- g = acceleration due to gravity,
- α = aquifer compressibility,
- η = porosity, and
- β = compressibility of the water.

Specific storage, S_s , is equivalent to the term $(\gamma_w m_w)$.

where:

- γ_w = $\rho_w g$, unit weight of water,
- m_w = $(\alpha + \eta \beta)$ system compressibility.

Therefore, the system compressibility, m_w is

$$m_w = \frac{S_s}{\gamma_w} \quad [8]$$

The system compressibility due to a change in pore-water pressure is defined by the variable, m_w .

The aquifer transmissivity, T is defined as:

$$T = k_w b \quad [9]$$

where:

- b = aquifer thickness, and
- k_w = hydraulic conductivity.

3 PDE'S FOR SEEPAGE ANALYSIS - SVENVIRO/GT

The flow law equations (Darcy law and Fick's law), and a water volume change constitutive equation must be combined with the continuity of water mass equation to obtain the partial differential equation that governs the conservation of water mass (i.e., both liquid and vapor). The next sections present the partial differential equations used by SVFLUX for the analysis of saturated-unsaturated soil seepage problems.

3.1 ONE-DIMENSIONAL SEEPAGE - SVENVIRO/GT

One-dimensional seepage analysis is often used for modeling large planar areas. Cover system design is one of many typical applications. The number of nodes normally used in one-dimensional analyses is relatively low when compared to the number of nodes used in two-dimensional analyses. Therefore, computation times are dramatically reduced when adopting a one-dimensional model.

3.1.1 1D Seepage – SVENVIRO/GT

Considering the reference volume, V_o , and assuming that water is incompressible, the following equation is obtained for one-dimensional transient saturated/unsaturated seepage:

$$\frac{\partial}{\partial y} \left[k_{wy} \frac{\partial h}{\partial y} + k_{vd} \frac{\partial u_w}{\partial y} \right] = -\gamma_w m_2^w \frac{\partial h}{\partial t} \quad [10]$$

where:

y = coordinate in vertical direction, (corresponding to elevation).

The PDE governing the flow and storage of water within a saturated/unsaturated soil is presented using total head, h , as the primary variable. However, pore-water pressure, u_w , can also be used producing identical results provided the geometry dimension in the y -coordinate is small. It is also possible to use pore-water pressure as the primary variable when studying the dissipation of excess pore-water pressures.

Three soil property functions can be identified for the transient seepage PDE; namely:

- hydraulic conductivity function, k_w ,
- vapor conductivity function, k_{vd} , and
- soil-water characteristic curve, whose derivative with respect to soil suction is represented by m_2^w .

The above-mentioned soil properties functions vary with soil suction. Therefore, the PDE is physically nonlinear.

The partial differential equation for water flow is based on the assumption that the rate of water mass flow across a REV is continuously distributed in space. Therefore, the spatial distribution of water flow rate can be described using the partial derivative of water flow in a particular direction. These comments apply to the all the seepage PDEs presented in the next sections.

For steady-state conditions, the PDE for liquid and vapor water flow reduces to the following equation:

$$\frac{\partial}{\partial y} \left[k_{wy} \frac{\partial h}{\partial y} + k_{vd} \frac{\partial u_w}{\partial y} \right] = 0 \quad [11]$$

The hydraulic conductivity can be considered as being constant when solving saturated seepage problems. Therefore, the PDE for saturated and unsaturated water seepage has the same form.

3.2 TWO-DIMENSIONAL SEEPAGE - SVENVIRO/GT

Two-dimensional seepage analysis is used for modeling cross-sections passed through elongated geometries, such as an earth dam.

3.2.1 2D Seepage – SVENVIRO/GT

Assuming the reference volume, V_o , remains constant and the water is incompressible, the following equation can be written for transient saturated/unsaturated seepage:

$$\frac{\partial}{\partial x} \left[k_{wx} \frac{\partial h}{\partial x} + k_{vd} \frac{\partial u_w}{\partial x} \right] + \frac{\partial}{\partial y} \left[k_{wy} \frac{\partial h}{\partial y} + k_{vd} \frac{\partial u_w}{\partial y} \right] = -\gamma_w m_2^w \frac{\partial h}{\partial t} \quad [12]$$

where:

- x = horizontal direction, and
 y = vertical direction, (corresponding to elevation).

The partial differential equation, PDE, is presented for anisotropic properties with the principal direction of anisotropy corresponding to the x- and y-directions. Anisotropic material properties that do not coincide with the Cartesian coordinate axis can be considered as presented in the previous chapter.

For steady-state conditions, the water storage portion of the equation is set to zero and the PDE reduces to the following equation:

$$\frac{\partial}{\partial x} \left[k_{wx} \frac{\partial h}{\partial x} + k_{vd} \frac{\partial u_w}{\partial x} \right] + \frac{\partial}{\partial y} \left[k_{wy} \frac{\partial h}{\partial y} + k_{vd} \frac{\partial u_w}{\partial y} \right] = 0 \quad [13]$$

The governing PDE for steady state seepage can be further reduced by assuming vapor flow is negligible and soil is saturated. The resulting PDE can be considered to be in its simplest form for two-dimensional seepage.

$$\frac{\partial}{\partial x} \left[k_{wx} \frac{\partial h}{\partial x} \right] + \frac{\partial}{\partial y} \left[k_{wy} \frac{\partial h}{\partial y} \right] = 0 \quad [14]$$

3.3 PLAN SEEPAGE - SVENVIRO

Plan seepage corresponds to the situation where water is assumed to only flow in directions perpendicular to the force of gravity direction. In other words, flow occurs in the x and z directions, perpendicular to the y gravity force direction.

$$\frac{\partial}{\partial x} \left[(k_{wx} + k_{vd}) \frac{\partial h}{\partial x} \right] + \frac{\partial}{\partial z} \left[(k_{wz} + k_{vd}) \frac{\partial h}{\partial z} \right] = -\gamma_w m_2^w \frac{\partial h}{\partial t} \quad [15]$$

where:

- x = first horizontal direction, and
 z = second horizontal direction, orthogonal to the x-direction and perpendicular to the y-direction.

The gravimetric component of seepage is omitted since there is no derivation with respect to elevation, (i.e., y-direction). For steady-state conditions and no consideration of vapor flow, the PDE for plane seepage reduces to the following equation:

$$\frac{\partial}{\partial x} \left[k_{wx} \frac{\partial h}{\partial x} \right] + \frac{\partial}{\partial z} \left[k_{wz} \frac{\partial h}{\partial z} \right] = 0 \quad [16]$$

This equation is similar to the simplest form for two-dimensional seepage problems modeled using SVFLUX.

3.4 AXIS-SYMMETRIC SEEPAGE - SVENVIRO

Axis-symmetric geometries are three-dimensional domains that can be viewed as the result of a two-dimensional geometry that is revolved around a central axis. The axis-symmetric representation of seepage problems is in practice a two-dimensional representation of a three-dimensional problem. In fact, plane triangular elements are used by the finite element model in SVFLUX.

Flow volumes computed across flux sections on axis-symmetric problems result in values that are integrated along a surface. This surface corresponds to the entire true area that is obtained by revolving the one-dimensional cross-section around the central axis, as shown in Figure 5.

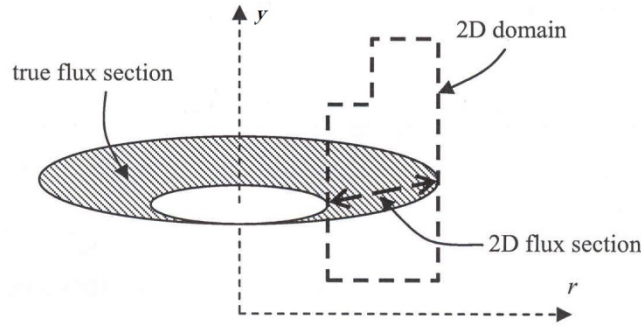


Figure 5 Representation of axis-symmetric problems

Axis-symmetric seepage is implemented in SVFLUX using the cylindrical coordinate system. The horizontal direction corresponds to the r -direction and the vertical direction corresponds to the y -direction. The mass conservation equation in cylindrical coordinates takes a new form. The direction derivatives are neglected based on axis-symmetry. The PDE governing axis-symmetric seepage is as follows:

$$\frac{\partial}{\partial r} \left[(k_{wr} + k_{vd}) \frac{\partial h}{\partial r} \right] + \frac{k_{wr} + k_{vd}}{r} \frac{\partial h}{\partial r} + \frac{\partial}{\partial y} \left[(k_{wr} + k_{vd}) \frac{\partial h}{\partial y} - k_{vd} \right] = -\gamma_w m_2^w \frac{\partial h}{\partial t} \quad [17]$$

where:

- r = horizontal direction, and
- y = vertical direction, corresponding to elevation.
- k_{wr} = hydraulic conductivity function in r -direction.

For steady-state conditions, the PDE for plan seepage reduces to the following equation:

$$\frac{\partial}{\partial r} \left[(k_{wr} + k_{vd}) \frac{\partial h}{\partial r} \right] + \frac{k_{wr} + k_{vd}}{r} \frac{\partial h}{\partial r} + \frac{\partial}{\partial y} \left[(k_{wr} + k_{vd}) \frac{\partial h}{\partial y} - k_{vd} \right] = 0 \quad [18]$$

Again, a simpler version of the governing PDE is used by SVFLUX when neglecting vapor. The PDE governing steady state seepage under these conditions reduces to:

$$\frac{\partial}{\partial r} \left[k_{wr} \frac{\partial h}{\partial r} \right] + \frac{k_{wr}}{r} \frac{\partial h}{\partial r} + \frac{\partial}{\partial y} \left[k_{wr} \frac{\partial h}{\partial y} \right] = 0 \quad [19]$$

3.5 THREE-DIMENSIONAL SEEPAGE - SVENVIRO/GT

Three-dimensional seepage analysis is often used when the problem geometry cannot be adequately represented by a one-dimensional column, a two-dimensional, a plan, or an axisymmetric model.

3.5.1 3D Seepage – SVENVIRO/GT

The PDE used in SVFLUX SVENVIRO for the solution of three-dimensional transient saturated/unsaturated seepage problems is as follows:

$$\begin{aligned} & \frac{\partial}{\partial x} \left[k_{wx} \frac{\partial h}{\partial x} + k_{vd} \frac{\partial u_w}{\partial x} \right] + \frac{\partial}{\partial z} \left[k_{wz} \frac{\partial h}{\partial z} + k_{vd} \frac{\partial u_w}{\partial z} \right] + \frac{\partial}{\partial y} \left[k_{wy} \frac{\partial h}{\partial y} + k_{vd} \frac{\partial u_w}{\partial y} \right] \\ & = -\gamma_w m_2^w \frac{\partial h}{\partial t} \end{aligned} \quad [20]$$

where:

- x = first horizontal direction,
- z = second horizontal direction, orthogonal to the x -direction, and
- y = vertical direction, corresponding to elevation

The partial differential equation for flow in the three main orthogonal directions is equal to the flow along each direction, (i.e., the x , y , and z -directions). For steady-state conditions, the PDE for seepage reduces to the following equation:

$$\frac{\partial}{\partial x} \left[k_{wx} \frac{\partial h}{\partial x} + k_{vd} \frac{\partial u_w}{\partial x} \right] + \frac{\partial}{\partial z} \left[k_{wz} \frac{\partial h}{\partial z} + k_{vd} \frac{\partial u_w}{\partial z} \right] + \frac{\partial}{\partial y} \left[k_{wy} \frac{\partial h}{\partial y} + k_{vd} \frac{\partial u_w}{\partial y} \right] = 0 \quad [21]$$

Neglecting vapor flow and assuming the soil is saturated, the PDE governing steady state seepage reduces to:

$$\frac{\partial}{\partial x} \left[k_{wx} \frac{\partial h}{\partial x} \right] + \frac{\partial}{\partial z} \left[k_{wz} \frac{\partial h}{\partial z} \right] + \frac{\partial}{\partial y} \left[k_{wy} \frac{\partial h}{\partial y} \right] = 0 \quad [22]$$

3.6 H-BASED VERSUS MIXED FORMULATION - SVENVIRO/GT

A transient-state seepage problem in which the permeability and volumetric water content variables change in accordance with soil suction is common to geotechnical engineering. The fluid motion in unsaturated soils is generally assumed to obey the partial differential equations presented in the previous chapter. These equations are similar to the classical Richards equation (Hillel, 1980). The PDEs for water seepage in unsaturated soils can be written in several forms. The three most common formulations of the unsaturated flow equation are identified as the “*h*-based” form, the “*q*-based” form, and the “mixed form”. There are advantages and disadvantages associated with each of the formulations. The advantages and disadvantages become apparent when solving particular unsaturated seepage problems.

There are several advantages associated with the *q*-based form. One advantage is that it can be formulated to be perfectly water mass conservative. It is not commonly used, however, because this form degenerates in fully saturated systems and material discontinuities produce discontinuous *q* profiles.

The *h*-based form of the PDE seepage equation is the most commonly implemented form. Its primary drawback is that it can suffer from poor water mass balance when solving transient seepage problems. The poor water mass balance problem is exacerbated in situations where the soil-water characteristic curve for the material is highly nonlinear.

Celia (1990) proposed a “mixed form” of the Richards equation. The “mixed form” was designed to improve the water mass-balance of the “*h*-based” formulation. SVFLUX implements both the “*h*-based” and “mixed” PDE formulations.

3.6.1 H-Based Formulation – SVENVIRO/GT

The most commonly implemented form of the governing partial differential equation for transient seepage is shown below. The SVFLUX SVENVIRO/GT formulation is presented here and is based on total head:

$$\frac{\partial}{\partial x} \left[(k_{wx} + k_{vd}) \frac{\partial h}{\partial x} \right] + \frac{\partial}{\partial y} \left[(k_{wy} + k_{vd}) \frac{\partial h}{\partial y} \right] - k_{vd} \frac{\partial h}{\partial t} = -\gamma_w m_2^w \frac{\partial h}{\partial t} \quad [23]$$

The partial differential equation governing water flow and the storage of water within a saturated/unsaturated soil is formulated using total head, *h*, as the primary variable. However, pore-water pressure, *u_w*, (written as a water head, *u_w*/*γ_w*), can be used when solving certain seepage problems.

The formulations presented above satisfy the condition that the difference between the water flow entering or leaving a unit volume is equal to the change in volumetric water content. Under steady-state conditions, the water flux entering and leaving a unit volume is the same and as a consequence, the storage term (i.e., right-hand side of the equation) becomes zero.

The above formulation makes the assumptions that there is no loading or unloading of the soil mass during the transient process. Pore-air pressures are assumed to remain constant and at atmospheric pressure. Changes in volumetric water content are assumed to be strictly dependent on changes in the soil suction state variable.

3.6.2 H-Based Formulation (Comprehensive) - SVENVIRO

The H-based comprehensive form of the governing partial differential equation for transient seepage is shown below.

$$\frac{\partial}{\partial x} \left[(k_{wx} + k_{vd}) \frac{\partial h}{\partial x} \right] + \frac{\partial}{\partial y} \left[(k_{wy} + k_{vd}) \frac{\partial h}{\partial y} \right] - k_{vd} \frac{\partial h}{\partial t} = \gamma_w m_2^w \frac{\partial h}{\partial t} + \gamma_w h \frac{\partial m_2^w}{\partial t} \quad [24]$$

This equation takes into account the change in *m₂^w* with time and $\frac{\partial m_2^w}{\partial t}$ is insignificant in most cases.

3.6.3 Mixed Formulation - SVENVIRO

The mixed-form of the governing partial differential equation for transient seepage is shown below.

$$\frac{\partial}{\partial x} \left[(k_{wx} + k_{vd}) \frac{\partial h}{\partial x} \right] + \frac{\partial}{\partial y} \left[(k_{wy} + k_{vd}) \frac{\partial h}{\partial y} - k_{vd} \right] = \frac{\partial \theta}{\partial t} \quad [25]$$

Volumetric storage is computed using a refined differentiation of the soil-water characteristic curve.

3.6.4 Density-Dependent Formulation - SVENVIRO

The density of water changes with temperature or the solute concentration. This situation comes into play when SVFLUX (water flow) is coupled with SVHEAT (heat flow) or SVCHEM (solute movement).

The density of water in the soil is assumed to satisfy the Boussinesq approximation which can be written as follows:

$$\rho_{mw} = \rho_w [1 + \beta_c C - \beta_T (T - T_o)] = \beta \rho_w \quad [26]$$

where the β variable can be written as follows:

$$\beta = \frac{\rho_{mw}}{\rho_w} = [1 + \beta_c C - \beta_T (T - T_o)] \quad [27]$$

where:

ρ_{mw}	= water density at the given temperature or solute concentration, kg/m^3 ,
ρ_w	= fresh water density at the reference temperature T_o , ($\rho_w = 999.937$ kg/m^3),
T	= water temperature, $^{\circ}C$,
T_o	= reference temperature, $T_o = 4^{\circ}C$,
C	= solute concentration, g/m^3 ,
β_T	= water thermal expansion coefficient, $1/^{\circ}C$,
β_c	= concentration expansion coefficient, $1/(g/m^3)$,

Based on the data presented in <http://physics.info/expansion/>, the water thermal expansion varies with temperature as shown in Figure 6. The default thermal expansion is set to $2.07 \times 10^{-3} \text{ } 1/^{\circ}C$ in SVFLUX.

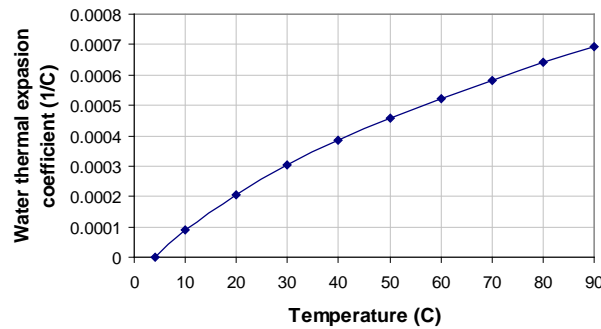


Figure 6 Thermal coefficient of expansion of water with respect to temperature

The thermal expansion of water, β_T , as the function of temperature is approximated using the following expression of data fitting.

$$\beta_T = 10^{-5} (-3 + T - 5 \times 10^{-3} T^2) \quad \text{if } T \geq 4 \quad [28]$$

where:

T	= water temperature, $^{\circ}C$.
-----	------------------------------------

The coefficient of expansion due to changes in salt concentration, β_c , is calculated using the following equation:

$$\beta_c = \frac{\rho_{\max} - \rho_w}{\rho_w C_{\max}} \quad [29]$$

where:

$$\begin{aligned} C_{max} &= \text{maximum solute concentration, } g/m^3, \\ \rho_{max} &= \text{water density at the maximum solute concentration, } kg/m^3, \end{aligned}$$

The water flow equation in one-dimension is modified as follows, when taking changes in water density into consideration as a result of temperature changes:

$$q_y = - \left(\frac{k_y^w}{\gamma_w} \frac{\partial u_w}{\partial z} + \beta k_w \right) \quad [30]$$

where:

$$\begin{aligned} q_y &= \text{water flow recharge in the y-direction, } m/s, \\ u_w &= \text{pressure on the fresh water at the reference temperature, } kPa, \\ k_z^w &= \text{hydraulic conductivity, } m/s, \\ \gamma_w &= \text{unit of weight of fresh water at the reference temperature } \gamma_w = \rho_w g, \\ &\quad kN/m^3, \text{ and} \\ \beta &= \text{defined in Equation [27].} \end{aligned}$$

The Equation [30] can be rewritten for vertical water flow when independently considering water head and elevation head.

$$q_y = - \left(k_w \frac{\partial h}{\partial y} + k_w buoy \right) \quad [31]$$

$$buoy = \frac{\rho_{mw} - \rho_w}{\rho_w} \quad [32]$$

According to the conservation of mass requirement,

$$\frac{\partial}{\partial y} (\rho_{mw} q_y) + \frac{\partial (\rho_{mw} \theta_w)}{\partial t} = 0 \quad [33]$$

The governing seepage PDE for SVFLUX when it is coupled with SVHEAT and SVCHEM is written as follows for the y-direction of flow:

$$\frac{\partial}{\partial y} \left[\frac{k_{wy}}{\gamma_w} \frac{\partial u_w}{\partial y} + \beta k_{wy} \right] = \frac{\partial \theta_w}{\partial t} + \frac{\theta_w}{\beta} \left(\beta_c \frac{\partial C}{\partial t} - \beta_T \frac{\partial T}{\partial t} \right) \quad [34]$$

The water flow PDE can also be written in terms of the water head.

$$\frac{\partial}{\partial y} \left[k_{wy} \frac{\partial h}{\partial y} + buoy k_{wy} \right] = \frac{\partial \theta_w}{\partial t} + \frac{\theta_w}{\beta} \left(\beta_c \frac{\partial C}{\partial t} - \beta_T \frac{\partial T}{\partial t} \right) \quad [35]$$

where:

$$\begin{aligned} \theta_w &= \text{volumetric water content, } m^3/m^3, \text{ and} \\ t &= \text{time, } s. \end{aligned}$$

4 BOUNDARY CONDITIONS IN SEEPAGE - SVENVIRO/GT

Several types of boundary conditions can be applied when solving seepage problems. The boundary conditions associated with seepage are as follows:

- Natural (or Neumann) boundary condition: flux,
- Essential (or Dirichlet) boundary conditions: imposed value, and
- Special boundary conditions: combinations of the above conditions.

The two basic boundary conditions intrinsically related to the formulations normally used in the finite element solutions are: Essential (or Value) boundary condition and Natural boundary conditions. Essential boundary conditions are assigned to nodes as fixed values. Natural boundary conditions are assigned to the sides of elements (and are defined by a surface integral). Natural boundary conditions correspond to the surface integral of the term inside the outer derivative of second order partial differential equations.

4.1 NATURAL BOUNDARY CONDITION - SVENVIRO/GT

Natural (or Neumann) boundary conditions arise from the integration by parts of second order derivatives. The integration results in a surface integral that corresponds to a flux quantity. Therefore, natural boundary condition associated with the seepage PDE corresponds to the total amount of water flow normal to the surface (m^3/s).

$$\text{Natural boundary condition} = \int_{\Gamma} (\mathbf{v} \cdot \mathbf{n}) dS \quad [36]$$

where:

- Γ = boundary area,
- \mathbf{v} = total flux vector,
- \mathbf{n} = outward surface-normal vector, and
- dS = an infinitesimal element at the boundary.

Natural boundary conditions are called “flux boundary conditions” in SVFLUX.

Natural boundary conditions are appropriate choices for the representation of situations such as simple soil-atmosphere fluxes, the water uptake inside a well, and the groundwater flow taking place at the bottom of a domain. The absence of a boundary condition corresponds to a zero flux natural boundary condition.

Natural boundary conditions can be applied as constant values or a set of data (or expressions in SVENVIRO only). An expression can be a function of time, space, or any other meaningful variable. Flux expressions can be used to represent several hypothetical and real world scenarios such as the increase in water uptake in a well during the course of a day or the increase in groundwater flow with depth.

The natural boundary conditions associated with the seepage PDEs do not make a distinction between the types of flow (i.e., whether it is liquid or vapor flow). The determination of the amount of flow taking place in the form of a liquid or a vapor is not required for the application of a natural boundary condition.

For instance, the imposition of a negative flux at a soil surface can result in both liquid and vapor fluxes at the surface. The partitioning of the imposed total flux into vapor and liquid flux will depend on the soil properties and pore-water pressures. Nevertheless, the total amount of flux at the surface will always correspond to the applied boundary conditions. The fractions of liquid and vapor flow can be determined from the resulting pore-water pressure gradients, temperature gradients and the soil property functions.

4.1.1 Differences Between Actual and Applied Boundary Flux – SVENVIRO/GT

It is possible that a natural boundary condition might apply more fluid at the boundary than the model can reasonably accept. This is particularly true when running numerical models which are saturated. The mass-balance of the modeling domain must be of primary consideration. Therefore, if the user applies a large boundary flux which cannot be accepted by the modeling domain, then the natural boundary condition will need to be reduced to represent the flux which can be applied while maintaining an appropriate mass balance over the modeling domain. The excess flux which is not applied is conceptually similar to “runoff” but this type of runoff may be present even if the “runoff” specifier in the software is not specified.

4.2 ESSENTIAL BOUNDARY CONDITION - SVENVIRO/GT

Essential (or Dirichlet) boundary conditions correspond to predetermined hydraulic head values.

$$\text{Essential Boundary Condition} = h$$

[37]

where:

$$h = \text{specified hydraulic (total) head value} = \frac{u_w}{\gamma_w} + y$$

u_w = pore-water pressure,
 γ_w = unit weight of water,
 y = elevation (y in a model).

This type of boundary condition is called “head” or “hydraulic head” in SVFLUX. Essential boundary conditions can be used to represent numerous situations such as the head imposed by a water reservoir (Figure 7) or the head at the bottom of a domain where the water table is relatively constant. Essential boundary conditions are always required in steady-state problems. Transient problem may or may not present an essential boundary condition.

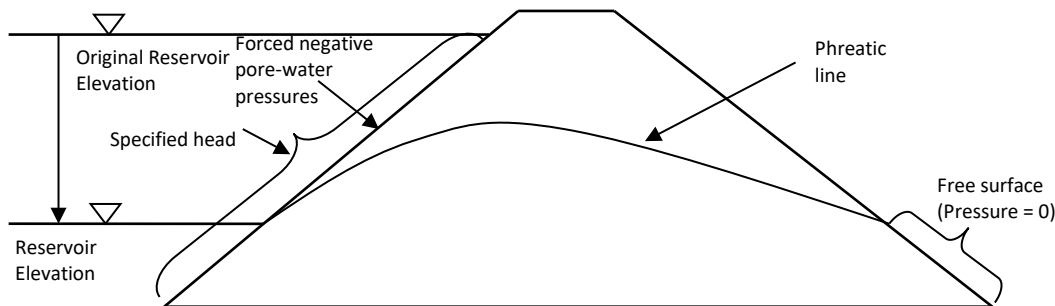


Figure 7 Head upstream boundary conditions in the case of rapid drawdown simulation

Essential boundary conditions can be applied as constant values or a set of data (or expressions in SVENVIRO only). Similar to the natural boundary condition, an expression can be a function of time, space, or any other meaningful variable. Head expressions can be used to represent several hypothetical and real world scenarios such as the increase in the filling of a reservoir or transient heads imposed by tides.

Essential boundary conditions must be consistent with the initial conditions of a problem. Discontinuity not only misrepresents the actual problem, but also results in numerical oscillations. For instance, the simulation of a sudden reduction in pore-water pressure at a surface should always be done using the ramping of head over time, starting with an initial head equal to initial conditions. An appropriate ramping time interval that represents the actual rate of change should be selected.

The user must be careful when applying a head boundary condition to the upstream side of an earth levee or dam during a rapid drawdown scenario. The head boundary condition may be inappropriate for some situations as it inherently forces unsaturated soil conditions above the water table. Professional judgment is needed to determine whether or not the “forcing” of negative pore-water pressures is appropriate within the context of the problem under consideration.

4.2.1 Review Boundary Condition (Drain) – SVENVIRO/GT

More complex boundary conditions are required in order to model certain seepage problems. An example is the situation of a free drainage surfaces with an unknown seepage exit point. This situation commonly occurs on the downstream slope of an earth fill dam (Figure 8). The downstream face of the dam can be represented as a modification of the natural and essential boundary conditions.

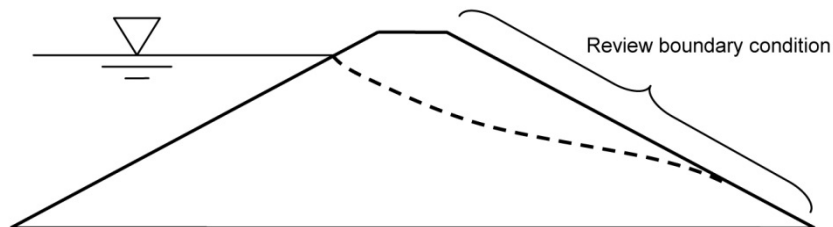


Figure 8 “Review boundary” condition for a free flow surface

The boundary condition used to represent the free flow condition is shown in Figure 8. The boundary is called a “Review boundary condition” in SVFLUX. The terminology “drain boundary condition” is sometimes used to refer to this type of boundary condition.

A review boundary condition is applied as follows:

- If pore-water pressures are negative, then the boundary condition has zero flux,
- If pore-water pressure is positive, then the boundary condition is equal to a negative (outward) flux that brings pore-water pressures on the surface to zero.

If the amount of negative flux is large, changes at the boundary will take place nearly instantaneously. A large negative flux is equivalent to setting the essential boundary condition equal to the elevation relative to the datum:

$$h = y \quad [38]$$

The essential boundary condition creates another degree of nonlinearity in the system that must be solved through the use of an iterative process. Another type of special boundary condition available in SVFLUX is called the "climate boundary condition".

Climate boundary conditions are used to model complex soil-atmosphere fluxes. Additional input data is required in order to use climatic boundary conditions. The following chapter presents the theory for this type of boundary condition.

4.2.2 Upstream Head and Flow Boundary Conditions – SVENVIRO/GT

The rapid drawdown or rapid filling behind an earth fill dam (or an embankment) requires the use of a special upstream head and flux boundary condition. The change in reservoir conditions creates a unique boundary condition where special boundary conditions need to be used in SVFLUX.

Consider the case where there is a rapid drawdown of the reservoir. This scenario can be represented using a standard Dirichlet (head) boundary condition where the reservoir elevations are entered into the software in the form of a data table. This type of boundary condition is simple to evaluate numerically and generally executes quickly. The downside of this type of representation lies in the fact that as the water table is lowered, there are negative pore-water pressures that are placed on the upper portions of the boundary.

The upstream "Head-Flow" boundary condition divides the upstream boundary into two segments; i) one segment below the reservoir level, and ii) another segment above the reservoir level. Below the reservoir level, the water is allowed to flow in or out of the soil depending upon whether the model is under rapid filling or rapid drawdown. Above the reservoir elevation, the boundary is treated as a "no flow" boundary condition. It is possible in this boundary condition that the phreatic surface may approach and touch the boundary during the rapid drawdown scenarios. The description of the "Head-Flow" boundary condition can be seen in Figure 9.

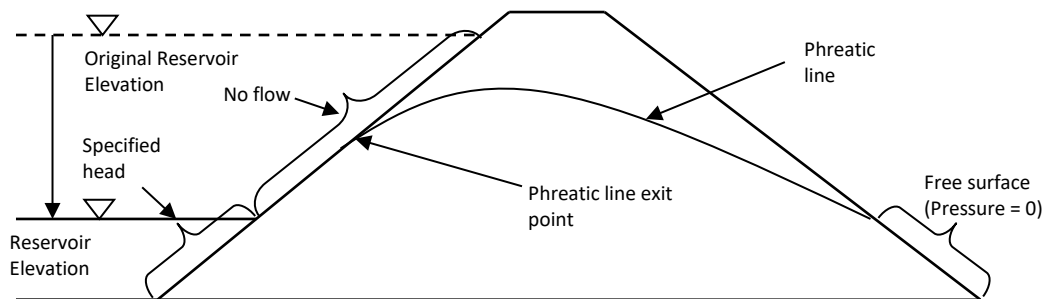


Figure 9 Description of the Head Flow boundary condition

4.2.3 Upstream Head Review Boundary Conditions – SVENVIRO/GT

There are three potential zones that must be considered in the numerical model when rapid drawdown is considered in a numerical model. These zones are illustrated in Figure 10. The Head Review boundary condition in SVFLUX is designed to handle all three of these conditions. Specifically, water is allowed to flow into or out of the model (depending on the difference in head) below the reservoir elevation. Between the phreatic line exit point and the reservoir elevation, water may exit the model if the pore-water pressures approach zero in this area. Unsaturated soil conditions above the phreatic line impose "no flow" conditions.

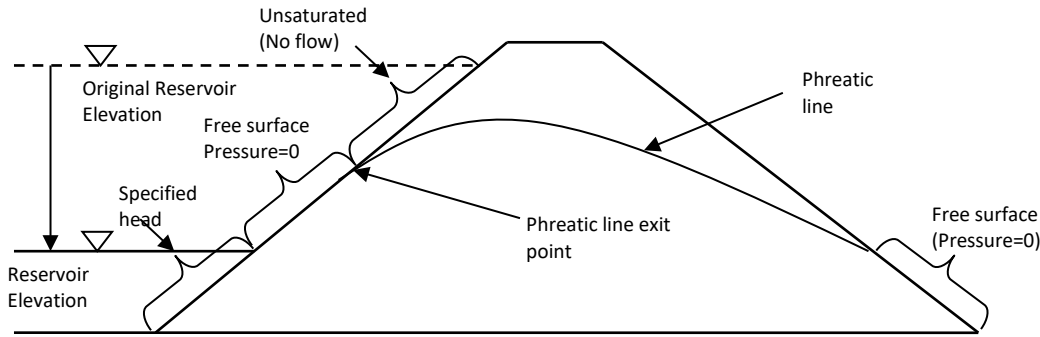


Figure 10 Three zones of potential consideration on the upstream side of a rapid drawdown scenario with the “Head Review” boundary condition

4.3 GEOMEMBRANE WITH CONTACT RESISTANCE - SVENVIRO

Geomembranes made from composite liner materials are typically thin and have a low hydraulic conductivity. SVFLUX implements an internal contact resistance boundary condition that allows for reasonable representation of geomembranes. Such representation does not require the large number of nodes typically required when representing a geomembrane with a separate region. Figure 11 illustrates the case of a geomembrane modeled as a semi-impermeable barrier to water. Geomembranes are often designed as part of a waste management system.

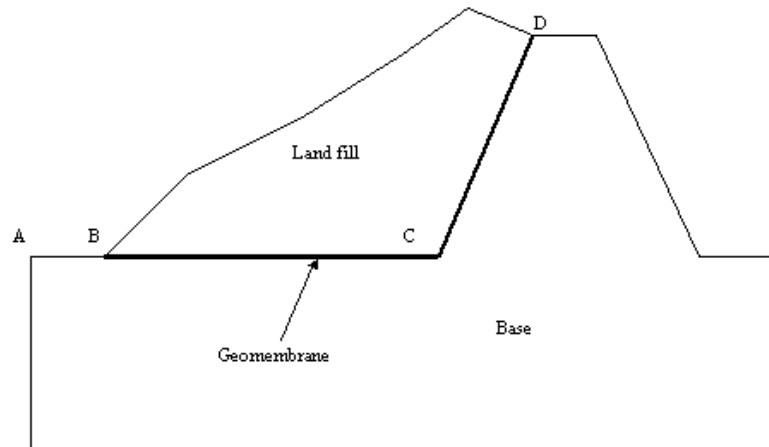


Figure 11 Illustration of model using geomembrane boundary condition

The geomembrane boundary condition called a geomembrane boundary condition. It is implemented as a contact boundary condition which can be expressed mathematically as,

$$contact(h) = \frac{Jump(h)}{R} \quad [39]$$

$$R = \frac{B_b}{k_b} \quad [40]$$

where:

- h = hydraulic head, m ,
- R = contact resistance, $1/s$,
- B_b = thickness of geomembrane, m , and
- k_b = hydraulic conductivity of geomembrane, m/s .

Note: time units used in a given model can be chosen, seconds are used in this example.

The thickness and hydraulic conductivity of the geomembrane must be specified when using the geomembrane boundary condition. In the example illustrated in Figure 11, only geometry for the “Land fill” and the “base” regions are required. The geomembrane boundary (i.e., boundary B-C-D) is applied as an internal boundary condition in the region of “Land fill”. The boundary B-C-D in the “Base” region can be specified as “NoBC”.

NOTE:

Because the geomembrane boundary condition is implemented as a contact boundary condition, a geomembrane internal boundary condition must terminate at an edge of the model. Figure 12 and Figure 13 shows the cases of an invalid geomembrane BC applied, while Figure 14 and Figure 15 are valid cases.

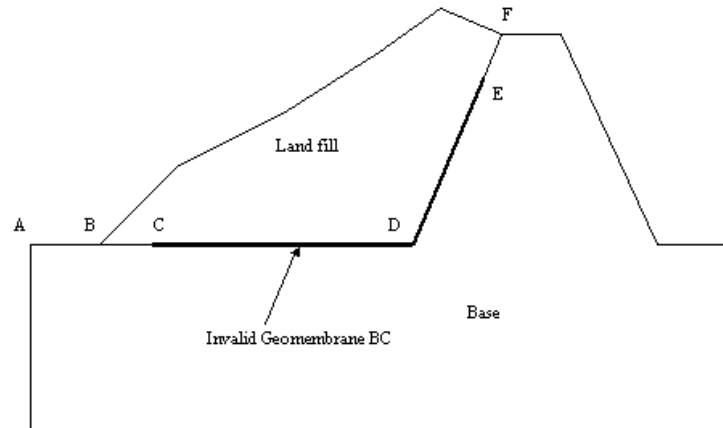


Figure 12 Invalid Geomembrane 1

- a. Invalid geomembrane designation because B-C and E-F are not a geomembrane boundary condition in the internal boundary B-C-D-E-F

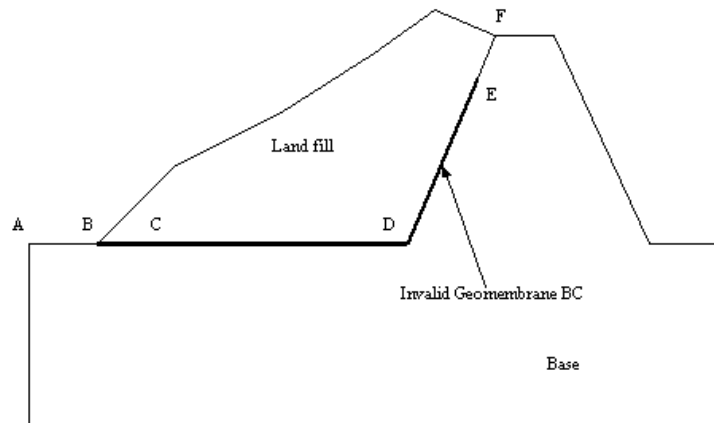


Figure 13 Invalid Geomembrane 2

- b. Invalid geomembrane designation because E-F is not a geomembrane boundary condition on the internal boundary B-C-D-E-F

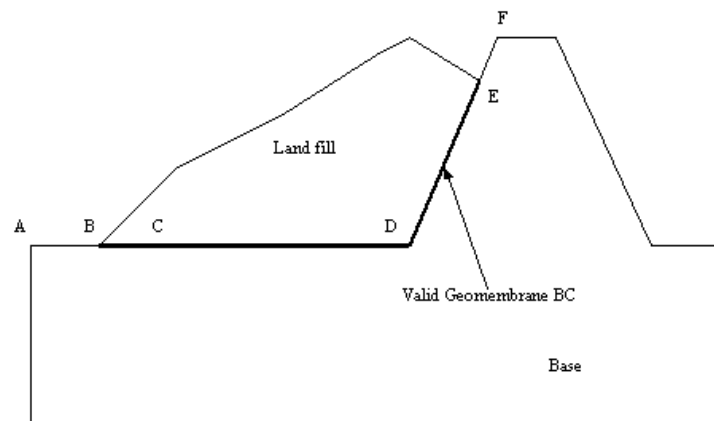


Figure 14 Valid Geomembrane 1

- c. Valid geomembrane condition because B-C-D-E is specified as geomembrane boundary condition on the internal boundary B-C-D-E

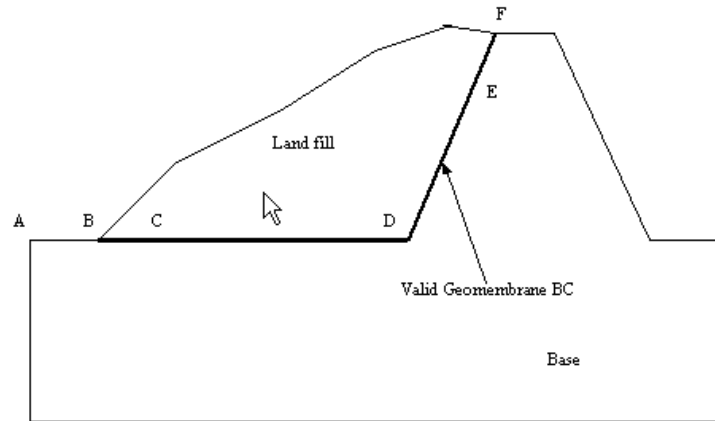


Figure 15 Valid Geomembrane 2

- d. Valid geomembrane condition because B-C-D-E-F is specified as a geomembrane boundary condition on the internal boundary B-C-D-E-F

4.4 INITIAL WATER TABLE - SVENVIRO/GT

Initial pore-water pressure conditions can be calculated assuming hydrostatic conditions and the following equation:

$$u_w = \gamma_w (h - y) \quad [41]$$

where:

u_w	= pressure, kPa ,
γ_w	= unit weight of water, kN/m^3 ,
h	= total water head, m , and
y	= elevation, m .

Therefore,

when	$h = y$	$u_w = 0$; represents the phreatic surface
when	$h > y$	$u_w > 0$; represents the saturated region
when	$h < y$	$u_w < 0$; represents the unsaturated region

Defining a water table as initial conditions is well-suited for some situations requiring a quick solution. For more complex situations, using hydrostatic conditions may not be realistic and may cause convergence problems. To overcome convergence problems with complex models it is best to import the initial head conditions from a steady-state run of the model.

5 WELLS AND TUNNELS - SINK/SOURCE METHOD - SVENVIRO/GT

5.1 INTRODUCTION - SVENVIRO

Wells are common occurrences that consist of a cylindrical hole drilled to a specified depth. A screen is placed through a particular water bearing zone. Tunnels are features such as mine shafts and drains. Wells and tunnels are often pumped on an ongoing basis to maintain the water level below a designated elevation.

Tunnels and wells are represented as localized sinks or sources in a numerical model. Tunnels and wells draw water out of cells (by pumping) or add water to cells (by injection). On a regional scale, the diameter of a well borehole or tunnel shaft is too small to model in a rigorous manner since it would require an extremely fine mesh resolution fine to model the physical borehole.

A traditional method of representing well and tunnel objects is through use of a line of nodes in a finite element model. Such a representation is efficient in terms of the generated mesh, but can result in extremely high gradients next to the line of elements. This is particularly true when the internal boundary condition applied to the well/tunnel differs greatly from the surrounding domain. Sharp gradients can lead to instabilities in the numerical model.

SVFLUX SVENVIRO/GT models wells as a sink (or source) term in the partial differential equation, rather than as a physical boundary condition. This eliminates the meshing issues associated with modeling a borehole that is small relative to the overall extent of the model.

The SVFLUX SVENVIRO methodology introduces an approximation that affects the distance at which the flux across a closed surface bounding the well screen becomes accurate. The user can set this *influence distance*, and experiment with the level that provides the right mix of accuracy in the solution and modeling speed.

In SVFLUX, wells are vertical features whereas tunnels can be inclined at any angle and can be a sequence of straight line segments. Wells differ from tunnels only in the definition of the *Review* boundary condition (See section 5.5). Otherwise, one may use the terms wells and tunnels interchangeably. Wells and tunnels can be included in two- and three-dimensional models.

In this document, tunnels are only referred to where the theory differs from that of wells. Otherwise, the theory applies for both tunnels and wells.

5.2 EQUATIONS - SVENVIRO/GT

Equation [42] is the groundwater flow equation in three Cartesian coordinate dimensions.

$$\frac{\partial}{\partial x} \left[k_{wx} \frac{\partial h}{\partial x} \right] + \frac{\partial}{\partial y} \left[k_{wy} \frac{\partial h}{\partial y} \right] + \frac{\partial}{\partial z} \left[k_{wz} \frac{\partial h}{\partial z} \right] + \bar{Q}_{well} = -\gamma_w m_2^w \frac{\partial h}{\partial t} \quad [42]$$

where:

h	= hydraulic head, m ,
k_{wx}	= hydraulic conductivity in the x -direction, m/day ,
k_{wy}	= hydraulic conductivity in the y -direction, m/day ,
k_{wz}	= hydraulic conductivity in the z -direction, m/day ,
γ_w	= $\rho_w g$ = the unit weight of water
m_2^w	= derivative of the soil-water characteristic curve

In SVFLUX SVENVIRO:

The source term, \bar{Q}_{well} , in Equation [43], can be used to simulate a well.

$$\bar{Q}_{well} = \frac{P}{\int_P PdV} Q_{well} \quad [43]$$

where, Q_{well} is the user-defined pumping/injection rate for the well, and P , in Equation [43], is a function that scales the source term.

$$P = \exp\left(-\frac{|\mathbf{r}|^2}{\alpha^2} \ln 20\right) \quad [44]$$

where, \mathbf{r} (described in Section 5.3) is the shortest vector from the well to a point in the model domain, and α is the user-defined *influence distance*. The Equation [44], definition of P , corresponds to $|\mathbf{r}| = \alpha$, and $P = \frac{1}{20}$. The integral $\int_P P dV$ in Equation [43] is taken over the entire volume, V , of the model, and normalizes P such that $\int_V \bar{Q}_{well} dV = Q_{well}$. Figure 16 shows some examples of P for example values of α .

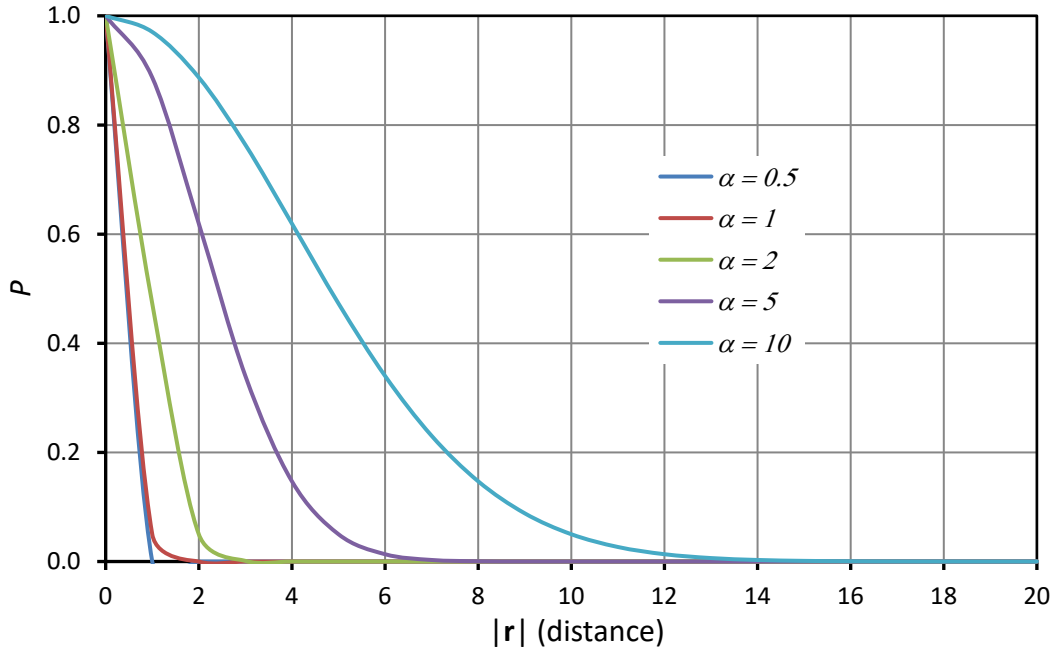


Figure 16: Examples of P for values of α .

In SVFLUX GT:

A unit cross-sectional area is assumed for the well. The total discharge Q_{well} from the well is partitioned to the various nodes on the well screen on the basis of contributory area of flow to the nodes such that:

$$Q_{well} = \int_V \bar{Q}_{well} dV = \sum_{i=1}^n Q_i \quad [45]$$

where n is the total number of nodes in the well screen and i is the index of sequential node numbers.

5.3 GEOMETRY - SVENVIRO

The vector, \mathbf{r} , in Equation [44] is either the vector perpendicular to the well screen from the model point, or the vector from the closest end of the screen to the point under consideration. Figure 17 shows \mathbf{r} when the model point is closest to a point in the screened segment, and Figure 18 shows \mathbf{r} when the model point is closest to an end of the screen.

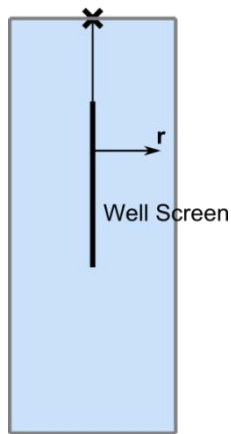


Figure 17: Shortest distance to a model point from the screened segment.

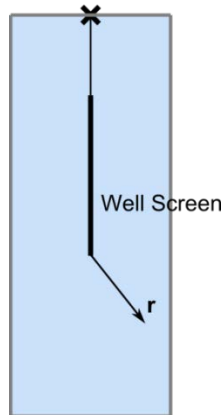


Figure 18: Shortest distance to a model point from an end.

5.4 SETTING THE INFLUENCE DISTANCE - SVENVIRO

The influence distance affects how far away from the screen Q_{well} becomes realized within the numerical model. Smaller influence distances will cause the well flux to be realized at closer distances to the screen than is the case with larger influence distances.

The influence distance should be set to a value that represents the scale at which the groundwater flux is important. In general, if the model extends horizontally for hundreds of meters, the seepage in a volume immediately surrounding the screen is less important than the overall effect that the well has on the flow in the region. Therefore, a larger value is appropriate for the influence distance (maybe in the order of ~ 10 m). Larger influence distances produce shallower gradients and prevent the computations related to the volume immediately surrounding the well from dominating the system.

For simpler models, the influence distance has little effect on the computational speed. Therefore, the influence distance can be set to a small value (say in the order of ~ 1 m).

5.5 BOUNDARY CONDITIONS - SVENVIRO/GT

Well and tunnel boundary conditions are implemented through use of a sink/source term, \bar{Q}_{well} , in Equation [42]. SVFLUX calculates an appropriate value for Q_{well} for each type of boundary condition.

5.5.1 Rate - SVENVIRO

The value of Q_{well} in Equation [43] is specified and applied along the well.

5.5.2 Head - SVENVIRO

A specified head, h_{well} , is maintained by determining the flow necessary to produce a head, h_{well} along the screen. The flow is specified as follows:

$$Q_{well} = \begin{cases} K(h_{well} - h)^2, & h \leq h_{well} \\ -K(h - h_{well})^2, & h > h_{well} \end{cases} \quad [46]$$

where, K is the *BIG_WELL* parameter that can be input. The K parameter can be used in a staged manner. The choices are *SQUARED* (as in Equation [46]), or *LINEAR* (as for a power of 1).

5.5.3 Head - GT

A specified head, h_{well} , is maintained in the same way as the application of Dirichlet boundary conditions described in section 4.2.

5.5.4 Review (Wells) - SVENVIRO

The review wells boundary condition implements a head boundary condition with a specified head equal to the elevation at the bottom of the screen.

5.5.5 Review (Wells and Tunnels) - GT

The review boundary condition on wells determines the natural water level in the well applying the principles as described in section 4.2.1.

For tunnels, the review boundary condition maintains the zero pore-water pressure along the entire tunnel length applying the same principles as described in section 4.2.1.

5.5.6 Review (Tunnels) - SVENVIRO

The review tunnel boundary condition maintains zero pore-water pressure along the tunnel. The zero pore-water pressure condition is implemented by ensuring that the flow, Q_{well} is equal to the head at that elevation. The equation can be written as follows.

$$Q_{well} = \begin{cases} 0, & h \leq y \\ -K(h - y)^2, & h > y \end{cases} \quad [47]$$

where, K is a *BIG_TUNNEL* parameter that can be input. The K parameter can also be used in a staged manner. An exponent of 2 can be set for Equation [47]. The choices are *SQUARED* (as in Equation [47]), or *LINEAR* (for a power of 1).

5.6 PARAMETERS - SVENVIRO

Wells and tunnels are controlled by three user definable parameters; namely, the *Influence Distance* α , the *Line Mesh Spacing* ζ , and the *Mesh Growth Coefficient* γ . The influence distance controls the spread of the sink that simulates the well, and the line mesh spacing and mesh growth coefficient control the mesh spacing near the well.

The well sink is computed using the following scale factor equation:

$$P = \exp\left(-\frac{|\mathbf{r}|^2}{\alpha^2} \ln 20\right) \quad [48]$$

The vector, \mathbf{r} , is described in detail in Section 5.3.

The mesh spacing is controlled using the following criteria.

$$m = \max\left(\xi, \gamma |\mathbf{r}|^{1.2}\right) \quad [49]$$

Equation [49] ensures that ζ is the smallest element size. The mesh spacing causes the mesh to grow at a rate proportional to $|\mathbf{r}|^{1.2}$. An exponent of 1.2 was selected to allow the mesh to grow at a rate that is generally appropriate for most models.

Figure 16 shows the scale function, P , for some values of influence distance, and Figure 19 shows the mesh spacing for some values of the mesh growth coefficient.

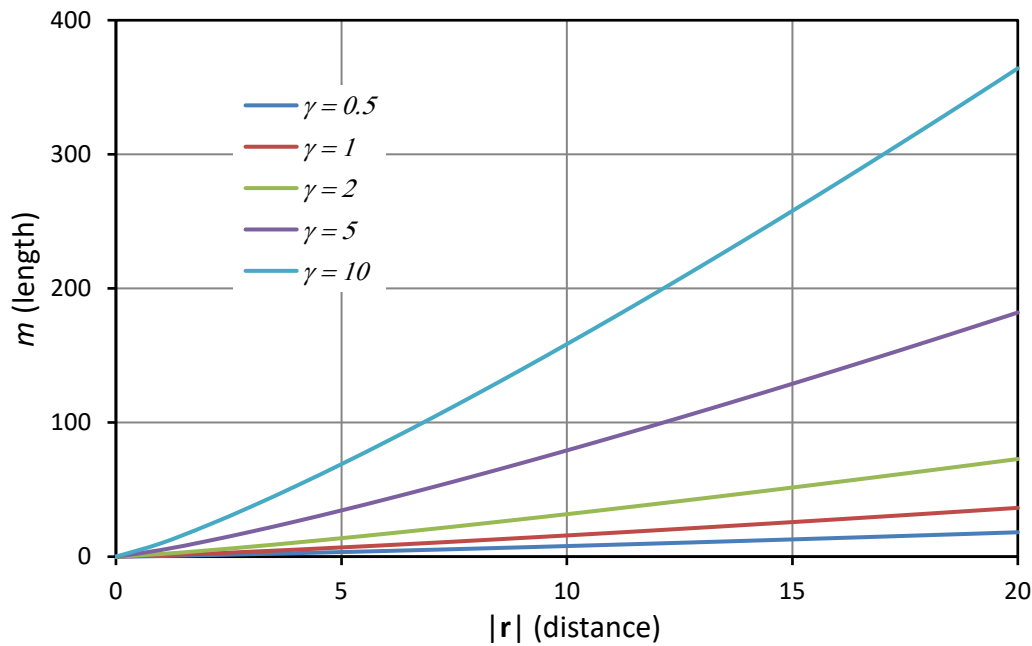


Figure 19: Mesh spacing (m) for various values of mesh growth coefficient (γ).

5.7 REMARKS - SVENVIRO

Changing the default mesh parameters in Equation [49] is only necessary if the automatically generated mesh is not suitable. The mesh may be too coarse or too fine near the well, and adjustment may be necessary to facilitate accurate and efficient modelling.

It is possible that the mesh generation will not be satisfactory around the well of large models. It is also possible that the modeler may fail to resolve the peak performance of the sink/source regardless of how the parameters are set. In this case, it is necessary to increase the mesh density of the model by decreasing the mesh size. It is often best to create a region that contains the well, and if necessary, decrease the mesh size for that region. Just creating the region around the well may not be sufficient to resolve the modeling issues. It should be noted that the regional mesh size will override the mesh size set by Equation [49].

When wells or tunnels are directly represented as a borehole in a model, it causes extremely dense meshing near the borehole. The dense mesh can generally be resolved by designating the model scale mesh. However, when the resulting mesh is extremely dense near to the well, the model may run slowly. The advantage of incorporating wells and tunnels as sinks/sources in the partial differential equation is that the mesh size is determined at the model scale. This computational procedure generally gives accurate results in much less time. Equations [48] and [49] provide control on the rate of decay of the sink/source.

FlexPDE takes several characteristics of the geometry into consideration when generating the mesh. It is possible that the mesh size set by Equation [49] will be overridden by another size parameter. Since FlexPDE will select the smallest mesh size out of all the possible sizes under consideration, this should not cause any problems with the simulation.

For complex models, particularly those for which the well or tunnel is screened across an aquitard/aquifer contact, the head gradients in the immediate vicinity of the well need to be monitored to guard against unrealistically large values.

The (*Rate*) boundary condition in a two-dimensional model is a volume per unit time. When determining the appropriate rate, the user must consider the well to be applied to a three-dimensional model with the third dimension having a unit length. This means that a rate that is suitable for a three-dimensional model may be too large for a corresponding two-dimensional model.

6 FLUX SECTIONS - SVENVIRO/GT

In SVFLUX, the flux of water across a user-defined section can be determined in either steady state or transient analysis. This flux section tool is used to calculate water fluxes into or out of a specific line segment, region segment or other places of interest. Some common applications are to determine the amount of seepage on the downstream face of a dam or below cut-off walls.

6.1 FLUX SECTION THEORY CALCULATION - SVENVIRO/GT

The theoretical calculation of flux section is illustrated in this section. Refer to Figure 20 for a diagram illustrating the theory. A 3-noded linear triangular element is used to demonstrate the theory and the flux of water across section A-A is calculated. The line section A-A crosses the element at points *a* and *b* with Cartesian (global) coordinates, (x_a, y_a) and (x_b, y_b), respectively. Point *C* (x, y) is at the center of the flux section, and water flux passing this point is defined as (Bathe, 1982):

$$\mathbf{q} = \begin{Bmatrix} q_x \\ q_y \end{Bmatrix} = -\mathbf{DB}(x, y)\mathbf{H} \quad [50]$$

where:

- q_x = flux in *x*-direction
- q_y = flux in *y*-direction
- D** = material property matrix
- B** = matrix for head gradient interpolation, and
- H** = vector of of total head at the element nodes

The **D** matrix for an isotropic material is defined as:

$$\mathbf{D} = \begin{bmatrix} k_x & 0 \\ 0 & k_y \end{bmatrix} \quad [51]$$

The **B** matrix is defined as:

$$\mathbf{B} = \begin{bmatrix} \frac{\partial N_1}{\partial x} & \frac{\partial N_2}{\partial x} & \frac{\partial N_3}{\partial x} \\ \frac{\partial N_1}{\partial y} & \frac{\partial N_2}{\partial y} & \frac{\partial N_3}{\partial y} \end{bmatrix} \quad [52]$$

where:

N_1, N_2, N_3 = shape functions at nodes 1, 2 and 3, respectively

The **H** is the total head vector of the element nodes:

$$\mathbf{H} = \begin{bmatrix} H_1 \\ H_2 \\ H_3 \end{bmatrix} \quad [53]$$

where:

H_1, H_2, H_3 = the total head at nodes 1, 2 and 3, respectively

The total head at a point (x, y) within the element can be defined using the shape functions and head values at the nodes as:

$$H(x, y) = \sum_{i=1}^3 N_i H_i \quad [54]$$

The above shape functions are usually expressed in local (natural) coordinates and for triangular elements (shown in Figure 21) they are defined as:

$$\begin{aligned} N_1 &= 1 - \alpha - \beta \\ N_2 &= \alpha \\ N_3 &= \beta \end{aligned} \quad [55]$$

The **B** matrix can be rewritten as:

$$\mathbf{B} = \begin{bmatrix} \frac{\partial x}{\partial \alpha} & \frac{\partial y}{\partial \alpha} \\ \frac{\partial x}{\partial \beta} & \frac{\partial y}{\partial \beta} \end{bmatrix}^{-1} \begin{bmatrix} \frac{\partial N_1}{\partial \alpha} & \frac{\partial N_2}{\partial \alpha} & \frac{\partial N_3}{\partial \alpha} \\ \frac{\partial N_1}{\partial \beta} & \frac{\partial N_2}{\partial \beta} & \frac{\partial N_3}{\partial \beta} \end{bmatrix} = \mathbf{J}^{-1} \begin{bmatrix} \frac{\partial N_1}{\partial \alpha} & \frac{\partial N_2}{\partial \alpha} & \frac{\partial N_3}{\partial \alpha} \\ \frac{\partial N_1}{\partial \beta} & \frac{\partial N_2}{\partial \beta} & \frac{\partial N_3}{\partial \beta} \end{bmatrix} \quad [56]$$

The matrix $\mathbf{J} = \begin{bmatrix} \frac{\partial x}{\partial \alpha} & \frac{\partial y}{\partial \alpha} \\ \frac{\partial x}{\partial \beta} & \frac{\partial y}{\partial \beta} \end{bmatrix}$ is called Jacobian matrix and \mathbf{J}^{-1} is the inverse of \mathbf{J} .

For iso-parameter elements, the same shape functions are used to determine coordinates of a point (x, y) within the element in global coordinates.

$$\begin{aligned} x &= \sum_{i=1}^3 N_i x_i \\ y &= \sum_{i=1}^3 N_i y_i \end{aligned} \quad [57]$$

Combining the equations [50], [51], [53] and [56], the flux vector $q(q_x, q_y)$ at the centre point of the flux section is determined. The flux crossing the flux section is determined as:

$$\begin{aligned} \|q\| &= \sqrt{q_x^2 + q_y^2} \\ l &= \sqrt{(x_a - x_b)^2 + (y_a - y_b)^2} \\ \begin{Bmatrix} Q_x \\ Q_y \end{Bmatrix} &= \begin{Bmatrix} q_x & 0 \\ 0 & q_y \end{Bmatrix} \begin{Bmatrix} \|x_a - x_b\| \\ \|y_a - y_b\| \end{Bmatrix} \end{aligned} \quad [58]$$

The normal flux across the flux section is determined as:

$$Q_n = (\mathbf{q} \cdot \mathbf{n}) \times l \quad [59]$$

where:

- \mathbf{n} = unit normal vector to the flux section shown in Figure 20
- l = length of the flux section
- Q_x, Q_y, Q_n = fluxes in x-, y-directions and normal flux across the flux section, respectively

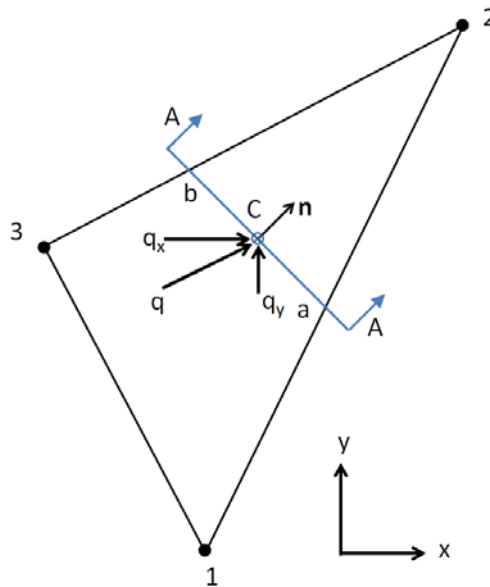


Figure 20. Flux section calculation for a 3-noded element

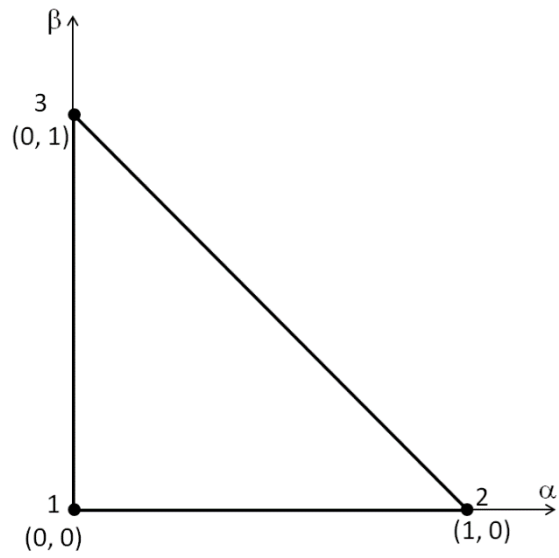


Figure 21. 3-noded element in local (natural) coordinates

7 MATERIAL PROPERTIES - SVENVIRO/GT

This section will present the theory behind material properties used in SVFLUX modeling software.

7.1 SOIL-WATER CHARACTERISTIC CURVE - SVENVIRO/GT

The *soil-water characteristic curve* is central to the application of unsaturated soil mechanics. It defines the nonlinear relationship between the amount of water in the soil (i.e., water content) and soil suction. Historically, the amount of water in the soil has been represented using the volumetric water content variable. However, other designations such as the degree of saturation of the soil prove to be superior designations of the amount of water in the soil when the soil undergoes volume change as soil suction is increased. Representation of the soil-water characteristic curve is accomplished either through fitting existing data or estimating the curve from grain-size information.

7.1.1 Fredlund and Xing (1994) Equation – SVENVIRO/GT

Fredlund and Xing (1994) presented a three-parameter equation with the flexibility to fit a wide range of materials. The equation also contained a correction variable that provided increased accuracy in the high suction range. The parameters of the equation were typically found using a least-squares algorithm. The original form of the equation was as follows.

$$\theta_w = \theta_s \left[1 - \frac{\ln\left(1 + \frac{\psi}{h_r}\right)}{\ln\left(1 + \frac{10^6}{h_r}\right)} \right] \left[\frac{1}{\ln\left[\exp(1) + \left(\frac{\psi}{a_f}\right)^{n_f}\right]} \right]^{m_f} \quad [60]$$

where:

- ψ = soil suction value (kPa).
- θ_w = volumetric water content at soil suction, ψ ,
- θ_s = saturated volumetric water content,
- a_f = material parameter which is primarily related to the air-entry value of the soil in kPa,
- n_f = material parameter which is primarily a function of the rate of water extraction from the soil once the air-entry value has been exceeded,
- m_f = material parameter which is primarily a function of the residual water content,
- h_r = suction at residual water content (kPa), and

Fitting method: Least squares nonlinear regression

Required input: Drying laboratory data consisting of points on the curve of volumetric water content versus soil suction.

Applicable material types: All soils

7.1.2 Fredlund (2000) Bimodal Equation – SVENVIRO/GT

The bimodal equation can be viewed as two superimposed unimodal SWCC curves. The fitting algorithm fits the bimodal equation by subdividing the overall curve into an upper and lower portion. Each of the two portions is then fit with a nonlinear least squares regression algorithm and the results are then combined through the use of superposition. The breaking point between the two curves is designated using the w parameter which must be selected by the analyst.

$$w = w_s \left\{ s \left[\frac{1}{\ln\left(\exp(1) + \left(\frac{a_{fb}}{\psi}\right)^{n_{fb}}\right)} \right]^{m_{fb}} + (1-s) \left[\frac{1}{\ln\left(\exp(1) + \left(\frac{j_{fb}}{\psi}\right)^{k_{fb}}\right)} \right]^{l_{fb}} \right\} \left[1 - \frac{\ln\left(1 + \frac{\psi}{3000}\right)}{\ln\left(1 + \frac{1000000}{3000}\right)} \right] \quad [61]$$

where:

- w = gravimetric water content at any soil suction,
- w_s = gravimetric water content at any soil suction,
- ψ = soil suction, kPa,

a_{fb}	= fitting parameter,
n_{fb}	= fitting parameter,
m_{fb}	= fitting parameter,
j_{fb}	= fitting parameter, <i>kPa</i> ,
k_{fb}	= fitting parameter,
l_{fb}	= fitting parameter, and
s	= Fredlund bimodal split

Fitting method:	Least squares nonlinear regression
Required input:	Drying laboratory data consisting of points on the curve of volumetric water content versus soil suction.
Applicable material types:	All soils

7.1.3 Fredlund 2-Point Estimation – SVENVIRO/GT

The soil-water characteristic curve has two primary defining points: (1) the water content and soil suction at the air-entry value for the soil and (2) the water content and soil suction at residual conditions. Additionally, there are two points that define the extreme limits on the curve: completely saturated conditions under zero suction and completely dry conditions (i.e., zero water content and a soil suction of 1,000,000 kPa). This fit allows the soil-water characteristic curve to be represented by physically meaningful inflection points. The benefit of these physically significant points is that the exact quantification this allows can then lead to an easier statistical analysis.

$$\begin{aligned}
 w &= w_s + S_1 \log \frac{\psi}{\psi_s} && \text{when } \psi < \psi_{aev} \\
 w &= w_{aev} + S_2 \log \frac{\psi}{\psi_{aev}} && \text{when } \psi_{aev} < \psi < \psi_r \\
 w &= w_r + S_3 \log \frac{\psi}{\psi_r} && \text{when } \psi_r < \psi
 \end{aligned} \tag{62}$$

where:

w_s	= gravimetric saturated water content,
ψ_s	= low suction corresponding to saturated conditions in <i>kPa</i> ,
w_{aev}	= gravimetric water content at air-entry value,
ψ_{aev}	= suction at air-entry value in <i>kPa</i> ,
w_r	= gravimetric residual water content in <i>kPa</i> , and
ψ_r	= residual suction

The slope variables in the above equations are defined as follows:

$$\begin{aligned}
 S_1 &= \frac{w_{aev} - w_s}{\log(\psi_{aev}) - \log(\psi_s)} \\
 S_2 &= \frac{w_r - w_{aev}}{\log(\psi_r) - \log(\psi_{aev})} \\
 S_3 &= \frac{-w_r}{\log(10^6) - \log(\psi_r)}
 \end{aligned} \tag{63}$$

7.1.4 Van Genuchten (1980) Equation – SVENVIRO/GT

Van Genuchten (1980) presented a three-parameter equation with the flexibility to fit a wide range of materials. The parameters of the equation could be found using a least-squares algorithm.

$$w_w = w_{avg} + (w_s - w_{avg}) \left[\frac{1}{\left[1 + (a_{vg} \psi)^{n_{vg}} \right]^{m_{vg}}} \right] \tag{64}$$

where:

w_w	= gravimetric water content at any soil suction,
w_{rvg}	= residual gravimetric water content,
w_s	= saturated gravimetric water content,
a_{vg}	= material parameter which is primarily a function of the air-entry value of the soil in kPa ,
n_{vg}	= material parameter which is primarily a function of the rate of water extraction from the soil once the air-entry value has been exceeded, and
m_{vg}	= fitting parameter, and
ψ	= soil suction (kPa).

Fitting method: Least squares nonlinear regression

Required input: Drying laboratory data consisting of points on the curve of gravimetric water content versus soil suction. It should be noted that data points well beyond residual suction conditions may distort the best-fit analysis.

Applicable material types: All soils

7.1.5 Van Genuchten (1980) and Mualem (1976) Equation – SVENVIRO/GT

Van Genuchten (1980) proposed a closed form simplification for solving the Mualem (1976) integral equation. The relationship between the m and n parameters of the van Genuchten (1980) equation was first prescribed in order to reduce the number of fitting parameters from three to two. The simplification proposed by Mualem (1976) is shown below.

$$w_w = w_{rm} + (w_s - w_{rm}) \left[\frac{1}{\left[1 + (a_m \psi)^{n_m} \right]^{\left(1 - \frac{1}{n_m} \right)}} \right] \quad [65]$$

where:

w_w	= gravimetric water content at any soil suction,
w_{rm}	= residual gravimetric water content,
w_s	= saturated gravimetric water content,
a_m	= material parameter which is primarily a function of the air-entry value of the soil in kPa ,
n_m	= material parameter which is primarily a function of the rate of water extraction from the soil once the air-entry value has been exceeded, and
ψ	= soil suction (kPa).

Fitting method: Least squares nonlinear regression

Required input: Drying laboratory data consisting of points on the curve of gravimetric water content versus soil suction.

Applicable material types: All soils

7.1.6 Vereecken, Maes, Feyen and Darius (1989) Estimation Method – SVENVIRO/GT

The Vereecken et al., (1989) Pede-Transfer Function (PTF) used a multiple linear regression method to estimate the parameters for the van Genuchten (1980) equation.

A number of different forms of the van Genuchten (1980) equation were analyzed by Vereecken et al., (1989). The models considered are shown below.

$$\begin{aligned} \text{Model 1: } s_e &= (1 + (\alpha h)^n)^{-m} \\ \text{Model 2: } s_e &= (1 + (\alpha h)^n)^{-1+1/n} \\ \text{Model 3: } s_e &= (1 + (\alpha h)^n)^{-1+2/n} \\ \text{Model 4: } s_e &= (1 + (\alpha h)^n)^{-1} \\ \text{Model 5: } \theta &= \theta_s (1 + (\alpha h)^n)^{-1} \end{aligned} \quad [66]$$

where:

$$s_e = \frac{\theta - \theta_r}{\theta_s - \theta_r}, \text{ normalized volumetric water content,}$$

$$h = \text{pressure head (cm),}$$

$$\alpha, n, m = \text{fitting parameters}$$

Statistic test results show that model 4 performs considerably better than models 2 and 3. Model 5 has the poorest performance.

7.1.7 Gardner (1958) Equation – SVENVIRO/GT

Gardner (1958) presented a continuous equation for the first coefficient of permeability function. The form of the equation has subsequently been the basis for the soil-water characteristic curve as well as many other equations proposed in subsequent literature. However, it should be noted that the equation was originally proposed as an equation to best-fit measured permeability data.

$$w_w = w_{rg} + (w_s - w_{rg}) \left[\frac{1}{1 + a_g \psi^{n_g}} \right] \quad [67]$$

where:

$$w_w = \text{gravimetric water content at any soil suction,}$$

$$w_{rg} = \text{residual gravimetric water content,}$$

$$w_s = \text{saturated gravimetric water content,}$$

$$a_g = \text{material parameter which is primarily a function of the air-entry value of the soil in kPa,}$$

$$n_g = \text{material parameter which is primarily a function of the rate of water extraction from the soil once the air entry value has been exceeded, and}$$

$$\psi = \text{soil suction (kPa).}$$

Fitting method: Least squares nonlinear regression
 Required input: Drying laboratory data consisting of points on the curve of gravimetric water content versus soil suction.
 Applicable material types: All soils

7.1.8 Brooks and Corey (1964) Equation – SVENVIRO/GT

Brooks and Corey (1964) proposed a power-law relationship for the SWCC. The model represented an attempt to use an equation to describe the soil-water characteristic curve. The equation can be written as follows:

$$w_w = w_r + (w_s - w_r) \left[\frac{a_c}{\psi} \right]^{n_c} \quad [68]$$

where:

$$w_w = \text{gravimetric water content at any soil suction,}$$

$$w_r = \text{residual gravimetric water content,}$$

$$w_s = \text{saturated gravimetric water content,}$$

$$a_c = \text{bubbling pressure (kPa),}$$

$$n_c = \text{pore size distribution index (dimensionless), and}$$

$$\psi = \text{soil suction (kPa).}$$

Fitting method: Least squares nonlinear regression
 Required input: Drying laboratory data consisting of points on the curve of gravimetric water content versus soil suction.
 Applicable material types: All soils

7.1.9 Zapata Estimation (2000) – SVENVIRO/GT

Zapata (2000) performed a statistical regression analysis on a sampling of soils from 50 states in the USA. The regression led to “average” recommended curves based on categorization groupings as fine or coarse-grained soils. The average values for the SWCCs were further grouped according to plasticity index (PI). This estimation method provides a simple approximate method for the user to enter simple information about the SWCC for a soil and can be best-fit with the Fredlund and Xing (1994) fitting parameters.

7.2 HYDRAULIC CONDUCTIVITY FIT METHODS – SVENVIRO/GT

The SVFLUX software implements Gardner’s equation for fitting unsaturated permeability data.

7.2.1 Gardner’s (1958) Equation – SVENVIRO/GT

Gardner (1958) permeability function for unsaturated soils is expressed as a function of suction:

$$k_w = \frac{k_s}{1 + a \left\{ \frac{\psi}{\rho_w g} \right\}^n} \quad [69]$$

where:

- k_w = hydraulic conductivity or permeability of the water phase,
- k_s = saturated hydraulic conductivity of the water,
- ρ_w = density of water,
- a = fitting parameter,
- n = fitting parameter,
- g = acceleration of gravity, and
- ψ = soil suction (kPa).

Fitting method: Least squares nonlinear regression
 Required input: Laboratory data consisting of at least three points.
 Applicable material types: All soils.

The Gardner (1958) equation provides a flexible permeability function that is defined using two parameters, a and n . The parameter, n defines the slope of the function, and a is a parameter related to the breaking point of the function. The Gardner (1958) equation is meant to be obtained from laboratory data.

Figure 22 shows the sensitivity of the parameters, a and n . The permeability function has been quite often used in saturated-unsaturated flow modeling. The Gardner (1958) equation is sensitive to the air-entry value of the soil and the rate of desaturation. These features are modeled in a continuous manner.

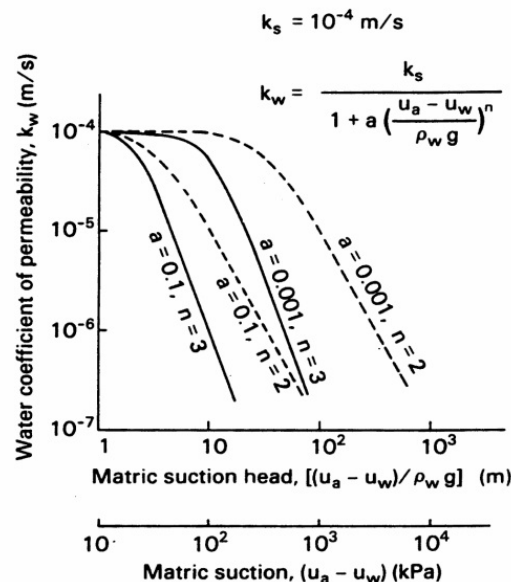


Figure 22 Sensitivity of Gardner's (1958) equation for the coefficient of permeability as a function of the matric suction (from Fredlund and Rahardjo, 1993)

A set of data is presented in Figure 23 to demonstrate the ability of the Gardner (1958) equation to fit laboratory data of the coefficient of permeability for various soils. The equation is easy to apply for saturated-unsaturated flow modeling.

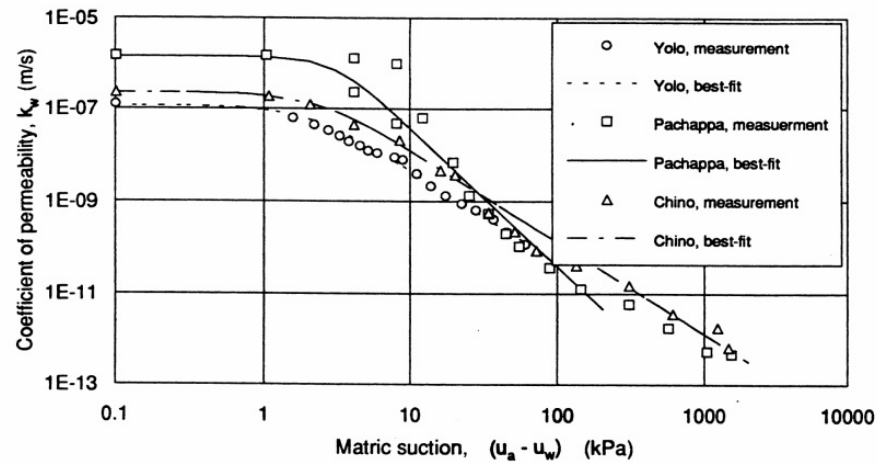


Figure 23 Comparison between the measured and the predicted coefficient of permeability values for different materials using the Gardner (1958) equation (from Huang et al., 1994)

7.3 HYDRAULIC CONDUCTIVITY ESTIMATION – SVENVIRO/GT

Estimation methods (also known as pedo-transfer functions) are provided in the SVFLUX software in order to facilitate the estimation of the unsaturated portion of the hydraulic conductivity curve. Most estimation methods are based on a description of the soil-water characteristic curve and therefore require a specific fit to be present in the software. Commonly used estimation methods are provided in the following sections.

7.3.1 Brooks and Corey Estimation – SVENVIRO/GT

Estimation methods (also known as pedo-transfer functions) are provided in the SVFLUX software in order to facilitate the estimation of the unsaturated portion of the hydraulic conductivity curve. Most estimation methods are based on a description of the soil-water characteristic curve and the saturated coefficient of permeability. Specific fits for the hydraulic conductivity are present in the SVFLUX software. Commonly used estimation methods are provided in the following sections.

$$k = k_{sat} \left(\frac{\psi_b}{\psi} \right)^{2+3\lambda} \quad \text{for suction, } \psi > \psi_b \quad [70]$$

$$k = k_{sat} \quad \text{for suction, } \psi \leq \psi_b$$

where:

- k = hydraulic conductivity (or coefficient of permeability) with respect to the water phase, m/s
- k_{sat} = saturated hydraulic conductivity with respect to the water, m/s
- ψ_b = Brooks and Corey (1964) soil-water characteristic curve fitting parameter,
- λ = Brooks and Corey (1964) soil-water characteristic curve fitting parameter,
- ψ = soil suction, kPa .

Required input: Saturated hydraulic conductivity and a fit of the soil-water characteristic curve using the Brooks and Corey (1964) equation.

Applicable material types: All soils

The Brooks and Corey (1964) equation that fits some soil-water characteristic curve data can be written in the form of a power-law relationship.

$$\Theta = \left(\frac{\psi_b}{\psi} \right)^\lambda \quad \text{for suction, } \psi \geq \psi_b \quad [71]$$

where:

- Θ = normalized water content (defined in Equation [72]),
- ψ_b = air-entry value,
- ψ = any suction, and
- λ = pore-size distribution index.

The normalized volumetric water content, Θ , is defined as follows:

$$\Theta = \frac{\theta - \theta_r}{\theta_s - \theta_r} \quad [72]$$

where:

- θ_s = saturated volumetric water content, and
- θ_r = residual volumetric water content.

Equation [74] is suitable for fitting laboratory SWCC data for coarse materials that have a low air-entry value.

Brooks and Corey (1964) also suggested a procedure for estimating the residual water content. The Brooks and Corey (1964) permeability function is based on the model of a porous media developed by Burdine (1953), Kozeny (1927), and Wyllie and Gardner (1958). The recommended function is shown below:

$$k_w = k_s \quad \text{for } \psi \geq \psi_b \quad [73]$$

$$k_w = k_s \Theta^\delta \quad \text{for } \psi < \psi_b \quad [74]$$

where:

- k_w = coefficient of permeability with respect to the water phase for the soil saturation (i.e., $S = 100\%$),
- δ = empirical constant.

The empirical constant, δ in turn is related to the pore-size distribution index.

The Brooks and Corey (1964) model is simple to use and appears to be quite reasonable for coarse-grained soils such as sands and gravels.

7.3.2 Modified Campbell (1973) Estimation – SVENVIRO/GT

The modified Campbell (1973) equation is implemented into SVFLUX to provide a hydraulic conductivity equation that levels off at high soil suctions. The shape of the function is consistent with theoretical considerations for hydraulic conductivity of an unsaturated soil when water flow transitions to the vapor phase. The point of residual suction can be assumed to be the point at which water movement becomes discontinuous or transitions to vapor flow. The Campbell (1974) equation was modified to produce an equation that tends to level off at approximately the residual suction for the soil. The modified equation as implemented into the SVFLUX software is presented below (Fredlund, 1996).

$$k(\psi) = (k_s - k_{min}) \left[\frac{\ln\left(1 + \frac{\psi}{h_r}\right)}{\ln\left(1 + \frac{10^6}{h_r}\right)} \right] \left[\frac{1}{\ln\left[\exp(1) + \left(\frac{\psi}{a_f}\right)^{n_f}\right]^{m_f}} \right]^p + k_{min} \quad [75]$$

where:

- k = hydraulic conductivity or permeability of the water phase, m/s
- k_s = saturated hydraulic conductivity of the water phase, m/s
- k_{min} = calculated minimum hydraulic conductivity, m/s
- p = parameter used to control the modified Campbell (1973) estimation of hydraulic conductivity,
- a_f = Fredlund and Xing (1994) soil-water characteristic curve fitting parameter,
- n_f = Fredlund and Xing (1994) soil-water characteristic curve fitting parameter,
- m_f = Fredlund and Xing (1994) soil-water characteristic curve fitting parameter,
- h_r = Fredlund and Xing (1994) soil-water characteristic curve fitting parameter, and
- ψ = soil suction.

Required input: Saturated hydraulic conductivity and a fit of the soil-water characteristic curve by the Fredlund and Xing (1994) equation.

Applicable material types: All soils

As a material dries, there is less and less water present in the soil matrix. The hydraulic conductivity then decreases accordingly as the volumetric water content decreases. The modified Campbell equation reflects this behavior by using the following equation.

$$k = k_s \Theta^p(\psi) \quad [76]$$

where:

- k = hydraulic conductivity at any level of suction, m/s
- k_s = saturated hydraulic conductivity, m/s ,
- ψ = soil suction, kPa ,
- Θ = normalized volumetric water content or θ_w/θ_s represented with any equation (i.e., van Genuchten, 1980; Fredlund and Xing, 1994), and
- p = power factor to adjust the prediction (same as in Equation [75]).

A modification was made to Campbell's (1974) equation before it was implemented into the SVFLUX software. The modification adjusts the Campbell equation such that the function flattens once a minimum permeability has been reached.

The hydraulic conductivity remains relatively constant once the water phase in the soil becomes discontinuous. Water flow in the soil is then primarily the result of vapor diffusion through air. The vapor phase flow can be accommodated through use of the Campbell (1974) equation as shown below:

$$k(\psi) = (k_s - k_{\min}) \Theta^P(\psi) + k_{\min} \quad [77]$$

where:

$$k_{\min} = \text{minimum permeability.}$$

The above equation allows the hydraulic conductivity versus soil suction function to level off after a particular soil suction has been reached. Initially, it was suggested that the equation could be set to level off once the residual water content conditions had been reached. However, it was observed for some laboratory data that the permeability function tended to flatten at about one log cycle of suction higher than the suction corresponding to the residual water content.

The method proposed by Campbell (1973) is implemented into SVFLUX. The implemented algorithm uses the soil-water characteristic curve and the saturated hydraulic conductivity to estimate the hydraulic conductivity of a soil at all levels of suction.

7.3.3 Fredlund, Xing and Huang (1994) Estimation – SVENVIRO/GT

Fredlund et al., (1994) presented a modification of the Mualem (1976) integration method for estimating the hydraulic conductivity of a material as a function of soil suction. The integration procedure is complex and a closed-form solution is not available. SVFLUX performs the integration and computes a series of data points that can be written onto a graph as x-y data.

Solution method:	Integration by Simpsons rule
Required input:	Saturated hydraulic conductivity and Fredlund and Xing (1994) fit of soil-water characteristic curve
Applicable material types:	All soils

Equations available in the literature for predicting the coefficient of permeability use the soil-water characteristic curve data only for a limited range of suction values (e.g., Brooks and Corey, 1964; Mualem, 1976; van Genuchten, 1980). These equations require knowledge of the residual water content. The residual water content θ_r is the water content below which a large increase in suction is required to remove additional water. Kunze et al., (1968) investigated the effect of using a partial soil-water characteristic curve for the prediction of coefficient of permeability and concluded that the accuracy of prediction significantly improved when the complete soil-water characteristic curve was used.

Fredlund et al., (1994) proposed an equation to estimate the coefficient of permeability of a soil over an extended range of soil suction values. The estimation procedure makes use of the soil-water characteristic curve data for the entire suction range of 0 to 1,000,000 kPa. This equation tends to be more practical for the estimation of the coefficient of permeability over a large range of suction values. The coefficient of permeability function is of interest at large suction values particularly for structures such as soil covers, as well as other near-ground-surface structures.

The equation suggested by Fredlund et al., (1994) for predicting the coefficient of permeability is given below:

$$k_r(\psi) = \frac{\int_{\ln(\psi)}^b \frac{\theta(e^y) - \theta(\psi)}{e^y} \theta'(e^y) dy}{\int_{\ln(\psi_{aev})}^b \frac{\theta(e^y) - \theta(\psi_{aev})}{e^y} \theta'(e^y) dy} \quad [78]$$

where:

b	= $\ln(1,000,000)$,
y	= dummy variable of integration representing the logarithm of suction, and
ψ	= soil suction, given a function of volumetric water content, and
ψ_{aev}	= air entry value of the soil under consideration.

The Fredlund et al., (1994) permeability equation makes use of the Fredlund and Xing (1994) equation (i.e., equation for fitting the soil-water characteristic curve data for the entire range of suctions). The Fredlund and Xing (1994) equation has been found to fit the soil-water characteristic data for essentially all type of soils and over all suction ranges (Benson et al., 1997; Leong and Rahardjo, 1997). More details are available in Fredlund et al., (1994).

7.3.4 Van Genuchten (1980) and Mualem (1976) Estimation – SVENVIRO/GT

The equation for calculating the permeability function by the van Genuchten (1980) and Mualem (1976) estimation method is based on Equation [65]. The van Genuchten and Mualem SWCC fitting equation is as follows.

$$k(\psi) = k_s \left[\frac{\left\{ 1 - (a\psi)^n \left(1 + (a\psi)^n \right)^{-\left(\frac{1}{n}\right)} \right\}^2}{\left[1 + (a\psi)^n \right]^{\left(\frac{1}{n}\right)/2}} \right] \quad [79]$$

where:

- k = hydraulic conductivity or permeability of the water phase, m/s ,
- k_s = saturated hydraulic conductivity of the water phase, m/s ,
- a = van Genuchten and Mualem soil-water characteristic curve fitting parameter,
- n = van Genuchten and Mualem soil-water characteristic curve fitting parameter, and
- ψ = soil suction, kPa .

Required input: Saturated hydraulic conductivity and van Genuchten and Mualem fit of the soil-water characteristic curve

Applicable material types: All soils

7.3.5 Van Genuchten (1980) Estimation – SVENVIRO/GT

Several investigators such as Brooks and Corey (1964) and Mualem (1976) have proposed closed-form equations for estimating the coefficient of permeability of unsaturated soils based on Burdine's theory (1953). Brooks and Corey (1964) equation may not converge rapidly when used in numerical simulations of seepage in saturated-unsaturated soils. The Mualem (1976) equation is in an integral form. However, it is possible to derive a closed-form analytical equation provided there is a fixed relationship between two of the fitting parameters.

The equation proposed for fitting the soil-water characteristic curve by *van Genuchten (1980)* is flexible, continuous and has a continuous slope. The closed-form equation proposed for estimating the coefficient of permeability function has been extensively used for saturated-unsaturated soils flow modeling.

$$k(\psi) = k_s \left[\frac{\left\{ 1 - (a\psi)^m \left[1 + (a\psi)^n \right]^{-m} \right\}^2}{\left[1 + (a\psi)^n \right]^{m/2}} \right] \quad [80]$$

where:

- k = hydraulic conductivity or permeability of the water phase, m/s ,
- k_s = saturated hydraulic conductivity of the water phase, m/s ,
- a = van Genuchten soil-water characteristic curve fitting parameter, kPa ,
- n = van Genuchten soil-water characteristic curve fitting parameter,
- m = van Genuchten soil-water characteristic curve fitting parameter, and
- ψ = soil suction, kPa .

Required input: Saturated hydraulic conductivity and van Genuchten fit of the soil-water characteristic curve

Applicable material types: All soils

The van-Genuchten's equation (1980) for fitting the soil-water characteristic curve data is given below:

$$\theta = \theta_r + \frac{(\theta_s - \theta_r)}{\left[1 + (a\psi^n) \right]^m} \quad [81]$$

where:

- θ = volumetric water content,
- θ_s = saturated volumetric water content,
- θ_r = residual volumetric water content, and
- a, n, m = material constants.

van Genuchten (1980) suggests the use of 1,500 kPa to represent residual conditions for a soil. For many soils, a volumetric water content corresponding to a residual suction of 1,500 kPa is a reasonable approximation. An analytical procedure has also been suggested for estimating the residual water content.

Figure 24 provides the comparison between the predicted and measured values of the soil-water characteristic curve along the drying and wetting paths with respect to suction for Guelph loam (van Genuchten, 1980). Also shown is the variation in the coefficient of permeability. The equations proposed by van Genuchten (1980) provide excellent fits for many soil types.

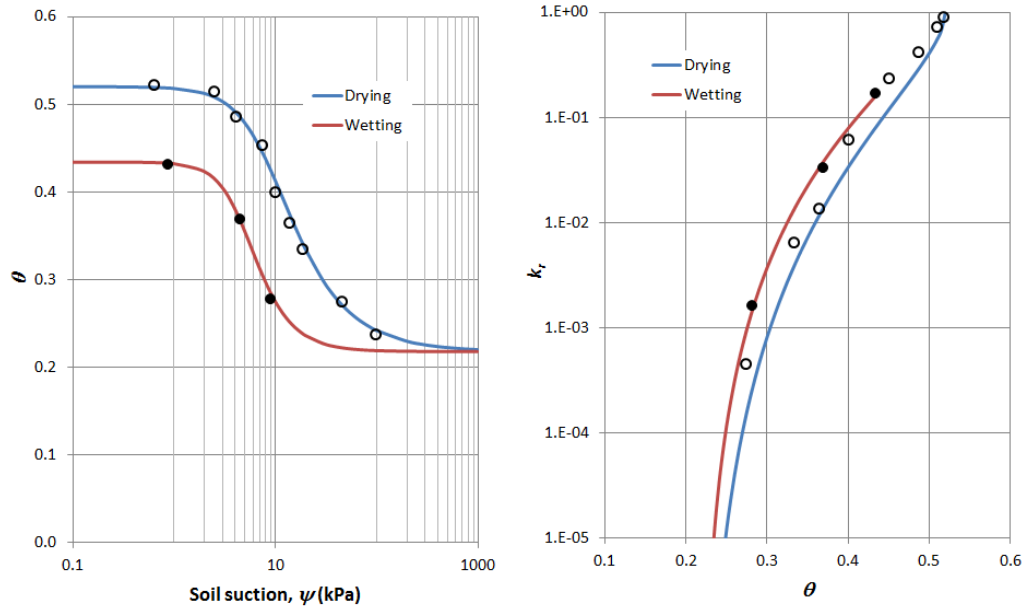


Figure 24 Comparison between the predicted (continuous solid lines) and measured values (circles) of the soil-water characteristic curve along drying and wetting paths and the variation of coefficient of permeability with respect to suction (from van Genuchten, 1980)

7.3.6 Leong and Rahardjo (1997) Estimation – SVENVIRO/GT

Leong and Rahardjo (1997) proposed a permeability function for predicting the unsaturated coefficient of permeability. The estimation is based on a fit of the soil-water characteristic curve with the Fredlund and Xing (1994) equation. The equation for estimation of the unsaturated soil permeability function can be written as follows:

$$k(\psi) = k_s \left[\frac{1}{\left[\ln \left[\exp(1) + \left(\frac{\psi}{a_f} \right)^{n_f} \right] \right]^{m_f}} \right]^p \quad [82]$$

where:

- k = hydraulic conductivity or permeability of the water phase, m/s ,
- k_s = saturated hydraulic conductivity of the water, m/s ,
- p = parameter used to control the Leong and Rahardjo (1997) estimation of hydraulic conductivity,
- a_f = Fredlund and Xing (1994) soil-water characteristic curve fitting parameter, kPa ,
- n_f = Fredlund and Xing (1994) soil-water characteristic curve fitting parameter,
- m_f = Fredlund and Xing (1994) soil-water characteristic curve fitting parameter,
- ψ = soil suction, kPa .

In Leong and Rahardjo (1997), the best fitted permeability function was used when comparing the predicted and measured coefficient of permeability for several soil types. The results were tested for both the wetting and drying curves. A good fit was obtained for a wide range of experimental data. It was found that if the exponent p was known for a given soil, the coefficient of permeability could be obtained indirectly from the soil-water characteristic curve. Otherwise, p needed to be determined using a curve fitting process with permeability data. The value of p varied from 4.3 to 52.1 for the soils studied.

8 SOIL ATMOSPHERE MODELING - SVENVIRO

Soil-atmosphere moisture fluxes can be modeled in SVFLUX by using "Climate boundary conditions". Soil-atmosphere moisture fluxes are influenced by the following types of processes:

- Infiltration fluxes – SVENVIRO,
- Runoff – SVENVIRO,
- Snow accumulation and melt – SVENVIRO,
- Evaporative fluxes – SVENVIRO, and
- Transpiration fluxes – SVENVIRO.

Moisture infiltration and runoff can be modeled by considering the amount of precipitation and the infiltration capacity of the soil. The infiltration capacity is determined by applying a modified version of the "Review boundary condition".

In cold regions, precipitation accumulates as snow cover during the winter period and subsequently melts during spring period. Melted snow may infiltrate into the ground in a slow manner because the underlying ground is still frozen and its hydraulic conductivity is low. Considerable runoff will occur during the spring period.

Evaporative fluxes are modeled by using an appropriate negative flow boundary condition and by considering moisture movement through vapor flow. Consideration of vapor flow becomes important when modeling soil-atmosphere fluxes. Liquid flow alone cannot represent the entire moisture migration associated with evaporation at the soil surface. Eventually there will essentially be a shut-off of both liquid and vapor moisture movement near the ground surface. The vapor flux component theory has been presented in the previous chapters.

Transpiration fluxes are simulated by taking into account the water uptake characteristics of the existing vegetation and applying negative fluxes at the near-surface soil. Again, vapor fluxes need to be considered when modeling transpiration fluxes. The following section presents a detailed description of the theory of soil-atmosphere modeling.

8.1 ATMOSPHERIC FLUX BALANCE - SVENVIRO

There is an atmospheric moisture flux balance and a thermal flux balance that must be satisfied at the ground surface when calculating *Actual Evaporation, AE*. Basically, water falling on the ground surface either infiltrates the soil (or runs off) or else rises to the sky through the process called "*Actual Evaporation, AE*". The ground surface moisture and thermal flux equation can be written as follows.

$$P = AE + NP + R_{off} \quad [83]$$

$$Q_n = Q_h + Q_l + Q_g \quad [84]$$

where:

P	= precipitation, $m^3/m^2/day$, or m/day
AE	= actual evaporation from ground surface, $m^3/m^2/day$ or m/day
NP	= net Percolation or infiltration, $m^3/m^2/day$ or m/day
R_{off}	= runoff, $m^3/m^2/day$ or m/day
Q_n	= net radiation, $kJ/m^2/day$, or equivalently converted into m/day ,
Q_h	= sensible heat transferring from ground surface to air, $kJ/m^2/day$, or equivalently converted into m/day ,
Q_l	= latent heat associated with the water phase change including evaporation or freezing, $kJ/m^2/day$, or equivalently converted into m/day , and
Q_g	= ground heat flux, $kJ/m^2/day$, or equivalently converted into m/day .

Precipitation information can be obtained from weather station records and is usually provided on a daily basis. Preferably precipitation data should be collected on an hourly basis when modeling near-ground-surface phenomena. The mechanics of net infiltration, NP , can be described by Darcy law. Net radiation, Q_n , can also be obtained from weather station records or it can be approximated using an equation suggested by Penman in (1948). The latent heat component, Q_l , can be estimated using actual evaporation, AE , or the formation of ice near the ground surface during freezing. The sensible heat component, Q_h , reflected from the ground surface to the air is described as follows (Penman, 1948; Gray, 1970; Wilson 1990):

$$Q_h = C_f \eta f(u)(T_s - T_a) \quad [85]$$

where:

Q_h	= sensible heat, m/day ,
-------	----------------------------

C_f	= conversion factor, (i.e., 1 $kPa = 0.0075 \text{ mHg}$),
η	= psychometric constant, $0.06733 \text{ kPa}/^\circ\text{C}$ at 20°C ,
$f(u)$	= function depending on wind speed, $f(u) = 0.35(1 + 0.146 W_w)$, and
W_w	= wind speed, km/hr .

Actual Evaporation, AE , is difficult to measure directly but can be calculated from fundamental thermodynamic considerations.

Equations [83] and [84] are fundamental to describing the coupling of moisture and heat flow processes. Actual evaporation, AE , depends on the water content and temperature of the soil at ground surface. In addition, the rate of evaporation also depends on the air temperature and air relative humidity. The air temperature and soil temperature at the ground surface are generally not the same but are inter-related through net radiation, Q_n , latent heat, Q_l , and sensible heat, Q_h . The available surface water is controlled by total precipitation, actual evaporation, and runoff. These variables play an important role in partitioning convective heat flux into sensible heat and latent heat (Wetzel and Boone, 1995).

8.2 INFILTRATION AND RUNOFF WITHOUT CONSIDERATION OF EVAPORATION - SVENVIRO

Infiltration, evaporation and runoff are determined simultaneously. If the moisture evaporation can be neglected, the moisture flux balance at the soil surface is rewritten:

$$P = NP + R_{off} \quad [86]$$

The amount of precipitation and the hydraulic properties of the soil are the main variables required when calculating net infiltration. Runoff is computed in an iterative manner and the amount of infiltration can be determined by consideration of previous conditions.

Normal flux boundary conditions in SVFLUX can be set to include the effects of runoff.

Depending on the amount of moisture flux applied to the uppermost boundary, the pore-water pressure, u_w , may tend to become higher than zero. The higher the influx, the higher the pore-water pressure, u_w becomes. If u_w becomes higher than zero, a condition occurs that corresponds to ponding.

However, if the ground surface is assumed to be well-drained with no ponding, a mechanism must be implemented in order to limit the amount of infiltration to a lowest possible value. The low value would keep the u_w value at the surface equal to zero. One common way of applying this limiting condition is to switch the boundary condition to an essential boundary condition equal to zero. This would occur when the pore-water pressure, u_w , becomes equal to zero. Another option, implemented in SVFLUX, switches the boundary condition to a different natural boundary condition that is equivalent to the essential boundary condition (Gitirana Jr., 2004).

The natural boundary condition is similar to the "Review Boundary Condition" presented in the previous chapter.

The ponding height for a model is by default set to zero. This means that when water is applied to the boundary of a model, the maximum pore-water pressure will be restricted to a maximum of 0 kPa. Any additional water applied which causes the upper boundary to exceed 0 kPa and will be re-classified as runoff. If a value greater than zero is specified for ponding then the maximum pressure allowed at the ground surface is increased to the pond height times γ_w . Runoff conditions will not occur until the increased maximum pressure is encountered.

The calculation of runoff adds significant complexity to the calculations in a numerical model. It is possible that adding a runoff calculation might double or triple computational times. A simple model should be set up and solved prior to the addition of a model implementing a runoff calculation.

8.2.1 Estimated Runoff Correction – SVENVIRO

This runoff correction option uses the equation presented by Gitirana (Gitirana Jr., 2004):

$$\text{Natural BC} = \begin{cases} \text{if } u_{ws} \geq 0 \text{ then } FAC \times \sqrt{k_{wx}^2 + k_{wy}^2} \times (pond \times \gamma_w - u_{ws}) \\ \text{if } u_{ws} < 0 \text{ then } n_p \cos \alpha \end{cases} \quad [87]$$

where:

u_{ws}	= pore-water pressure at the surface, kPa
k_{wx}, k_{wy}	= hydraulic conductivities in the x and y directions,
γ_w	= unit weight of water,
FAC	= a large number, usually from 10 to 100,

- $pond$ = the height of the pond, being 0 if no pond is allowed,
 n_p = is the net precipitation available at the ground surface, and
 α = slope of the ground surface with the horizontal direction.

When the number FACTOR, or FAC becomes large, this natural boundary condition is closer to the equivalent essential boundary condition. The reasoning behind the equivalent boundary condition comes from the fact that an essential boundary condition is equivalent to an extremely large natural boundary condition flux driving the value of pore-water pressure, u_w , at the boundary to the desired value. This occurs nearly instantaneously. Once this calculation is performed, the amount of runoff can be obtained by subtracting the amount of infiltration from the net precipitation available.

8.2.2 Pressure Head Calculated Runoff Correction – SVENVIRO

This runoff correction option is similar to the equation presented by Gitirana (Gitirana Jr., 2004), but uses the pressure head variable instead of the hydraulic conductivities and the FAC. This equation, developed by SoilVision Systems Ltd., is able to achieve the same goal as the Estimated Runoff Correction option, while offering increased stability. It also removes the need for a user-defined FACTOR input.

$$\text{Natural BC} = \begin{cases} \text{if } u_{ws} \geq 0 \text{ then } (pond - h_{ps}) \\ \text{if } u_{ws} < 0 \text{ then } n_p \cos \alpha \end{cases} \quad [88]$$

where:

- u_{ws} = pore-water pressure at the surface, kPa ,
 h_{ps} = pressure head at the surface, m ,
 $pond$ = the height of the pond, being 0 if no pond is allowed,
 n_p = is the net precipitation available at the ground surface, and
 α = slope of the ground surface with the horizontal direction.

This is the recommended runoff correction option in SVFLUX.

8.2.3 Gradient Calculated Runoff Correction – SVENVIRO

This runoff correction option, developed by SoilVision Systems Ltd. uses a similar technique to the Estimated and Pressure Head Calculated correction options. This option offers some numerical stability improvements over the Estimate method, but not as much as the Pressure Head Calculated option. It also removes the need for a user-defined FACTOR input in favor of a depth entry parameter.

$$\text{Natural BC} = \begin{cases} \text{if } u_{ws} \geq 0 \text{ then } \frac{(k_{ys} + k_{yd})}{2} \frac{(h_d - y_s + pond)}{d} \\ \text{if } u_{ws} < 0 \text{ then } n_p \cos \alpha \end{cases} \quad [89]$$

where:

- u_{ws} = pore-water pressure at the surface, kPa ,
 k_{ys} = vertical hydraulic conductivity at the ground surface, m/s ,
 k_{yd} = vertical hydraulic conductivity at the gradient depth below the ground surface, m/s ,
 h_d = head at the gradient depth below the ground surface, m ,
 y_d = ground surface elevation, m ,
 d = gradient depth,
 $pond$ = the height of the pond, being 0 if no pond is allowed,
 n_p = is the net precipitation available at the ground surface, and
 α = slope of the ground surface with the horizontal direction.

This option is only available in a vertical 1D model.

8.3 SNOW ACCUMULATION AND MELT - SVENVIRO

In SVFLUX SVENVIRO, the snow is modeled as a virtual layer over the applied boundary, as illustrated in Figure 25. During the winter time, the precipitation event is accumulated as a snow cover in a virtual layer above the upper boundary at which the climate boundary is applied. Snow cover is accumulated due to new snow falling or the redistribution of old snow with wind, and it can be considered as a water reservoir in winter until melting occurs in the spring.

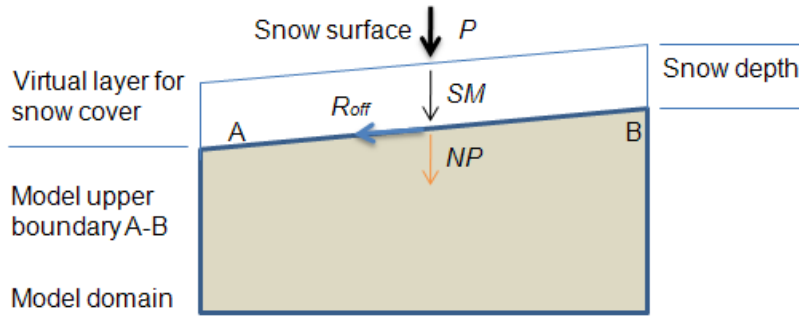


Figure 25 Virtual layer of snow cover for the applied boundary A-B

The amount of water stored in the snowpack is evaluated in tem of *snow water equivalent* (S_{WE}) in SVFLUX. Without consideration of snow redistribution with wind, the change rate of S_{WE} at the applied ground surface is described with the following equation:

$$\left. \frac{\partial(S_{WE})}{\partial t} \right|_{surface} = S_P - S_M \quad [90]$$

where:

- S_{WE} = snow water equivalent at the applied ground surface, m ,
- S_P = snow precipitation rate at the applied ground surface, m/day , and
- S_M = snow melt rate at the applied ground surface, m/day .

Please note that Equation [90] is associated with a specific ground surface that is applied at the model boundary as a boundary condition. This is because the snowmelt may experience different behaviors depending on different types of ground surfaces. For example, the snowmelt rate is larger for a bare and sunny ground surface than for a shady ground surface.

Snow precipitation is determined according to the amount of precipitation and air temperature that are recorded at the weather station. When the air temperature is greater than a threshold, T_{rmin} , the precipitation event is considered as rainfall; when the air temperature is below the freezing point of ice, T_{smax} , the precipitation is regarded as snowfall. The mixture of snow and rain happens if the air temperature is within the range from T_{smax} to T_{rmin} . The following equation is used for the partition of snow precipitation based on the precipitation event and air temperature record (Gustafsson et al., 2001):

$$S_P = Q_P P \quad [91]$$

$$Q_P = \begin{cases} 0 & \text{if } T_a > T_{rmin} \\ 1 - \theta_{smax} + \theta_{smax} \frac{T_a - T_{rmin}}{T_{smax} - T_{rmin}} & \text{if } T_{smax} \leq T \leq T_{rmin} \\ 1 & \text{if } T_a < T_{smax} \end{cases} \quad [92]$$

where:

- P = precipitation, m/day ,
- Q_P = thermal quality, changing from 0 to 1,
- T_a = air temperature, $^{\circ}C$,
- T_{rmin} = minimum temperature of rain, by default $T_{rmin} = 2^{\circ}C$,
- T_{smax} = maximum temperature of snow, by default $T_{smax} = 0^{\circ}C$, and
- θ_{smax} = maximum volumetric water content of snow, m^3/m^3 .

Two approaches are commonly used to estimate the rate of snow melt; namely, i) degree-day-factor and ii) energy balance. SVFLUX has implemented the degree-day-factor method.

8.3.1 Temperature-index based snow melt – SVENVIRO

Snow starts to melt when air temperature is above the snow melting temperature. The temperature-index based Equation [93] is utilized to estimate the water equivalent of snow melt:

$$S_M = \max\left(0, f_m (T_a - T_{smax})\right) \quad [93]$$

where:

f_m = melting factor, $m/day-^{\circ}C$, and
 T_{smax} = snow melting temperature, $^{\circ}C$.

Please note that the tem of snow melting temperature or snow freezing point have the same meaning; however, the terms are used in different contexts.

The snow melting factor is an empirical parameter. It varies with ground surface types and time. The mean value of melting factor $f_m = 0.00242 \text{ m/day-}^{\circ}C$ is used for forest area, and $f_m = 0.00351 \text{ m/day-}^{\circ}C$ is for open ground (Kuusisto, 1980).

To consider the melt factor changing with time seasonally, the value of f_m can be expressed with the sine function. Figure 26 is an example showing the snow melting factor changing with time.

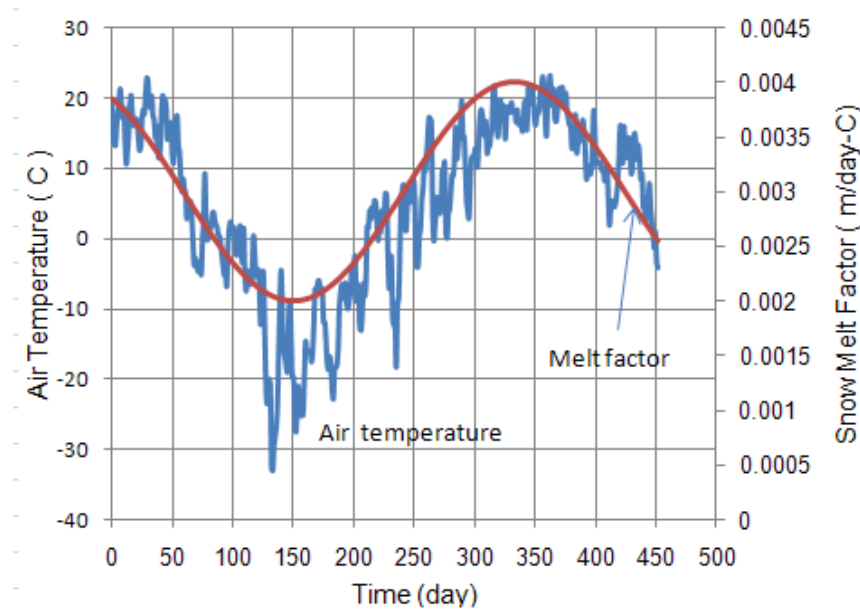


Figure 26 Snow melting factor and air temperature

8.3.2 Snow depth – SVENVIRO

The snow depth, snow water equivalent, and snow density are interrelated by the following equation:

$$D_{sn} = \frac{\rho_w}{\rho_{sn}} S_{WE} \quad [94]$$

where:

D_{sn} = snow depth, m ,
 ρ_{sn} = snow density, kg/m^3 ,
 ρ_w = water density, kg/m^3 , and
 S_{WE} = snow water equivalent height (see Equation [90]), m .

The snow density largely depends on the age of snow and overburden pressure. The density for new snow is mainly related to the air temperature:

8.3.2.1 New snow density – Anderson approach (1976)

Anderson (1976) used the following expression to estimate the density for new snow:

$$\rho_{newsn} = \begin{cases} \rho_{smin} + 1.7(T_{rmin} + 15)^{1.5} & \text{if } T_a > T_{rmin} \text{ } ^\circ C \\ \rho_{smin} + 1.7(T_a + 15)^{1.5} & \text{if } T_a > -15 \text{ } ^\circ C \\ 0 & \text{if } T_a \leq -15 \text{ } ^\circ C \end{cases} \quad [95]$$

where:

ρ_{smin} = minimum snow density, 50 kg/m^3 .

8.3.2.2 Density varying with the age of old snow

The snow density increases with the age of snow due to the action of snow compaction, but the maximum snow density is usually less than the value of 500 kg/m^3 . Figure 27 illustrates the various snow densities at different time and locations. According to the data as shown in Figure 27, the average of snow density is about 300 kg/m^3 .

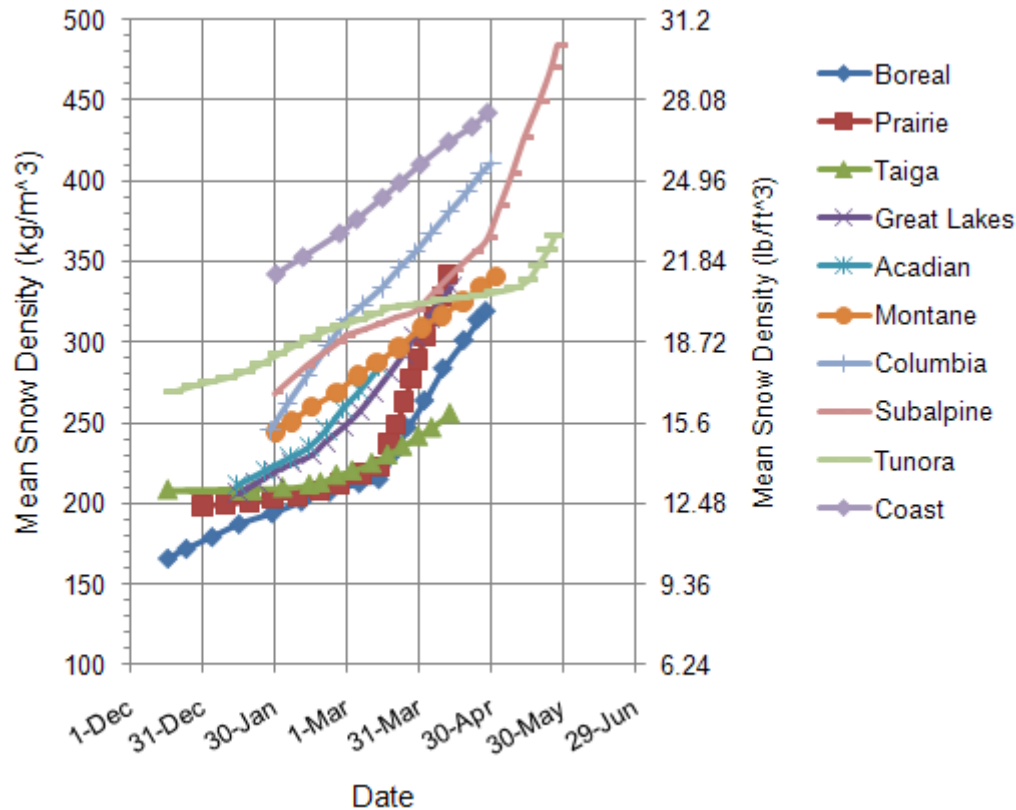


Figure 27 Snow density varying with time and location (from Hwang, 1976)

8.3.3 Infiltration boundary condition with snow cover

In the case without consideration of evaporation, the net percolation at the applied upper boundary condition (see Figure 25) can be generally expressed as

$$NP = P - S_P + S_M + R_{off} \quad [96]$$

where:

NP = net percolation at the upper boundary, m/day ,
 P = precipitation, m/day ,
 S_P = snow precipitation, m/day ,
 S_M = snow melt rate, m/day , and
 R_{off} = runoff, m/day .

During winter time, $S_P = P$, and $S_M = 0$, $R_{off} = 0$, and $NP = 0$. This implies that the precipitation event is stored as snow cover. During the early spring, when snow starts to melt, $S_P = 0$. The soil ground surface is still in the frozen state and the rainfall or melted snow barely infiltrates the ground, (i.e., $NP = 0$). Consequently, $R_{off} = P + S_M$, which means that the precipitation event and the melted snow runoff.

8.4 EVAPORATION - SVENVIRO

The effects of evaporation on a soil near the ground surface depend on the vapor pressure gradient between the soil surface and the atmosphere. Atmospheric coupling is achieved in SVFLUX in the form of an evaporative flux boundary condition. SVFLUX provides a number of methods for defining the evaporative flux in terms of potential evaporation (PE) or actual evaporation (AE).

When an evaporative boundary condition is being considered in SVFLUX, the governing equations must include vapor pressure gradients.

8.4.1 Potential Evaporation – SVENVIRO

Potential evaporation, PE , is the amount of evaporation that would occur from a saturated soil surface. The potential evaporation can be entered in SVFLUX: i.) as time data, ii.) as a constant, iii.) as an equation, or iv.) it can be calculated using a modified Penman formulation (Gitirana, 2005).

- **Penman (1948)**

The original Penman method is used for the calculation of potential evaporation (PE). The Penman method is one method available in SVFLUX which can be used to calculate potential evaporation.

The potential evaporation at a material-atmosphere boundary can be calculated using the following formulation (Penman, 1948):

$$PE = \frac{\Gamma Q_n + \eta E_a}{\Gamma + \eta} \quad [97]$$

where:

PE	= potential evaporation, m/day ,
E_a	= flux associated with "mixing"; $f(u) C_f u_{vo}^{air} (1 - h_r)$, m/day ,
$f(u)$	= $0.35 (1. + 0.146 W_w)$,
W_w	wind speed, km/hr ,
C_f	conversion factor, (i.e., $1 \text{ kPa} = 0.00750 \text{ mHg}$),
h_r	= relative humidity in the air above the ground (i.e., $h_r = u_v^{air}/u_{vo}^{air}$), obtained from weather station record,
u_v^{air}	= water vapor pressure in the air above ground surface, kPa ,
u_{vo}^{air}	= saturated vapor pressure at the mean air temperature, kPa ,
Γ	= slope of saturation vapor pressure versus temperature curve, $kPa/^{\circ}C$,
Q_n	= net radiation at the water surface, m/day ,
η	= psychrometric constant, $(kPa/^{\circ}C)$, $\eta = 0.06733 \text{ kPa}/^{\circ}C$.

The u_v^{air} , u_{vo}^{air} and Γ can be calculated from temperature as proposed by Lowe (1977).

The net radiation can be calculated (as suggested by Penman) in the following manner:

$$Q_n = (1-r)R_c - \sigma(273.5 + T_a)^4 \left(0.56 - 0.92 \left(p_{vsat}^{air} \right)^{0.5} \right) (0.10 + 0.90n/N) \quad [98]$$

where:

Q_n	= net radiation, m/day ,
r	= reflection coefficient,
R_c	= $0.95 R_a(0.18 + 0.55n/N)$ = shortwave radiation, m/day ,
0.95	= coefficient suggested by Penman for evaporation from a wet and bare soil as compared to evaporation from an open water surface,
R_a	= solar radiation, $MJ/m^2/day$,
σ	= Stefan Boltzman's constant, $W/m^2/K^4$,
T_a	= air temperature, $^{\circ}C$,
p_{vsat}^{air}	= vapor pressure of the air above the surface, $mmHg$, and
n/N	= sunshine ratio (actual/possible hours of bright sunshine).

Note: The vapor pressure, p_{vsat}^{air} in Equation [98] must be in $mmHg$.

In addition to the above equation suggested by Penman (1948), the net radiation data can be measured in the field, and is a typical weather station reading. The net radiation is usually measured in units of $MJ/day-m^2$. Entry of the measured net radiation in SVFLUX is also in units of $MJ/day-m^2$. SVFLUX will automatically convert the net radiation from units of $MJ/day-m^2$ into the units of m/day used in the evaporation calculations in the following expression:

$$Q_n = 10^6 Q_{mn} / (L_v) \quad [99]$$

where:

$$\begin{aligned} Q_{mn} &= \text{measured net radiation, } MJ/day-m^2, \\ L_v &= \text{latent heat of evaporation, } L_v = 4.187 \times 10^6 (591 - 0.51T_a), \text{ } J/m^2. \end{aligned}$$

8.4.2 Actual Evaporation – SVENVIRO

Actual Evaporation, AE , is difficult to measure directly but it can be calculated from fundamental thermodynamic considerations. There are several procedures that have emerged for the calculation of the actual evaporative flux. However, there have been few studies that assess the relationship between each of the suggested solution procedures. As well, the reliability of the proposed procedures seems to not have been completely verified.

In 1994 Wilson proposed a modification to the well-known Penman (1948) equation for the calculation of Potential Evaporation, PE . The modified equation has become known as the Wilson-Penman (1994) equation. The Wilson-Penman equation took into consideration the difference in temperature and relative humidity (and therefore vapor pressure) between the soil surface and the overlying air. The difference in conditions between the air and the water at ground surface has formed the basis for the Soil-Atmospheric Model which was subsequently implemented into the *SoilCover*, version 1.0, computer code (1994).

In 1997 a “Limiting Function” type relationship was proposed by Wilson, Fredlund and Barbour. The “Limiting Function” related Actual Evaporation and Potential Evaporation by scaling the vapor pressures associated with the relative humidity at ground surface and the relative humidity in the air above ground surface. Inherent in the derivation was the assumption that the air and soil temperatures were the same.

Wilson (1994) also presented experimental results that showed a unique relationship between total suction at any soil surface and the ratio of Actual Evaporation to Potential Evaporation, AE/PE . Wilson et al., (1997) presented a unique equation that passed through the experimental data. As a consequence, there was now another way to empirically relate Actual Evaporation and Potential Evaporation fluxes.

The above-mentioned relationships give rise to different possibilities for the calculation of Actual Evaporation from the ground surface. The major difference in the methodologies is related to the assumption regarding the air and soil temperatures. For example, the soil temperature can be assumed to be equal to the air temperature. This is known to not be the case but there does not appear to have been a thorough study performed that quantifies the magnitude of the error in calculating AE based on this assumption.

The **Case 1 Solution** presented below for Actual Evaporation considers the isothermal case (i.e., no ground thermal flux, $Q_g = 0$). This assumption greatly simplifies the solution for AE since all temperature values are taken as equal to the air temperature recorded above ground surface. The “Limiting Function” proposed by Wilson et al., (1997) was used to relate Actual Evaporation and Potential Evaporation. The procedure for solving this case is referred to as the **Case 1 Solution**.

The second solution procedure considered for calculating Actual Evaporative, AE , utilizes the Wilson-Penman (1994) equation for SVFLUX model case where ground thermal flux, Q_g , is equal to zero beneath the soil surface. *However, the soil temperature at ground surface can be different from the air temperature above ground surface.* The solution procedure is referred to as the **Case 2 Solution**.

The third solution procedure is quite similar to the **Case 1 Solution**, except that the Actual Evaporative, AE , is approximated using an empirical expression that is best-fit with Wilson’s 1994 experimental results. This solution procedure is referred to as the **Case 3 Solution**.

The fourth solution procedure for calculating Actual Evaporative, AE , utilizes the Wilson-Penman (1994) equation based on the coupled SVFLUX and SVHEAT model. In other words, there is a ground thermal flux beneath soil surface. This calculation procedure involves a full coupling of heat and moisture flow and is referred to as the *Soil-Atmospheric Model*. This solution procedure is referred to as the **Case 4 Solution**. This is the most rigorous solution procedure proposed to-date.

The fifth solution procedure utilizes the “Limiting Function” proposed by Wilson et al., (1997) for the calculation of Actual Evaporation while giving consideration to moisture flow and heat flow in a coupled mode. The solution procedure is referred to as the **Case 5 Solution**.

The sixth solution procedure is quite similar to the Case 5 Solution except that the empirical relationship of Actual Evaporation to Potential Evaporation is used when analyzing moisture flow and heat flow in a coupled manner. The solution procedure is referred to as the **Case 6 Solution**. This procedure allows the relative humidity of the air to be taken into consideration when calculating Actual Evaporation, AE .

Not all of the above-mentioned six solution procedures are presently implemented into SVFLUX or the coupled version of SVFLUX and SVHEAT. A flowchart showing the layout of all six possible solution procedures is shown in Figure 28. The

following sections explain the details related to each of the solution procedures. Note that Case 4, Case 5, and Case 6 are not available in SVFLUX GT.

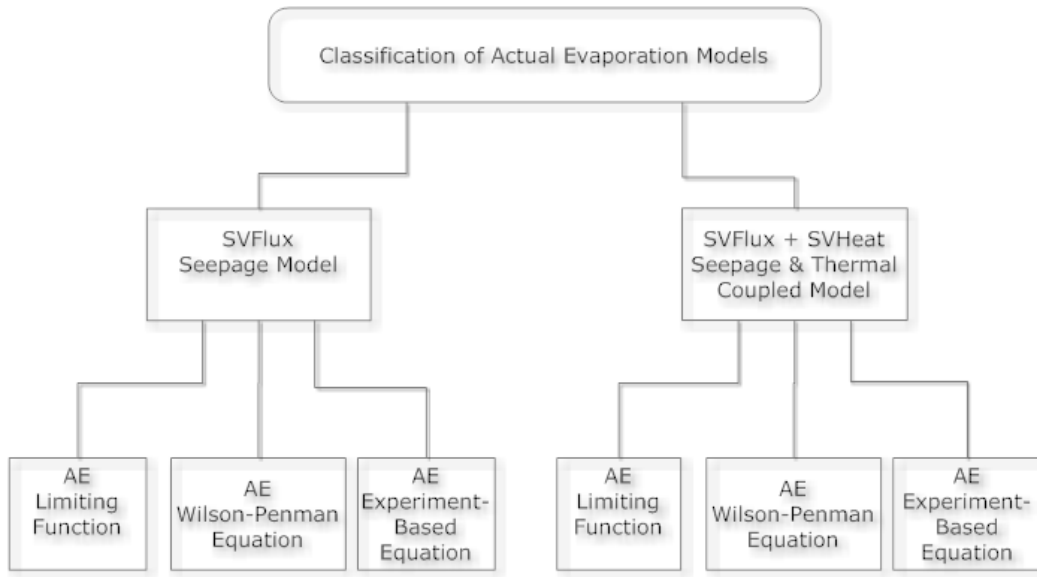


Figure 28 Classification of actual evaporation, AE, models

8.4.3 Case 1 Solution: “Limiting-Function” for AE/PE SVFLUX Model – SVENVIRO

The following assumptions are made in the isothermal, “*Limiting-Function*” SVFLUX model.

- There can be liquid and vapor flow through the soil, (i.e., liquid and vapor flow is in response to a hydraulic head gradient and a vapor pressure gradient, respectively).
- The soil temperature in the entire domain is assumed to be the same, and equal to the air temperature above the soil surface. (i.e., ground thermal flux is neglected, $Q_g = 0$).
- The ground surface temperature is assumed to be equal to the air temperature.
- Actual evaporation is calculated using the “Limiting Function” proposed by Wilson et al., (1997).

8.4.3.1 Mass Flow Governing Equation

Moisture flow in one-dimension beneath the soil surface is described using the following partial differential equation,

$$\frac{\partial}{\partial y} \left[(k_{wy} + k_{vh}) \frac{\partial h}{\partial y} - k_{vh} \right] = -\gamma_w m_2^w \frac{\partial h}{\partial t} \quad [100]$$

$$k_{vh} = \frac{\beta \theta_a g D_v \omega_v \rho_{sv0} h_r}{\rho_w R (273.15 + T)} \quad [101]$$

$$D_v = 2.29 \times 10^{-5} \left(1 + \frac{T}{273.15} \right)^{1.75} \quad [102]$$

$$\beta = (\theta_a)^{2/3} = (n - \theta_L)^{2/3} \quad [103]$$

$$h_r = e^{\frac{-g \omega_v \Psi}{\gamma_w R (273.15 + T)}} \quad [104]$$

$$\psi = (u_a - u_w) + \pi \quad [105]$$

where:

- | | |
|------------|---|
| h | = water head, m , |
| γ_w | = unit weight of water, kN/m^3 , |
| k_w | = hydraulic conductivity, m/s , |
| k_{vh} | = water vapor conductivity by diffusion within the air phase, m/s , |
| β | = soil tortuosity of a dimensionless factor, |
| θ_a | = volumetric air content, $\theta_a = n - \theta$, m^3/m^3 , |

θ	= volumetric water content, m^3/m^3 ,
n	= porosity,
D_v	= molecular diffusivity of vapor through soil, m^2/s ,
ω_v	= molecular weight of water vapor, 0.018016 kg/mol ,
ρ_{sv0}	= saturation vapor density that is dependent of temperature, kg/m^3 ,
h_r	= relative humidity,
ρ_w	= water density, kg/m^3 ,
R	= universal gas constant, 8.314 $J/(mol-K)$,
T	= temperature, $^{\circ}C$, and
Ψ	= total suction, kPa ,
u_a	= pore-air pressure, kPa ,
u_w	= pore-water pressure, kPa ,
π	= osmotic suction, kPa , and
y	= elevation, m .

The osmotic suction in a soil is related to the salt content in the soil. For typical field water content conditions, osmotic suction may range from 100 kPa to 1000 kPa or more. As the soil dries, the salt contents increase, and the osmotic component increases (Fredlund, 1991).

It should be noted that SVFLUX supports one-dimensional, two-dimensional, and three-dimensional formulations for moisture flow; however, only the one-dimensional partial differential equation is shown (i.e., Equation [100]).

8.4.3.2 Initial soil water contents

The soil moisture can be initialized using an initial set of values for pore-water pressure, water head. It is also possible to designate the location of the water table (i.e., phreatic line) and assume that hydrostatic conditions exist above and below the phreatic line.

8.4.3.3 Boundary condition for moisture flow

Using Equation [83] infiltration to the ground surface (i.e., the boundary condition for moisture flow) can be defined as.

$$q_y \Big|_{surface} = P - AE - R_{off} \quad [106]$$

where:

q_y	= moisture flow rate at soil surface, m/day ,
P	= precipitation flux, m/day ,
R_{off}	= water runoff, m/day ,
AE	= actual evaporation, m/day

8.4.3.4 Actual Evaporation

The "limiting function" proposed by Wilson et al., (1997) is written as follows.

$$AE = PE \left[\frac{u_v^{soil} - u_v^{air}}{u_{vo}^{soil} - u_v^{air}} \right] \quad [107]$$

where:

AE	= actual evaporation, m/day ,
PE	= potential evaporation, m/day ,
u_v^{soil}	= actual vapor pressure at the soil surface, kPa ,
u_{vo}^{soil}	= saturated vapor pressure in the soil at the ground surface, kPa , and
u_v^{air}	= vapor pressure in the air above the soil surface, kPa .

For the **Case 1 Solution**, it is assumed that $T_s = T_a$, and this leads to the vapor pressure in the air being equal to the saturated vapor pressure in the soil (i.e., $u_{vo}^{air} = u_{vo}^{soil}$). Equation [107] can also be written in term of relative humidity as follows (Wilson et al., 1997):

$$AE = PE \left[\frac{h_s - h_r}{1 - h_r} \right] \quad [108]$$

where:

h_r = relative humidity of the air above the ground surface, and
 h_s = relative humidity at the soil surface.

Equations [100], [106], and [107] or [108] together with the initial water content conditions are the equations required to solve for Actual Evaporation, AE.

8.4.3.5 Determining vapor pressure values throughout each day

The daily air temperature, T_a , and daily relative humidity, h_r , of the air above the ground surface are usually measured at a weather station. Minimum and maximum daily temperature and relative humidity values are generally recorded for each day. However, usually the hourly values of these variables are also recorded. The amount of data becomes quite excessive when hourly values are obtained. When minimum and maximum values are given for temperature and relative humidity, then an assumption can be made regarding their distributions throughout each day.

Figure 29 and Figure 30 shows two options of several possible methods implemented in SVFLUX to describe the daily changing pattern of air temperature and relative humidity based on the daily minimum and maximum value. Figure 29 indicates that the relative humidity has a maximum value at about 6:00 a.m. and a minimum value at about 1:00 p.m. The time at minimum and maximum value can be specified with other value. In Figure 30, the maximum value of relative humidity is assumed at the midnight (24:00 a.m.), and minimum value is at noon (12:00 p.m.). The daily changing pattern of air temperature is in general, opposite to the pattern for relative humidity.

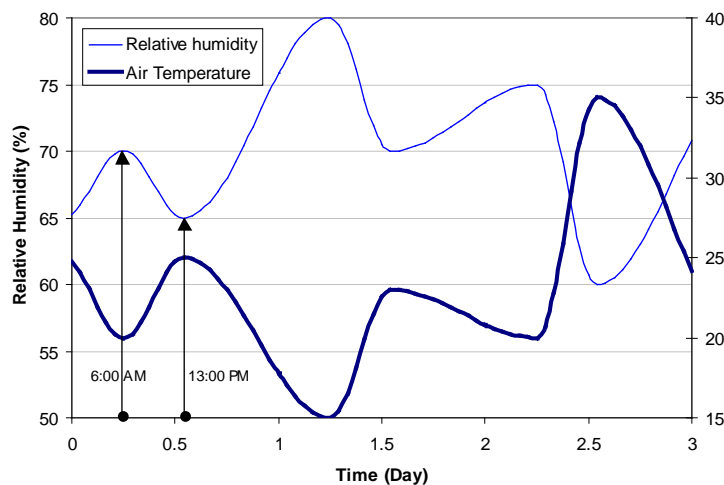


Figure 29 Daily changing pattern of air temperature and relative humidity of overlying air

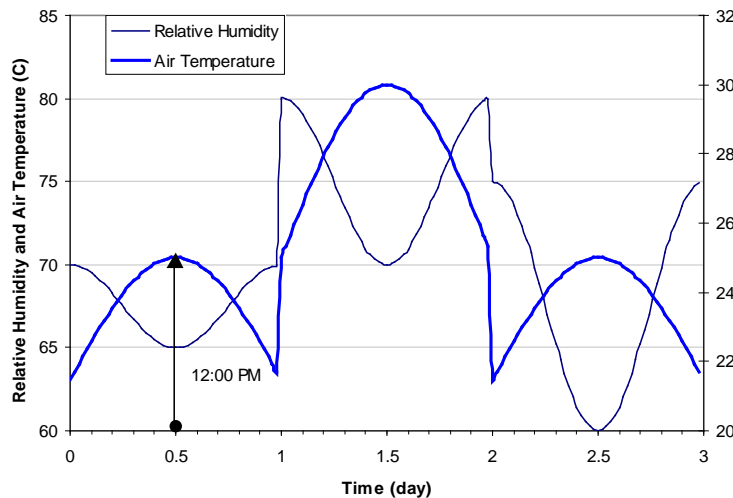


Figure 30 Symmetric distributions of daily changing of air temperature and relative humidity

The calculated relative humidity at the unsaturated soil surface based on Edlefsen and Anderson (1943) equation may be larger than the actual value particularly for an unsaturated sand. It can be seen from Figure 31 that when the total suction in

soil is less than about 3000 kPa , the relative humidity at the soil surface approaches 100% (i.e., $h_s \rightarrow 1$). Consequently, $AE = PE$, which is not valid for sand soil since the sand may have desaturated at a suction considerably below 100 kPa .

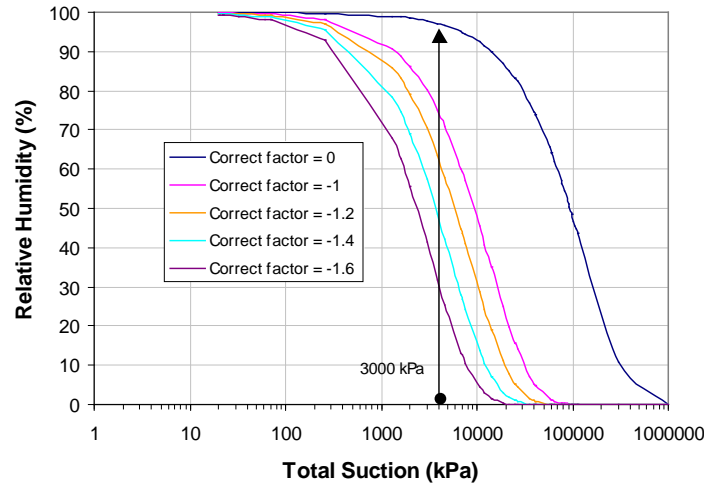


Figure 31 Relationship between relative humidity and total suction using Edlefsen and Anderson (1943) equation

SVFLUX provides three options to improve the accuracy and stability of evaporative and atmospheric modeling.

Apply Surface Suction Correction

When the Surface Suction Correction option is selected, the total suction that is used to calculate the relative humidity at the soil surface is adjusted based on an empirical correction factor (Alvenas and Jansson, 1997). In other words, the relative humidity at soil surface is modified in accordance with the following expression:

$$h_s = \frac{u_v^{soil}}{u_{vo}^{soil}} = \exp\left(\frac{-g\omega_v\psi\delta_{corr}}{\gamma_w R(273.15 + T_s)}\right) \quad [109]$$

$$\psi = (u_a - u_w) + \pi \quad [110]$$

$$\delta_{corr} = 10^{-(f_{corr})} \quad [111]$$

where:

- ψ = total suction, kPa ,
- ω_v = molecular weight of water, 0.018 kg/mol ,
- γ_w = unit weight of water, 9.807 kN/m^3 ,
- g = gravity acceleration, m/s^2 ,
- R = universal gas constant, 8.314 J/(mol-K) ,
- T_s = soil surface temperature, $^{\circ}C$,
- T_a = air temperature obtained from weather station, $^{\circ}C$
- u_a = pore-air pressure, kPa ,
- u_w = pore-water pressure, kPa ,
- π = osmotic suction, kPa .
- δ_{corr} = correction factor of soil surface suction ranging between 1 to $10^{3.48}$ (see section 8.4.7 for further details), and
- f_{corr} = empirical number changing from 0 to -2 . By default, $f_{corr} = -1.2$, which corresponds to $\delta_{corr} = 15.8$.

Figure 31 illustrates the correction factor effect on the relative humidity.

Apply Gradient Limit

When the Apply Gradient Limit option is selected, it is possible for extremely high gradients to develop at the upper boundary during evaporative conditions when using the Wilson-Penman climate boundary condition. Extremely high surface gradients can lead to unreasonable numerical instability. Limiting the gradient to a reasonable maximum value can improve convergence of climate-based numerical models. A reasonable Gradient Limit might be between 50 to 1000; however, it could go as high as 10,000.

None

When the None option is selected, the suction at the soil surface is not modified. (This option is equivalent to using a correction factor equivalent to f_{corr} equal to zero in the first option). Please note that with this option the calculated actual evaporation may be over-estimated for a coarse-grained unsaturated soil.

The vapor pressure of u_v^{soil} used in diffusive flow Equation [107] can be calculated using the following equation.

$$u_v^{soil} = u_{vo}^{soil} h_s = u_{vo}^{soil} \exp\left(\frac{g \omega_v \psi \delta_{corr}}{\gamma_w R (273.15 + T_s)}\right) \quad [112]$$

The saturated vapor pressure is a function of soil surface temperature as given by the following expression (Lowe, 1977; Gitirana, 2004):

$$u_{v0}^{soil} = a_0 + a_1 T_s + a_2 T_s^2 + a_3 T_s^3 + a_4 T_s^4 + a_5 T_s^5 \quad [113]$$

where:

$$\begin{aligned} a_0 &= 0.6183580754 \\ a_1 &= 0.0411427320 \\ a_2 &= 0.0017217473 \\ a_3 &= 0.0000174108 \\ a_4 &= 0.0000003985 \\ a_5 &= 0.0000000022 \end{aligned}$$

Note : $T_s = T_a$ in this case.

The Potential Evaporation, PE , in Equation [108] can be determined using one of several possible procedures, such as:

- Using Measured data (i.e., Pan evaporation),
- Calculated with the Penman (1948) equation,
- Calculated with the Thornwaite (1948) equation, or
- Calculated with the Priestley-Taylor (1972) equation.

Note: Currently only options a) and b) have been implemented in SVFLUX. Options c) and d) may be added in a later version of SVFLUX.

Penman (1948) Potential Evaporation

Penman (1948) proposed the following equation for the calculation of potential evaporation, (PE), from a saturated soil surface.

$$PE = \frac{\Gamma Q_n + \eta E_a}{\Gamma + \eta} \quad [114]$$

where:

$$\begin{aligned} PE &= \text{potential evaporation, } m/day, \\ E_a &= \text{flux associated with "mixing"; } f(u) C_f u_{vo}^{air} (1 - h_r), \text{ } m/day, \\ f(u) &= 0.35 (1. + 0.146 W_w), \\ W_w &= \text{wind speed, } km/hr, \\ C_f &= \text{conversion factor, (i.e., } 1 \text{ } kPa = 0.00750 \text{ } mHg), \\ h_r &= \text{relative humidity in the air above the ground (i.e., } h_r = u_v^{air}/u_{vo}^{air}), \\ &\text{obtained from weather station record,} \\ u_v^{air} &= \text{water vapor pressure in the air above ground surface, } kPa, \\ u_{vo}^{air} &= \text{saturated vapor pressure at the mean air temperature, } kPa, \\ \Gamma &= \text{slope of saturation vapor pressure vs. temperature curve, } kPa/^{\circ}C, \\ Q_n &= \text{net radiation at the water surface, } m/day, \text{ and} \\ \eta &= \text{psychrometric constant, (} kPa/^{\circ}C), \eta = 0.06733 \text{ } kPa/^{\circ}C. \end{aligned}$$

8.4.4 Case 2 Solution: Wilson-Penman (1994) SVFLUX Model – SVENVIRO

In Case2, the SVFLUX model assumes that

- Moisture and vapor flow occurs through the soil.
- Soil temperatures in the entire domain are the same. In other words, the ground thermal flux is neglected (i.e., $Q_g = 0$).
- The soil temperature at soil surface can be different from the air temperature. The heat exchanged between air and soil surface follows the convection law as given the closed-form Equations [84] or [85]. However, the surface temperature is not imposed as a boundary condition for distribution through the underlying soil.
- Actual Evaporation, AE , is calculated using Wilson-Penman (1994) equation.

8.4.4.1 Governing Equations

Moisture flow in one-dimension is defined by equation [115], (note: same as Equation [100]):

$$\frac{\partial}{\partial y} \left[(k_{wy} + k_{vh}) \frac{\partial h}{\partial y} - k_{vh} \right] = -\gamma_w m_2^w \frac{\partial h}{\partial t} \quad [115]$$

Since the soil temperature is different from the air temperature, it is necessary to use another equation to determine the soil temperature. Because this is an isothermal model (i.e., $Q_g = 0$), controlled by Equations [84] and [85], a closed-form for the soil temperature can be written (Wilson, 1994):

$$T_s = T_a + \frac{1}{C_f \eta f(u)} (Q_n - AE) \quad [116]$$

where:

T_s	= soil temperature at soil surface, °C,
T_a	= air temperature, °C,
C_f	= conversion factor (i.e., 1 kPa = 0.00750 mHg),
η	= psychometric constant, 0.06733 kPa/°C,
$f(u)$	= function depending speed, $f(u) = 0.35 (1. + 0.146 W_w)$,
W_w	= wind speed, km/hr,
Q_n	= net radiation, m/day, and
AE	= actual evaporation, m/day.

8.4.4.2 Initial soil water content profile

The water content in the soil can be initialized using an initial set of values for pore-water pressure or water pressure head. It is also possible to designate the location of the water table (i.e., the phreatic line) and assume that hydrostatic conditions exist below and above the water table.

8.4.4.3 Initial soil surface temperature

Temperature can be initialized to the air temperature. The initialized air temperature is:

$$T_s = T_a \quad [117]$$

8.4.4.4 Boundary condition for moisture flow

The boundary condition for moisture flow at the ground surface is defined using equation [118].

$$q_y \Big|_{\text{surface}} = P - AE - R_{\text{off}} \quad [118]$$

where:

q_y	= moisture flow rate at soil surface, m/day,
P	= precipitation flux. m/day,
R_{off}	= water runoff, m/day, and
AE	= actual evaporation, m/day

8.4.4.5 Actual Evaporation

The Wilson-Penman (1994) equation for actual evaporation, AE , can be re-written as follows:

$$AE = \frac{\Gamma Q_n + \eta E_a}{\Gamma + \eta / h_s} \quad [119]$$

where:

AE	= actual evaporation, m/day ,
PE	= potential evaporation, m/day
E_a	= flux associated with "mixing"; $f(u) C_f u_v^{air} (1/h_r - 1/h_s)$, m/day ,
$f(u)$	= $0.35 (1. + 0.146 W_w)$,
W_w	wind speed, km/hr ,
C_f	conversion factor, (i.e., $1 \text{ kPa} = 0.00750 \text{ mHg}$),
h_r	= relative humidity in the air above the ground (i.e., $h_r = u_v^{air}/u_{v0}^{air}$),
h_s	= relative humidity at the soil surface (i.e., $h_s = u_v^{soil}/u_{v0}^{soil}$),
u_v^{air}	= water vapor pressure in the air above ground surface, kPa ,
u_{v0}^{air}	= saturated vapor pressure at the mean air temperature, kPa ,
u_v^{soil}	= vapor pressure in the soil at ground surface, kPa ,
u_{v0}^{soil}	= saturated vapor pressure in the soil at ground surface, kPa ,
Γ	= slope of saturation vapor pressure vs. soil temperature curve ($kPa/^\circ C$),
Q_n	= net radiation at the water surface, m/day , and
η	= psychrometric constant, $kPa/^\circ C$, $\eta = 0.06733 \text{ kPa/}^\circ C$.

The governing Equations [115] and [116], initial condition Equation [117], boundary condition Equations [118] and [119] are essential for solving the isothermal model with atmospheric coupling.

Note: To calculate Actual Evaporation, AE , using Equation [119], the soil temperature at the ground surface must be known. But when using Equation [116] to calculate the soil temperature, the Actual Evaporation, AE , must be known. In other word, the Equations [116] and [119] are coupled to each other (i.e., must be solved simultaneously). The coupling Equation [116] is one of governing equations. Therefore, it must be initialized to a specific value. The Actual Evaporation can be calculated initially using Equation [119].

8.4.4.6 Determining Vapor Pressure Values throughout each Day

The saturated vapor pressure, u_{v0}^{air} in Equation [119], is calculated based on air mean temperature.

$$u_{v0}^{air} = a_0 + a_1 T_a + a_2 T_a^2 + a_3 T_a^3 + a_4 T_a^4 + a_5 T_a^5 \quad [120]$$

where:

T_a	= air mean temperature, measured at a weather station.
-------	--

The parameters of a_0 , a_1 , a_2 , a_3 , a_4 and a_5 are previously given in Equation [113]. The water vapor pressure in the air, u_v^{air} , is defined as follows:

$$u_v^{air} = u_{v0}^{air} h_r \quad [121]$$

where:

h_r	= relative humidity of the air above the soil surface.
-------	--

The relative humidity, h_r , of the air above the soil surface is measured at a weather station. The relative humidity, h_s , and water vapor pressure, u_v^{soil} , at the soil surface are calculated using Equations [109] and [112]. It should be noted that soil surface temperature, T_s , in Equations [109], [112], or [113] are calculated using Equation [116].

8.4.5 Case 3 Solution: "Experimental-Based" for AE/PE SVFLUX Model – SVENVIRO

For case 3, it is assumed that

- Moisture flow and vapor flow beneath the soil surface are driven by the hydraulic head gradient and the vapor pressure gradient, respectively.
- Soil temperatures in the model domain are the same, and assumed to be equal to the air temperature above the soil surface. In other words, the ground thermal flux can be neglected (i.e., $Q_g = 0$).
- The soil surface temperature is assumed to be equal to the air temperature.
- The actual evaporation is calculated using an empirical “experimental-based” equation proposed by Wilson et al., (1997).

8.4.5.1 Governing Equation

The partial differential equation for the one-dimensional flow of water through a saturated –unsaturated soil is defined as follows:

$$\frac{\partial}{\partial y} \left[(k_{wy} + k_{vh}) \frac{\partial h}{\partial y} - k_{vh} \right] = -\gamma_w m_2^w \frac{\partial h}{\partial t} \quad [122]$$

8.4.5.2 Initial water content conditions

The water contents of the soil can be initialized using an initial set of values for pore-water pressure or water pressure head. It is also possible to designate the location of the water table (i.e., the phreatic line) and assume that hydrostatic conditions exist below and above the phreatic line.

8.4.5.3 Boundary condition for moisture flow

Using the water balance Equation [83], the boundary condition for moisture flow at the ground surface is defined as:

$$q_y|_{\text{surface}} = P - AE - R_{\text{off}} \quad [123]$$

where

- q_y = moisture flow rate at soil surface, *m/day*,
 P = precipitation flux, *m/day*,
 R_{off} = water runoff, *m/day*, and
 AE = actual evaporation, *m/day*.

8.4.5.4 Determine an empirical expression for the ratio of actual evaporation, AE, to potential evaporation, PE

If the soil suction is known at the ground surface, then the rate of evaporation from the ground surface can be estimated from the empirical “experimental-based” relationship shown in Figure 32.

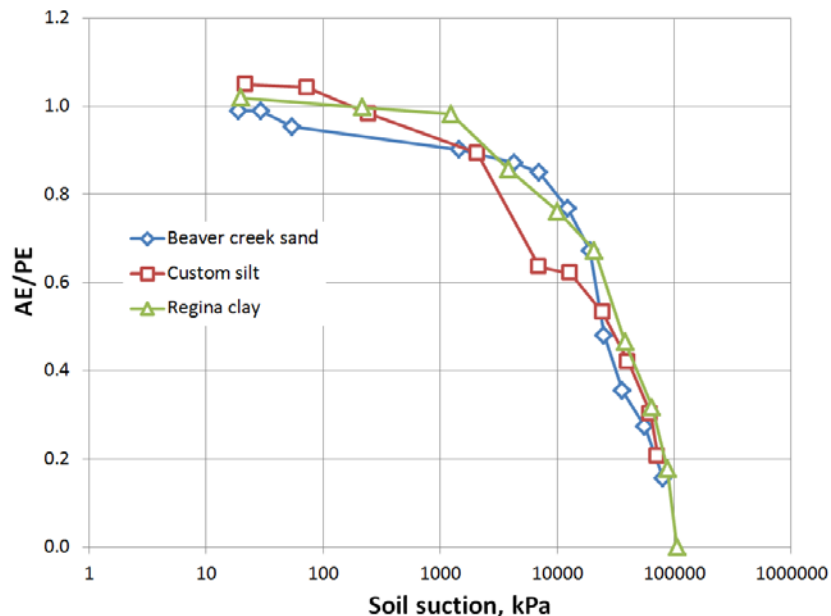


Figure 32 Relationship between ratio of AE/PE and total suction

The ratio of actual evaporation to potential evaporation, AE/PE , can be approximated using the form of the thermodynamic equilibrium relationship between relative humidity and total suction. (Edlefsen and Anderson, 1943). However, a correction factor, δ_{corr} , must be applied to the calculation of AE and the magnitude of the correction is dependent upon the type of soil near the ground surface. The ratio of AE/PE has a format similar to that used for Equation [109]. The ratio of AE/PE has a format similar to that used for Equation [109].

$$AE / PE = \exp\left(\frac{-g\omega_v\psi\delta_{corr}}{\gamma_w R(273.15 + T_s)}\right) \quad [124]$$

$$\delta_{corr} = 10^{-f_{corr}} \quad [125]$$

where:

AE	= Actual evaporation, m/day ,
PE	= Potential evaporation, m/day ,
ψ	= total suction (i.e., matric suction plus osmotic suction), kPa ,
ω_v	= molecular weight of water, 0.018 kg/mol ,
γ_w	= unit weight of water, 9.807 kN/m^3 ,
g	= gravity acceleration, m/s^2 ,
R	= universal gas constant, 8.314 J/(mol-K) ,
T_s	= soil surface temperature, $^{\circ}C$, and
f_{corr}	= correction variable, and
δ_{corr}	= correction factor by which total suction must be multiplied.

The correction factor, δ_{corr} , is computed based on the difference between the residual suction of the soil and a total suction of 3000 kPa . Equation [143] (section 8.4.7) shows how the correction factor is computed. The variable f_{corr} , is determined based on the shift of the SWCC of the soil and Lord Kelvin's thermodynamic equilibrium equation. The f_{corr} , variable is typically about 1.8 for a coarse sand soil.

To include the relative humidity of the overlying air in equation [124], the equation can be modified to the following format:

$$AE / PE = \exp\left(\frac{-g\omega_v\psi\delta_{corr}}{\zeta(1-h_a)\gamma_w R(T_s + 273.15)}\right) \quad [126]$$

where:

ζ	= a dimensionless empirical parameter with a suggested value of 0.7, and
h_a	= relative humidity overlying air.

Figure 33 shows the predicted values for the ratio of AE to PE when using Equation [108], equation [124], and Equation [126]. In Figure 33, the data for the "Limiting Function (1997)" is calculated using Equation [108]. The data for the Wilson-Penman (1994) ratio of AE to PE is calculated using Equation [124]. The data for the empirical "experimental-based" ratio of AE to PE is calculated using Equation [126].

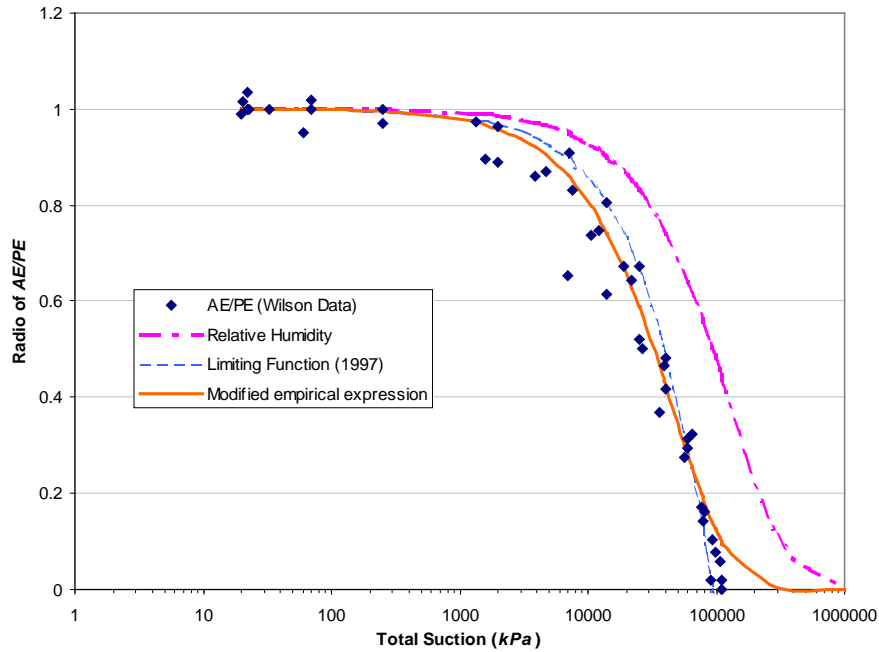


Figure 33 Comparison of predicted values of AE/PE using different suggested equations

Note: Equation [126] is currently utilized in SVFLUX for obtaining the **Case 3 Solution**.

8.4.6 Case 4 Solution: Coupled Moisture and Heat Modeling (SVFLUX & SVHEAT Using “Wilson-Penman (1994)” for AE – SVENVIRO

In the coupled moisture flow and thermal flow model, the following assumptions are made:

- Moisture and vapor flow beneath soil surface is governed by hydraulic head gradients, vapor pressure gradients and temperature gradients.
- The heat transfer beneath soil surface (i.e., ground thermal flux in Equation [84]) is mainly governed by thermal conduction. Heat transfer by thermal convection is included but it can be neglected for Soil Cover applications.
- Soil freezing/thawing processes are considered when soil temperature goes below the freezing point. In the frozen soil, the reduction of hydraulic conductivity is taken into account through the existence of ice in the frozen soil.
- The latent heat due to phase change, including evaporation and freezing/thawing is considered in heat transfer beneath the soil surface.
- The soil surface temperature can be different from the air temperature. The heat exchanged between air and soil surface is determined by thermal balance as given in Equation [84].
- Actual evaporation is calculated using the Wilson-Penman (1994) equation.

8.4.6.1 Moisture flow governing equation

The coupling moisture and vapor flow equation (Wilson 1990, and Gitirana, 2004):

$$\frac{\partial}{\partial y} \left[k_{y11} \frac{\partial(u_w)}{\partial y} + k_{y12} \frac{\partial T}{\partial y} + k_{wy} \right] + S_{\sin k} = \frac{\partial \theta_u}{\partial t} + \frac{\rho_i}{\rho_w} \frac{\partial \theta_i}{\partial t} \quad [127]$$

8.4.6.2 Heat flow equation

The heat flow beneath soil surface is modified based on the equation given by Jame (1977), Wilson (1994), Gitirana (2005), and other works related soil freezing and thawing. Please see SVHEAT Theory Manual for the detailed derivation.

$$\frac{\partial}{\partial y} \left(k_{y21} \frac{\partial u_w}{\partial y} + k_{y22} \frac{\partial T}{\partial y} + L_f k_{wy} \right) - \left(C_w q_y^L + C_v q_y^v \right) \frac{\partial T}{\partial y} + Q_{\sin k} = \left(C + L_f m_2^i \right) \frac{\partial T}{\partial t} \quad [128]$$

where:

$$k_{y11} = \frac{k_{wy} + k_{vh}}{\gamma_w}, \quad k_{y12} = k_{yLT} + k_{vT}, \quad k_{yLT} = m_2^{\phi} \frac{k_{wy}}{\gamma_w} \quad [129]$$

$$k_{y21} = \frac{L_f k_{wy} + L_v k_{vh}}{\gamma_w}, \quad k_{y22} = \lambda_y + L_v k_{vT} + L_f k_{yLT} \quad [130]$$

$$k_{vT} = \frac{k_{vh}}{\gamma_w} \left[\frac{\rho_w}{\rho_{sv0}} \left(\frac{\partial u_{sv0}}{\partial T} - \frac{u_{sv0} + u_{atm}}{(273.15 + T)} \right) + \frac{u_a - u_w}{(273.15 + T)} \right] \quad [131]$$

where:

u_w	= pore-water pressure as part of hydraulic head, kPa ,
u_a	= pore-air pressure, kPa ,
u_{sv0}	= saturated vapor pressure, kPa ,
u_{atm}	= atmospheric air pressure, kPa .
θ_u	= volumetric unfrozen water content, m^3/m^3 ,
θ_i	= volumetric ice content, m^3/m^3 ,
ρ_w	= water density, kg/m^3 ,
ρ_i	= ice density, kg/m^3 ,
ρ_{sv0}	= saturation vapor density that is dependent of temperature, kg/m^3 ,
T	= material temperature, $^{\circ}C$,
t	= time, s ,
k_{wy}	= hydraulic conductivity, m/s ,
k_{vh}	= pore-water vapor conductivity by vapor diffusion within the air phase, see Equation [101], m/s ,
k_{vT}	vapor diffusion due to temperature gradient, m/s ,
k_{LT}	= hydraulic conductivity introduced by temperature gradient, $m^2/s-^{\circ}C$,
γ_w	= unit weight of water, kN/m^3 ,
λ_y	= thermal conductivity, $J/s-m-^{\circ}C$,
L_v	= volumetric latent heat of water vaporization or condensation, J/m^3 . $L_v = 2.5 \times 10^9 J/m^3$ if $T > T_{ef}$, otherwise, $L_v = 0$.
L_f	= volumetric latent heat of water freezing or thawing, J/m^3 , $L_f = 3.34 \times 10^8 J/m^3$ if $T_{ef} > T > T_{ep}$, otherwise $L_f = 0$,
T_{ef}	= temperature at soil freezing point, $^{\circ}C$,
T_{ep}	= the temperature at which soil phase change is finished during freezing, $^{\circ}C$,
C	= volumetric heat capacity of material, J/m^3 ,
C_w	= volumetric heat capacity of water, J/m^3 ,
C_v	= volumetric heat capacity of water vapor, J/m^3 ,
q_y^L	= water flow velocity, m/s ,
q_y^V	= vapor flow velocity, m/s ,
S_{sink}	= water sink or source, m^3/m^3-s ,
Q_{sink}	= heat sink or source, J/m^3-s ,
m_2^i	= slope of Soil-Freezing Characteristic Curve (SFCC) (i.e., the relationship between unfrozen water content and soil temperature), and
m_2^{θ}	= slope of the relation of matric suction to the soil temperature, $kPa/^{\circ}C$.

It should be noted that $k_{LT} = 0$ in the current software.

8.4.6.3 Initial water content conditions

The water content of the soil can be initialized using an initial set of values for pore-water pressure, water pressure head. It is also possible to designate the location of the water table (i.e., the phreatic line) and assume that hydrostatic conditions exist below and above the water table.

8.4.6.4 Initial temperature conditions

The soil temperatures in the domain are initialized using a specific value or an expression. For example, the air temperature can be used for the initial soil temperature.

$$T = T_a \quad [132]$$

8.4.6.5 Thermal boundary condition at soil surface

The thermal boundary condition at the ground surface is specified as thermal flux. According to Equation [84], the ground heat flux is expressed as

$$Q_g \big|_{\text{surface}} = Q_n - Q_L - Q_h \quad [133]$$

8.4.6.6 Boundary condition for moisture flow

The atmospheric moisture flux at the ground surface should satisfy equation [134].

$$q_y \big|_{\text{surface}} = P - AE - R_{\text{off}} \quad [134]$$

8.4.6.7 Actual Evaporative, AE

Wilson-Penman (1994) actual evaporation flux equation is shown as follows.

$$AE = \frac{\Gamma Q_n + \eta E_a}{\Gamma + \eta / h_s} \quad [135]$$

where:

AE	= actual evaporation, m/day ,
PE	= potential evaporation, m/day
E_a	= flux associated with "mixing"; $f(u) C_f u_v^{air} (1/h_r - 1/h_s)$, m/day ,
$f(u)$	= $0.35 (1. + 0.146 W_w)$,
W_w	wind speed, km/hr ,
C_f	conversion factor, (i.e., $1 \text{ kPa} = 0.00750 \text{ mHg}$),
h_r	= relative humidity in the air above the ground (i.e., $h_r = u_v^{air}/u_{vo}^{air}$),
h_s	= relative humidity at the soil surface (i.e., $h_s = u_v^{soil}/u_{vo}^{soil}$) defined in equation [109],
u_v^{air}	= water vapor pressure in the air above ground surface, kPa ,
u_{vo}^{air}	= saturated vapor pressure at the mean air temperature, kPa ,
u_v^{soil}	= vapor pressure in the soil at ground surface, kPa ,
u_{vo}^{soil}	= saturated vapor pressure in the soil at ground surface, kPa ,
Γ	= slope of saturation vapor pressure vs. soil temperature curve, $kPa/^\circ C$,
Q_n	= net radiation at the water surface, mm/day , and
η	= psychrometric constant, $kPa/^\circ C$, $\eta = 0.06733 \text{ kPa}/^\circ C$.

The moisture and heat flow coupled problem can be solved using the governing Equation [127] and Equation [128], the initial thermal condition Equation [132], thermal boundary condition Equation [133], and moisture flow boundary condition Equation [134] together with actual evaporation Equation [135].

8.4.6.8 Calculation Procedure

1. Initialize the water content profile.
2. Initialize the soil temperature using Equation [132].
3. Apply the moisture flux boundary condition in accordance with Equation [134].
4. Apply the thermal boundary condition at the ground surface using Equation [133].
5. Once the model domain is initialized, the following steps must be performed:

6. Calculate the actual evaporation, AE , using Equation [135] based on the soil temperature at the ground surface. Initially the soil temperature can be specified as the air temperature using Equation [132].
7. Solve the moisture flow Equation [127], and the thermal flow Equation [128], based on initial conditions, boundary conditions using equation [99] and Equation [134].
8. Calculate net percolation, NP , or infiltration at soil surface. The net infiltration flux at the ground surface is defined as

$$k \frac{\partial h}{\partial y},$$

9. Calculate runoff, R_{off} , using Equation [83], using the known value of precipitation, P , actual evaporation, AE , and net infiltration, NP , at the ground surface.
10. Check the solution to see if the convergence has been reached for both seepage head and soil temperature, T . The difference between iteration must less than the designated tolerances.
11. If the solution has not yet converged, repeat step 6) to 11) iteratively until the convergence is achieved.

8.4.7 Case 5 Solution: SVFLUX and SVHEAT Coupled Using the Wilson-Fredlund-Barbour “Limiting Equation” – SVENVIRO

The **Case 5 solution** is based on the following assumptions:

- The soil temperature at the ground surface is equal to the air temperature,
- The moisture flow and heat transfer beneath the ground surface are the same as in **Case 4 Solution**.
- Soil freezing/thawing processes are considered when the soil temperature falls below the freezing point. In the frozen soil regiment, the hydraulic conductivity is reduced for the existence of ice in the frozen soil,
- The latent heat due to phase change, including evaporation and freezing/thawing, is considered in the heat transfer beneath the ground surface, and
- Actual Evaporation, AE , is calculated using Limiting Equation proposed by Wilson et al., (1997).

8.4.7.1 Moisture flow governing equation

The following partial differential equation accounts form the flow of liquid and vapor water through a soil in addition to water movement related to phases changes that occur upon freezing and thawing.

$$\frac{\partial}{\partial y} \left[k_{y11} \frac{\partial u_w}{\partial y} + k_{y12} \frac{\partial T}{\partial y} + k_{wy} \right] + S_{\sin k} = \frac{\partial \theta_u}{\partial t} + \frac{\rho_i}{\rho_w} \frac{\partial \theta_i}{\partial t} \quad [136]$$

8.4.7.2 Heat flow equation:

The following heat flow partial differential equation accounts for heat flow and phases changes between the liquid and solid (ice) states.

$$\frac{\partial}{\partial y} \left(k_{y21} \frac{\partial u_w}{\partial y} + k_{y22} \frac{\partial T}{\partial y} + L_f k_{wy} \right) - \left(C_w q_y^L + C_v q_y^v \right) \frac{\partial T}{\partial y} + Q_{\sin k} = \left(C + L_f m_2^i \right) \frac{\partial T}{\partial t} \quad [137]$$

8.4.7.3 Initial water content conditions

The water content of the soil can be initialized using an initial set of values for pore-water pressures or water pressure head. It is also possible to designate the location of the water table (i.e., phreatic line) and assume that hydrostatic conditions exist below and above the phreatic line.

8.4.7.4 Initial temperature conditions

The temperature of the soil in the domain is initialized using a specific value or an expression. For example, the air temperature can be used for the initial soil temperature.

$$T = T_a \quad [138]$$

8.4.7.5 Thermal boundary condition at soil surface

The thermal boundary condition at the ground surface can be specified as thermal flux:

$$Q_g \Big|_{surface} = Q_n - Q_L - Q_h \quad [139]$$

8.4.7.6 Boundary condition for moisture flow

The atmospheric moisture flux at the ground surface should satisfy the following:

$$q_y \Big|_{surface} = P - AE - R_{off} \quad [140]$$

8.4.7.7 Actual evaporation

The calculation of actual evaporation, AE , is computed using the “limiting function” (Wilson et al., 1997), as shown in Equation [141].

$$AE = PE \left[\frac{u_v^{soil} - u_v^{air}}{u_{vo}^{soil} - u_v^{air}} \right] \quad [141]$$

where:

- AE = Actual evaporation, m/day ,
- PE = Potential evaporation, m/day ,
- u_v^{soil} = actual vapor pressure at the soil surface, kPa ,
- u_{vo}^{soil} = saturated vapor pressure in the soil at the ground surface temperature, kPa , and
- u_v^{air} = vapor pressure in the air above the soil surface, kPa .

Assuming the air, water and soil temperatures are approximately equal, allows soil temperature to be used in Equation [142].

$$AE = PE \frac{\left(\exp\left(\frac{-g\omega_v\psi\delta_{corr}}{\gamma_w R(273.15 + T_s)}\right) - u_v^{air} / u_{v0}^{air} \right)}{1 - u_v^{air} / u_{v0}^{air}} \quad [142]$$

where:

- AE = Actual evaporation, m/day ,
- PE = Potential evaporation, m/day ,
- u_v^{air} / u_{v0}^{air} = relative vapor pressure (or relative humidity, h_r) of the air,
- ψ = total suction (i.e., matric suction plus osmotic suction), kPa ,
- δ_{corr} = correction factor for the suction at the soil surface (see Equation [111], and
- T_s = soil temperature at ground surface, $^{\circ}C$.

Fredlund et al., (2016) used the residual suction of the drying SWCC as a reference point to calculate the correction factor, δ_{corr} . This correction factor translates the SWCC to a suction value of 3000 kPa on the Lord Kelvin’s curve (Fredlund et al., 2016). Equation [143] shows the relationship between the residual suction and the correction factor, δ_{corr} and the equation is plotted in Figure 34. For coarse-grained soils, the maximum correction factor, δ_{corr} , is 3.48 and there is no correction factor required for fine-grained soils with a high air-entry value (Fredlund et al., 2016).

$$\delta_{corr} = \log 3000 - \log \psi_{residual} \quad [143]$$

where:

- $\psi_{residual}$ = residual soil suction on the drying SWCC, kPa .

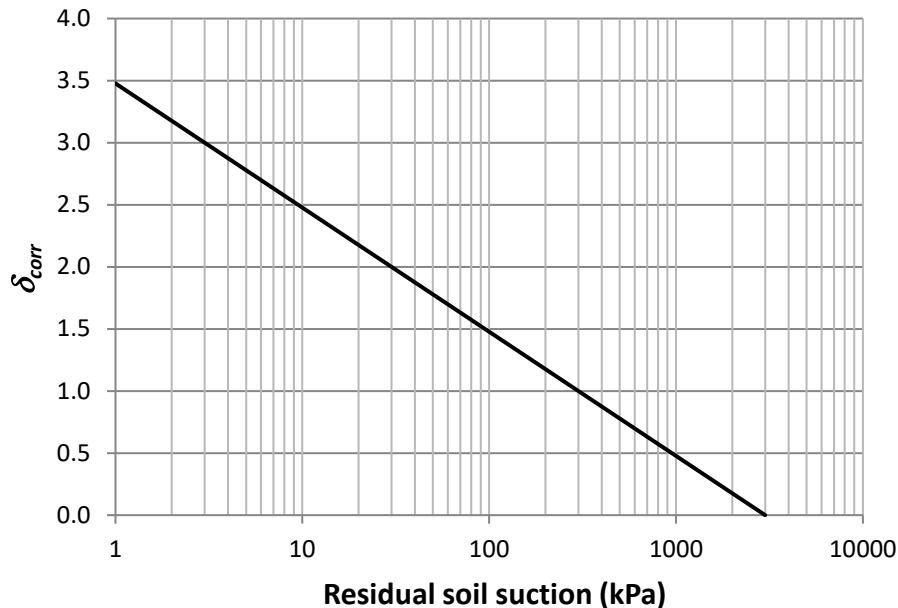


Figure 34 The δ_{corr} correction factors for various residual suction values

8.4.7.8 Potential Evaporative

The potential evaporation, PE , can be determined using one of several approaches, such as,

- Using measured data (i.e., Pan evaporation),
- Calculated using the Penman (1948) equation,
- Calculated using the Thornwaite (1948) equation, or
- Calculated using the Priestley-Taylor (1972) equation.

Note: Currently only options a) and b) have implemented in SVFLUX. Option c) and d) may be added in a later version of SVFLUX.

Penman (1948) approach

The Potential Evaporation, PE , can be approximated using Penman equation as follows.

$$PE = \frac{\Gamma Q_n + \eta E_a}{\Gamma + \eta} \quad [144]$$

where:

- PE = potential evaporation, m/day ,
- E_a = flux associated with "mixing"; $f(u) C_f u_{vo}^{air} (1 - h_r)$, m/day ,
- $f(u)$ = $0.35 (1. + 0.146 W_w)$,
- W_w = wind speed, km/hr ,
- C_f = conversion factor, (i.e., $1 kPa = 0.00750 mHg$),
- h_r = relative humidity in the air above the ground surface
(i.e., $h_r = u_v^{air} / u_{vo}^{air}$),
- u_v^{air} = water vapor pressure in the air above ground surface, kPa ,
- u_{vo}^{air} = saturated vapor pressure at the mean air temperature, kPa ,
- Γ = slope of saturation vapor pressure vs. temperature curve, $kPa/^{\circ}C$,
- Q_n = net radiation at the water surface, mm/day , and
- η = psychrometric constant, $kPa/^{\circ}C$, $\eta = 0.06733 kPa/^{\circ}C$.

8.4.8 Case 6 Solution: Coupled Moisture and Heat Modeling (SVFLUX & SVHEAT) by Using the Empirical "Experimental-Based" for AE/PE – SVENVIRO

It is assumed that:

- Soil temperature at the soil surface is equal to the air temperature,

- The moisture flow and heat transfer beneath the soil surface are the same as that in **Case 4 Solution** and **Case 5 Solution**.
- Soil freezing/thawing processes are considered when soil temperature goes below the freezing point. The hydraulic conductivity is reduced for the existence of ice in the frozen soil.
- The latent heat due to phase change including evaporation and freezing/thawing is considered in heat transfer beneath the soil surface, and
- Actual Evaporative is based on an empirical expression as Equation [126] defined in **Case 3 Solution**.

8.4.8.1 Moisture flow governing equation

The following partial differential equation describes liquid and vapor flow of water as well as taken phase changes associated with freezing (and thawing) into consideration.

$$\frac{\partial}{\partial y} \left[k_{y11} \frac{\partial u_w}{\partial y} + k_{y12} \frac{\partial T}{\partial y} + k_{wy} \right] + S_{\sin k} = \frac{\partial \theta_u}{\partial t} + \frac{\rho_i}{\rho_w} \frac{\partial \theta_i}{\partial t} \quad [145]$$

8.4.8.2 Heat flow equation:

The following heat flow equation accounts for heat flow and phases changes between the liquid and solid (ice) states.

$$\frac{\partial}{\partial y} \left(k_{y21} \frac{\partial u_w}{\partial y} + k_{y21} \frac{\partial T}{\partial y} + L_f k_{wy} \right) - \left(C_w q_y^L + C_v q_y^v \right) \frac{\partial T}{\partial y} + Q_{\sin k} = \left(C + L_f m_2^i \right) \frac{\partial T}{\partial t} \quad [146]$$

8.4.8.3 Initial water content conditions

The water content of the soil can be initialized using an initial set of values for pore-water pressures or water pressure head. It is also possible to designate the location of the water table and assume that hydrostatic conditions exist.

8.4.8.4 Initial temperature conditions

The soil temperature in the domain is initialized using a specific value or an expression. For example, the air temperature can be used for the initial soil temperature.

$$T = T_a \quad [147]$$

8.4.8.5 Thermal boundary condition at soil surface

The thermal boundary condition at the ground surface can be specified as thermal flux according to heat balance equation.

$$Q_g \Big|_{\text{surface}} = Q_n - Q_L - Q_h \quad [148]$$

8.4.8.6 Moisture flow boundary condition at soil surface

The atmospheric moisture flux at the ground surface should satisfy as follows.

$$q_y \Big|_{\text{surface}} = P - AE - R_{\text{off}} \quad [149]$$

8.4.8.7 Actual evaporation, AE

Actual Evaporation, AE , is obtained in the **Case 6 Solution** through use of the empirical “Experimental-Based” Equation [126]:

$$AE / PE = \exp \left(\frac{-g \omega_v \psi \delta_{\text{corr}}}{\zeta (1 - h_a) \gamma_w R (T_s + 273.15)} \right) \quad [150]$$

where:

AE	= Actual evaporation, m/day ,
PE	= Potential evaporation, m/day ,
ψ	= total suction (i.e., matric suction plus osmotic suction), kPa ,

ω_v	= molecular weight of water, 0.018 kg/mol,
γ_w	= unit weight of water, 9.807 kN/m ³ ,
g	= gravity acceleration, m/s ² ,
R	= universal gas constant, 8.314 J/(mol-K),
T_s	= soil surface temperature, °C,
δ_{corr}	= correction factor for the suction at the soil surface,
ζ	= a empirical parameter, that is recommended to be 0.7, and
h_a	= air relative humidity.

8.4.8.8 Determine Potential Evaporation PE

The potential evaporation, PE , can be determined in different ways, including

- Using measured data (i.e., Pan evaporation),
- Calculated using the Penman (1948) equation,
- Calculated using the Thornwaite (1948) equation, or
- Calculated using the Priestley-Taylor (1972) equation.

Note: Currently only options a) and b) have implemented in SVFLUX. Option c) and d) may be added in a later version of SVFLUX.

8.5 TRANSPIRATION - SVENVIRO

Evapotranspiration consists of the combined processes of evaporation and transpiration. Evaporation was described in the previous section. This section describes the transpiration process which can be, applied as a sink term below a specified evaporation boundary condition. Transpiration has been implemented in SVFLUX based on the methodology proposed by Tratch (1995).

Vegetation plays a significant and dynamic role in the overall evapotranspiration process (Saxton, 1982). There are a number of factors that control the amount of water that can be transpired by the vegetation including bare soil potential evaporation, leaf-area index (LAI), plant limiting function (PLF) as it relates to soil suction, and the root zone profile. Lack of available plant water and/or high evaporative demands will cause most plants to biologically react by closing stoma, reducing transpiration, and reducing metabolic reactions (Saxton, 1982). Under continued and increasing stress the plant will reach its wilting point. The wilting point results in leaf drop and tissue death (Saxton, 1982).

Tratch (1995) suggested a four step methodology for the prediction of moisture uptake from transpiration of a plant population:

1. The determination of the potential evaporation which is a measure of the maximum evapotranspiration rate possible under specified atmospheric conditions.
2. Determination of the potential transpiration rate based upon the potential evaporation and the plant population characteristics at the site. This is a measure of the maximum transpiration rate possible in the specified atmospheric conditions.
3. Distribution of the potential transpiration, which is a surface flux, into a potential root uptake profile throughout the active root zone.
4. Modification of the potential root uptake based upon the moisture availability to deliver the actual root uptake profile.

The determination of the bare soil potential evaporation, PE , is described in the previous section. The potential evaporation is applied as a boundary flux in SVFLUX and depends on the atmospheric conditions specified. Natural boundary conditions are assigned to the sides of a finite element and correspond to the surface integral of the term inside the outer derivative of a second order partial differential equation. Potential evaporation is the maximum potential cumulative sum of bare soil evaporation and plant transpiration (Granger, 1989).

The determination of the potential transpiration, PT , is the second step in evaluating the transpiration flux. The potential transpiration is the potential evaporation modified by the leaf-area index. Ritchie (1972) observed that the transpiration component depends on the leaf area index values of the plant canopy. The calculation of potential transpiration is as follows:

$$PT = 0, \quad LAI < 0.1 \quad [151]$$

$$PT = PE(-0.21 + 0.7 \cdot LAI^{0.5}), \quad 0.1 \leq LAI < 2.7 \quad [152]$$

$$PT = PE$$

$$2.7 \leq LAI$$

[153]

where:

PT = potential transpiration rate per unit time (e.g., m/day),

LAI = leaf-area index (unit less), and

PE = potential evaporation rate per unit time (e.g., m/day).

The leaf area index by definition is the surface area of the leaves divided by the surface area of the soil covered. Depending on this ratio, evaporation only, combined evaporation and transpiration, or transpiration only conditions can be selected.

If SVFLUX LAI versus time data is entered, the accuracy of the solution will depend on the accuracy and density of the data provided. The SVFLUX solver will perform a linear interpolation between data points. The pre-defined LAI curves for excellent, good, and poor cover were provided in SoilCover (MEND, 1993). Figure 35 shows these curves for a standard year.

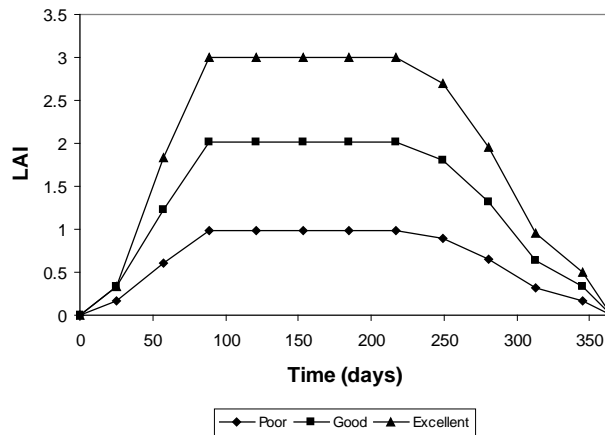


Figure 35 Leaf Area Index Functions (SoilCover, MEND, 1993)

Step 3 suggested by Tratch (1995) involves the partitioning of the available potential evaporation energy between the energy available for potential transpiration by the plants and the energy available for actual evaporation at the boundary. The PT calculation above describes the amount of energy partitioned to the plants. Partitioning of the energy into the AE at the boundary is achieved by the following equation:

$$AE = AE_{bs}, \quad LAI < 0.1 \quad [154]$$

$$AE = AE_{bs} (1 - (-0.21 + 0.7 * LAI^{0.5})), \quad 0.1 \leq LAI < 2.7 \quad [155]$$

$$AE = 0 \quad 2.7 \leq LAI \quad [156]$$

where:

AE = actual evaporation rate per unit time (e.g., m/day),

LAI = leaf-area index (unit less), and

AE_{bs} = actual bare soil evaporation rate per unit time (e.g., m/day).

The term AE_{bs} is the actual evaporation calculated by the various Actual Evaporation methods described in previous section, which assumes bare soil conditions.

The fourth step is to distribute this flux through the soil profile. The mass flux due to transpiration has so far been defined as a surface flux. SVFLUX supports 2 shape functions for describing root distribution, triangular and rectangular. Both functions will result in the same volume of water extracted from the system, but it will be extracted at different volumes spatially.

- **Triangular Root Distribution**

The triangular root distribution shape function describes a decreasing root uptake with depth as illustrated in Figure 36.

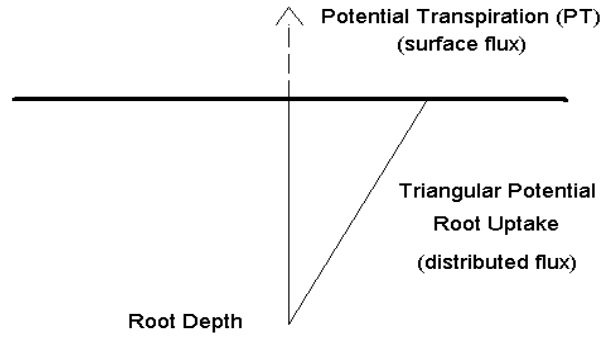


Figure 36 Triangular Potential Root Uptake distribution

- **Rectangular Root Distribution**

The rectangular root distribution shape function describes a decreasing root uptake with depth as illustrated in Figure 37.

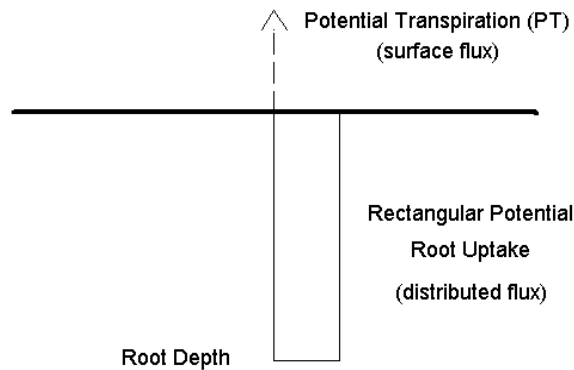


Figure 37 Rectangular Potential Root Uptake distribution

The potential root uptake (PRU) at a given point in the material is defined as follows:

$$PRU = \frac{RSF \times PT}{R_T} \left(1 - \frac{R_n}{R_T} \right) \quad [157]$$

where:

- PRU = potential root uptake rate per unit time (e.g., m^3/day),
- RSF = root distribution shape factor (2 – triangular, 1 – rectangular),
- PT = potential transpiration rate per unit time (e.g., m/day),
- R_T = total thickness of the root zone in length units (e.g., m), and
- R_n = depth to the given point in length units (e.g., m).

The SVFLUX solver will integrate the potential root uptake, PRU , over the root zone below each specified evapotranspiration boundary to determine the potential transpiration sink.

The actual transpiration sink (S_{root}) is found by modifying the potential transpiration sink by a reducing term that is based on the moisture availability (matric suction) as shown below.

$$S_{root} = PRU \times PLF \quad [158]$$

where:

- S_{root} = actual transpiration sink term (e.g., m^3/day),
- PRU = potential root uptake rate per unit time (e.g., m^3/day), and
- PLF = plant limiting factor.

The *PLF* is a reduction term that describes a decrease in transpiration with an increase in matric suction. This relationship is illustrated in Figure 38.

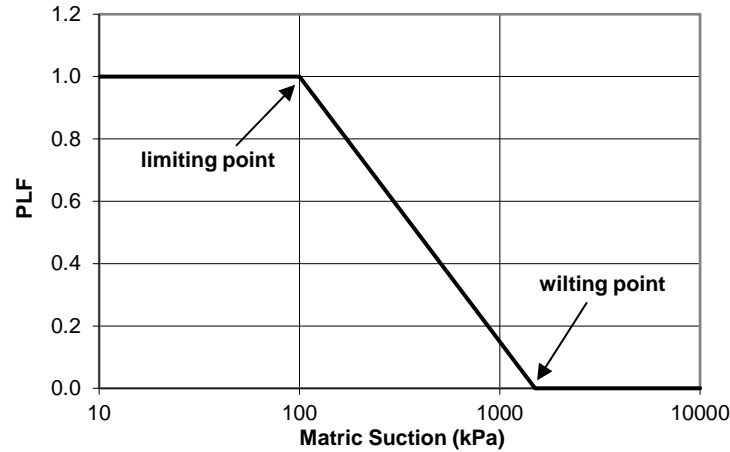


Figure 38 Plant Limiting Factor versus Matric Suction

The actual transpiration sink is maintained at the potential values when the matric suction is below the wilting point. Once the limiting point is exceeded the actual fluxes decrease exponentially until the wilting point is reached. At suctions above the wilting point the transpiration will be zero. Tratch (1995) suggests that the limiting and wilting points are generally 100 and 1500 kPa, respectively.

The transpiration sink term is added to the partial differential equation as shown below. A negative value indicating that water is being pulled from the system.

8.6 OSMOTIC CRUST EFFECT ON ACTUAL EVAPORATION - SVENVIRO

It is often observed that a thin layer of salt crust forms at the soil surface. The crust can be built up on top of the soil surface during the evaporation process. The existence of the salt crust can significantly reduce the evaporation of water from the underlying material. The process leading to the build-up of a salt crust can be described as follow:

1. During the evaporation process, water is pulled out of the soil. This process delivers salt in the soil to the surface and after drying a crust comprised largely of salts is formed.
2. Once the crust is formed, there will be a reduction in future evaporation of water from the material.
3. At the time of a rain-fall event, water will tend to dissolve some of the salts on the surface of the material and water will flow into the material. Therefore infiltration into the soil is not affected.

The formation of a salt crust on the material surface will decrease the vapor pressure near the soil surface. Decreasing the vapor pressure near the soil surface reduces evaporation of the water from the soil. Modeling of the seepage process needs to take into account the existent of the salt crust. The salt crust can be accounted for by assuming that there is a certain value of osmotic suction associated with the salt concentration at the material surface.

The relationship between soil suction and relative humidity can be written as follows (Fredlund and Rahardjo, 1993):

$$\psi = -\frac{R(273.17 + T)}{v_{w0}w_v} \ln\left(\frac{\bar{u}_v}{\bar{u}_{v0}}\right) \quad [159]$$

where:

- ψ = soil suction or total suction, *kPa*,
- R = universal gas constant (i.e., 8.314 *J/(mol-K)*),
- T = temperature, *°C*,
- v_{w0} = specific volume of water or inverse of density of water, *m³/kg*,
- w_v = molecular mass of water vapor,
- \bar{u}_v = partial pressure of pore-water, *kPa*,
- \bar{u}_{v0} = saturation pressure of water vapor over a flat surface of pure water at the same temperature, *kPa*.

The total suction can be calculated from the relative humidity of pore-air in the soil using equation (1). A relative humidity of 20% is equivalent to a soil suction of 200,000 *kPa* which means that at this soil suction, there is almost no evaporation of water from the soil. A range of osmotic suctions from 0 to 200,000 *kPa* will cover the possible range for osmotic suction. A mean value for the osmotic suction associated with the salt crust is about 70,000 *kPa* (i.e., equivalent to a relative humidity of around 60%). It is suggested that the standard deviation of the osmotic suction is equal to a half of the mean value (i.e., 35,000 *kPa*).

When an osmotic suction is entered into the software the osmotic suction is added to the suction calculated in the model domain. The additive value is taken as the total suction. The calculation of actual evaporation (*AE*) from potential evaporation (*PE*) is then based on the total suction. Reasonable values of osmotic suction have been suggested by Wilson (1997) and are shown in the following table:

Table 2 Values of osmotic suction as determined from vacuum desiccators at 20 degrees Celsius (Wilson, 1997)

Salt Solution	Activity coefficient	Osmotic suction (<i>kPa</i>)
Lithium chloride [LiCl H ₂ O] and [LiCl 2H ₂ O]	0.115	292,400
Magnesium chloride [MgCl ₂ 6H ₂ O]	0.330	152,400
Magnesium nitrate [Mg(NO ₃) ₂ 6H ₂ O]	0.543	84,000
Sodium chloride [NaCl]	0.755	38,600
Potassium sulphate [K ₂ SO ₄]	0.970	4,190

8.7 PHYSICAL CRUST EFFECT ON ACTUAL EVAPORATION - SVENVIRO

Crusts are common when dealing with the mining of waste rocks. The existence of the salt crust can significantly reduce the evaporation of water from the material. The process can lead to the build-up of a crust which can be described as follows:

1. During the evaporation process, water is pulled out of the soil. This process delivers salt or other precipitates in the soil to the surface, and crust begins to form. After a certain period of drying, the crust formation is complete.
2. Once the crust is formed, there will be a reduction in future evaporation of water from the material. The ratio of evaporation reduction is referenced as crust coverage.
3. At the time of a rainfall event, and if the rainfall is over a certain amount, water will tend to dissolve some the precipitate on the surface of the material and water will flow into the material.

A salt crust can be modeled in the SVFLUX software through a specification of the time for a crust to begin forming after a precipitation event, the time until a crust is complete, and the percentage coverage of the crust material. When considering the crust effect on evaporation, the actual evaporation *AE* is modified as follows.

$$AE_c = C_f \times AE \quad [160]$$

where:

- AE_c = actual evaporation after consideration of crust effect
 C_f = factor of crust effect on evaporation. C_f changes from 0 to 1

C_f is related to crust drying day C_{dd} ,

$$\begin{aligned} C_f &= 1 & \text{if } C_{dd} < F_s \\ C_f &= 1 - C_v & \text{if } C_{dd} < F_c \\ C_f &= 1 + C_v \frac{(F_s - C_{dd})}{F_c - F_s} & \text{if } F_s < C_{dd} < F_c \end{aligned} \quad [161]$$

where:

- C_{dd} = crust drying day,
 F_s = crust starting formulation
 F_c = crust formulation completion
 C_v = crust coverage in percentage. If $C_v = 100\%$ meaning no evaporation happens after the crust is formulated.

The crust drying days is calculated precipitation, and is calculated with following formula:

$$\begin{aligned}
 C_{dd} &= 0 && \text{if } P_T > P_h \\
 C_{dd} &= C_{dd} - 1 && \text{if } P_T = 0 \\
 C_{dd} &= C_{dd}(1 - P_T / P_h) && \text{otherwise}
 \end{aligned}
 \quad [162]$$

where:

P_T = daily precipitation

P_h = dissolved threshold of precipitation. If a daily precipitation is over this threshold, the crust effect will be dissolved.

Figure 39 illustrates how the crust factor is calculated with the changing daily climate. In this figure, the crust starting formulation = 1 day, crust formation completion = 4 days, crust coverage = 80%, and dissolved threshold of precipitation = 0.5 mm.

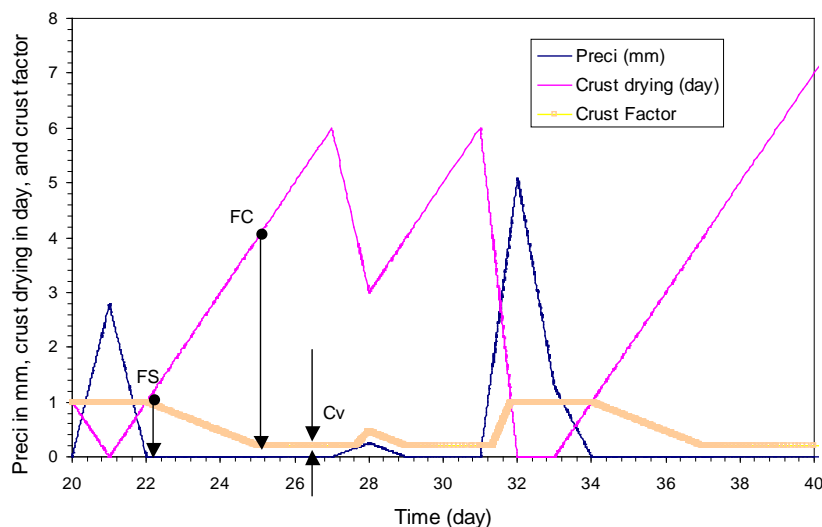


Figure 39 Illustration of crust factor changing with precipitation

9 STREAM TRACES - SVENVIRO/GT

SVFLUX provides the functionality to plot the stream traces by clicking on the model. For seepage models, the underground water flow velocity can be expressed using the following formulas. With v_x and v_y , the direction of the stream trace can be determined at a specific point.

$$\begin{aligned}V_x &= k_x \frac{\partial h}{\partial x} = flux_x \\V_y &= k_y \frac{\partial h}{\partial y} = flux_y\end{aligned}\quad [163]$$

where:

- k_x = hydraulic conductivity in the x-direction,
- k_y = hydraulic conductivity in the y-direction,
- h = total head,
- $flux_x$ = the flow in the x direction,
- $flux_y$ = the flow in the y direction.

10 PARTICLE TRACKING - SVENVIRO/GT

The Particle Tracking feature implemented in SVFLUX allows the user to track the advective movement of contaminant particles in a solution. Clicking a location in the mesh will initiate the plotting of a path of a particle moving from the clicked location. The calculations assume zero diffusion.

The particle tracking feature is only for transient models. The theory behind the particle tracking is straightforward and is defined as follows:

$$\begin{aligned}x_1 &= x_0 + \theta_w k_x \frac{\partial h}{\partial x} \Delta t \\y_1 &= y_0 + \theta_w k_y \frac{\partial h}{\partial y} \Delta t\end{aligned}\quad [164]$$

11 SPATIAL VARIABILITY - SVENVIRO

Natural soils are spatially variable and non-homogeneous. In order to investigate how spatial variability affects geotechnical behavior, soils can be modeled as one dimensional (1D), two dimensional (2-D) or multi-dimensional (3-D) randomly varying processes. SVFLUX implements 2D Spatial Variation.

11.1 2D SPATIAL VARIABILITY - SVENVIRO

2D Spatial Variability Option is used to generate a 2D random field for the properties of a soil using the Random Field Theory proposed by Fenton and Vanmarcke (1990).

11.1.1 General - SVENVIRO

SVFLUX uses Random Field Theory to generate a 2D discrete random field. It represents local averages of a homogeneous random function defined by its mean and covariance function. The averaging is performed over incremental domains formed by different levels of discretization of the field.

The approach is motivated first by the need to represent engineering properties as local averages (since many properties are not well defined at a point and show significant scale effects), and second to be able to easily condition the realization to incorporate known data or change resolution within sub-regions. The Ornstein-Uhlenbeck and fractional Gaussian noise processes are used as illustrations (Fenton and Vanmarcke, 1990).

11.1.2 Covariance Function - SVENVIRO

Five covariance functions (*dlavx2*, *dlsep2*, *dlsp2*, *dlaf2*, *dlfr2*) are available for 2D random field generation as described as follows:

1. *dlavx2*: 2D exponentially decaying (Markov) model

This function returns the covariance between two points in a 2D Markov random field, separated by lag vector $\{x, y\}$. The covariance function for this process is given by:

$$B(x, y) = \text{var} \times \exp\left(-\sqrt{(2 \times x / dthx)^2 + (2 \times y / dthy)^2}\right) \quad [165]$$

where:

- $B(x, y)$ = covariance function,
- var = the point variance,
- $dthx$ = the scales of fluctuation in the x-direction,
- $dthy$ = the scales of fluctuation in the y-direction,
- x = component of the lag vector between the points (or the dimensions of the averaging area, if $\text{var} < 0$), and
- y = component of the lag vector between the points (or the dimensions of the averaging area, if $\text{var} < 0$).

If $\text{var} < 0$, then this function returns the variance of a local average of the process, $|\text{var}| * V(x, y)$, averaged over the domain. This variance is obtained by 16-pt Gauss quadrature integration of the covariance function. The 4-fold integral is reduced to 2-fold integration by taking advantage of the quadrant symmetry of the covariance function.

Note that when the element is non-square, extremely small scales of fluctuation tend to yield inaccurate local average variances (either directly here using $\text{var} < 0$, or through *dcvaa2*). More Gauss points are needed in the integration.

2. *dlsep2*: 2D separable (1D x 1D) Markov model

This function returns the covariance between two points, separated by lag vector $\{x, y\}$, in a 2D random field having separable Markovian covariance function. The covariance function for this field is given by:

$$B(x, y) = \text{var} \times \exp\left(-(2|x| / dthx)\right) \times \exp\left(-(2|y| / dthy)\right) \quad [166]$$

where:

- $B(x, y)$ = covariance function,

- var = the point variance,
 $dthx$ = the scales of fluctuation in the x-direction,
 $dthy$ = the scales of fluctuation in the y-direction,
 x = component of the lag vector between the points (or the dimensions of the averaging area, if $var < 0$), and
 y = component of the lag vector between the points (or the dimensions of the averaging area, if $var < 0$).

NOTE: this function is NOT isotropic even if $dthx = dthy$.

If $var < 0$, then this function returns the variance of a local average of the process, $|var| * V(x, y)$, averaged over the domain x by y . For a separable covariance function, the variance function is also separable and can be written as the product of two 1D variance functions corresponding to the exponential correlation function

$$V(x, y) = V(x) \times V(y) \quad [167]$$

where:

- $V(x, y)$ = covariance function,
 $V(x), V(y)$ = individual functions are based on the 1D analytical model

$$\begin{aligned}
 V(x) &= 2 \frac{dthx^2}{4x^2} \left[\left(2|x|/dthx + \exp(-2|x|/dthx) - 1 \right) \right] \\
 V(y) &= 2 \frac{dthy^2}{4y^2} \left[\left(2|y|/dthy + \exp(-2|y|/dthy) - 1 \right) \right]
 \end{aligned} \quad [168]$$

The variance of the local average is then given by $var * V(x, y)$.

3. *dlspx2*: 2D separable Gaussian decaying model

This function returns the covariance between two points, separated by lag vector $\{x, y\}$, in a 2D random field having separable (and mean-square differentiable) covariance function.

$$B(x, y) = var \times \exp\left(-\pi(|x|/dthx)^2\right) \exp\left(-\pi(|y|/dthy)^2\right) \quad [169]$$

where:

- $B(x, y)$ = covariance function,
 var = the point variance,
 $dthx$ = the scales of fluctuation in the x-direction,
 $dthy$ = the scales of fluctuation in the y-direction,
 x = component of the lag vector between the points (or the dimensions of the averaging area, if $var < 0$), and
 y = component of the lag vector between the points (or the dimensions of the averaging area, if $var < 0$).

4. *dlafr2*: 2D isotropic fractional Gaussian noise model

This function computes and returns the covariance between two points, separated by the distance T , in a 2D fractional Gaussian noise (fGn) process. The radial covariance function of the fractional noise process is given by:

$$B(s) = \frac{var}{2(pb)^{2H}} \left[|s + pb|^{2H} - 2|s|^{2H} + |s - pb|^{2H} \right] \quad [170]$$

where:

- $B(s)$ = radial covariance function,
 var = point variance of the fGn process,
 pb = length over which the fractional Brownian motion is averaged in order to make this, the derivative process, exist, Normally 'pb' is selected to be quite

- small (of the order of the size of the discretization interval),
- s = Euclidean length of the lag vector $\{x, y\}$, $s = \sqrt{x^2 + y^2}$,
- H = Hurst exponent. In this implementation, $0.5 < H < 1$; values of H near 1 yield a correlation structure which remains very high (and thus a covariance matrix which may be nearly singular). Values of H near 0.5 yield a band-limited white noise process.

If $var < 0$, then this function returns the variance of a local average of the process, $|var| * V(D)$, averaged over the domain 'D' (see below). The variance function which yields a close approximation to the above radial covariance function is given by

$$V(D) = \frac{|D + pb|^r - 2(|D|^r + |pb|^r) + |D - pb|^r}{D^2(2H+1)(2H+2)(pb)^{2H}} \quad [171]$$

where:

- r = $(2H+2)$,
- D = $|x| + |y|$, the 1-norm of $\{x, y\}$,
- pb = length over which the fractional Brownian motion is averaged in order to make this, the derivative process, exist. Normally 'pb' is selected to be quite small (of the order of the size of the discretization interval).

NOTE: The actual covariance function corresponding to [172] is equal to [171] along the coordinate axes, and remains close to [171] for $H > 0.8$. For $H < 0.7$, the covariance in the diagonal direction is too high, but since the covariance in such fields dies off very rapidly, the error is believed negligible.

5. *dlsfr2*: 2D separable fractional Gaussian noise model

This function computes and returns the covariance between two points, separated by the lag vector $\{x, y\}$, in a random field, which is a separable 2D fractional Gaussian noise. The covariance function for such a field is separable, and given by:

$$B(x, y) = var \times r(x) \times r(y) \quad [172]$$

For two points separated by distance $\{x, y\}$, where $r(x)$ and $r(y)$ are the directional correlation functions,

$$\begin{aligned} r(x) &= \frac{1}{2(pb)^{2H}} \left[|x + pb|^{2H} - 2|x|^{2H} + |x - pb|^{2H} \right] \\ r(y) &= \frac{1}{2(pb)^{2G}} \left[|y + pb|^{2G} - 2|y|^{2G} + |y - pb|^{2G} \right] \end{aligned} \quad [173]$$

where:

- pb = the length over which the fractional Brownian motion is averaged in order to make this, the derivative process, exist. Normally 'pb' is selected to be quite small (of the order of the size of the discretization interval)
- H = self-similar parameter, the Hurst exponent governing the process in the x-direction. In this implementation, $0.5 < H < 1$; values of H near 1 yield a correlation structure which remains very high (and thus a covariance matrix which may be nearly singular). Values of H near 0.5 yield a band-limited white noise process.
- G = self-similar parameter, the Hurst exponent governing the process in the y-direction. In this implementation, $0.5 < G < 1$; values of G near 1 yield a correlation structure which remains very high (and thus a covariance matrix which may be nearly singular). Values of G near 0.5 yield a band-limited white noise process.

If $var < 0$, then this function returns the variance of a local average of the process, $|var| \times V(x, y)$, averaged over the domain x by y . If the covariance function is separable, then so too is the variance function.

$$V(x, y) = V(x) \times V(y) \quad [174]$$

where:

- x, y = dimensions of the averaging region,

$V(x), V(y)$ = 1-D variance functions.

$$V(x) = \frac{|x+pb|^r - 2(|x|^r + |pb|^r) + |x-pb|^r}{x^2(2H+1)(2H+2)(pb)^{2H}}$$

$$V(y) = \frac{|y+pb|^r - 2(|y|^r + |pb|^r) + |y-pb|^r}{y^2(2G+1)(2G+2)(pb)^{2G}}$$
[175]

where:

$$r = 28H + 2,$$

NOTE: As the variable, x goes to zero $V(x)$ or $V(y)$ becomes 0/0, but its limiting value is 1.0.

11.1.3 Parameters - SVENVIRO

In order to generate a random field, users are allowed to determine Distribution Type, Mean Value, Standard Deviation, Correlation Length and Number of Grid for each soil's property as described as follows:

1. Distribution

SVFLUX simulates up to 5 soil property fields (cohesion, friction angle, unit weight, PWP, Suction. Individual fields are generated as standard Gaussian random fields using the 2D Local Average Subdivision (LAS) algorithm. These fields are then combined to produce correlated standard Gaussian fields using the Covariance Matrix Decomposition approach. Finally the individual fields are transformed so that they have the desired marginal distributions. These transformations are as follows;

a. Normal

$$P(x, y) = \mu + \sigma G(x, y)$$
[176]

b. Lognormal

$$P(x, y) = \exp[\mu_{\ln} + \sigma_{\ln} G(x, y)]$$

$$\sigma_{\ln}^2 = \ln \left(1 + \frac{\sigma^2}{\mu^2} \right)$$

$$\mu_{\ln} = \ln(\mu) - \frac{1}{2} \sigma_{\ln}^2$$
[177]

c. Bounded

$$P(x, y) = a + 0.5(b - a) \left\{ 1 + \tanh \left[\left(\mu + \sigma G(x, y) \right) / 2 / \pi \right] \right\}$$
[178]

where:

- $P(x, y)$ = desired random field (one of the soil properties),
- $G(x, y)$ = standard correlated Gaussian field,
- μ = mean value,
- σ = standard Deviation,
- μ_{\ln} = mean value of a lognormal distribution,
- σ_{\ln} = standard Deviation of a lognormal distribution,
- a = lower bound for bound distribution,
- b = upper bound for bound distribution,
- m = location parameter for Bounded distribution, and
- s = scale parameter for Bounded distribution.

2. Correlation Length

Correlation lengths give the scale of fluctuation in x-direction and y-direction. Correlation lengths govern the decay rate of correlation between points in the random field as a function of the distance between them. Loosely speaking, the scale of fluctuation can be thought of as the distance over which points on the random field show substantial correlation.

The effect of Correlation Length can be summarized as follows:

- a. When correlation length is small, random fields tend to be rough,
- b. As correlation length is close to zero, all points in the field become uncorrelated with one another and field becomes infinitely rough. This is called white noise and physically unrealizable,
- c. As correlation length increases, the field becomes smoother,
- d. As correlation length is close to ∞ , all points in the fields become completely correlated for finite-scale correlation functions. If the field is stationary, this means that the random field becomes completely uniform like a traditional soil model.

3. Number of Grid

Number of grid gives the number of divisions for a soil mass in x-direction and y-direction.

11.1.4 Random Field - SVENVIRO

Figure 40 shows a random field for c in a simple slope.

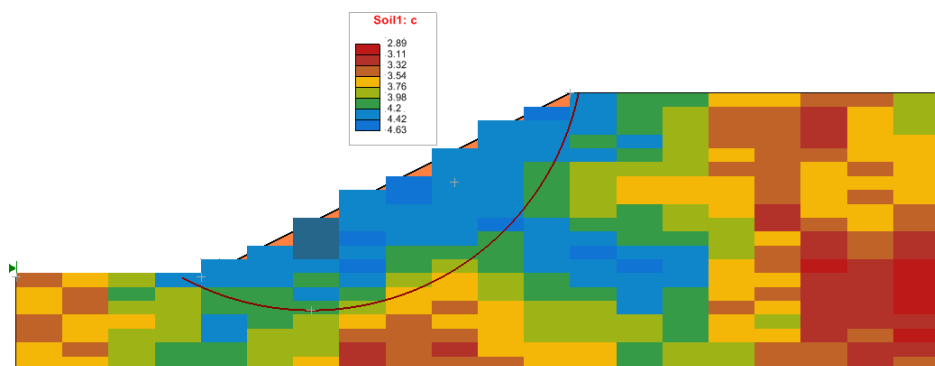


Figure 40 2-D Random Field Distribution (Mean = 3, SD = 1, normal) (Correlation Length $x = 100\text{m}$, $y = 100\text{m}$)

12 NUMERICAL IMPLEMENTATION - SVENVIRO

The SVFLUX finite element software makes use of a generic finite element solver called FlexPDE. FlexPDE has been designed and maintained by Bob Nelson of PDE Solutions Inc. over the course of the past 31 years and is the result of many years of rigorous testing and peer review. The most detailed source of documentation of the numerical schemes used in the FlexPDE software can be found in the User's Guide and Reference Manual provided with the software. The following sections provide a brief overview of some of the more significant numerical methods used in the software.

Primary advantages of the FlexPDE finite element solver are as follows:

- Fully automatic mesh generation,
- Fully automatic mesh refinement based on any model variable,
- Fully implicit approach in the solver, which provides for a robust solution of difficult models with convergence issues,
- 3, 6, or 10-noded triangles as elements for 2D analysis and 4, 10, or 20-noded tetrahedrons in 3D elements,
- Adaptive time-stepping with automatic generation and control of time steps,
- Newton-Raphson convergence iteration schemes, and
- Use matrix preconditioning in conjugate-gradient solutions. The default preconditioner is the diagonal-block inverse matrix.

12.1 EQUATION ANALYZER

A symbolic *equation analyzer* expands defined parameters and relations, performs spatial differentiation, and symbolically applies integration by parts to reduce second order terms to create symbolic Galerkin equations. It then differentiates these equations to form the Jacobian coupling matrix.

12.2 MESH GENERATION

A *mesh generation* module constructs a triangular finite element mesh over an arbitrary two-dimensional model domain. In three-dimensional models, the 2D mesh is extruded into a tetrahedral mesh covering an arbitrary number of non-planar layers in the extrusion dimension. Bilinear interpolation is used in 3D models to approximate a curved surface.

FlexPDE uses an "advancing front" mesh generation method, triangular in 2D and tetrahedral in 3D (the specific algorithm is proprietary, but similar mesh generation methods are widely reported in the literature). The mesh generator allows spatially-varying node density, in order to concentrate cells in regions of structural detail.

12.3 MESH REFINEMENT

The FlexPDE solver implements fully automatic mesh refinement. The mesh refinement may be triggered based on any model variable through a combination of the RESOLVE statement as well as the XERRLIM variable.

FlexPDE automatically adapts the computation mesh to the needs of the solution. Error estimates are formed in each cell, and cells with high error are split into two new cells, resulting in a new computation mesh and a repeat of the solution process. The reference error is user-selectable (ERRLIM). The exact algorithm is proprietary, but similar techniques are discussed in the open literature.

The error estimation process is based on the following observation. In the finite element method, each nodal value is computed by minimizing the residual of the partial differential equation, PDE, weighted by a node-specific weighting function and integrated over all cells surrounding the node. A centrally-weighted integral of the PDE residual over an individual cell provides an independent measure of the residual, and provides the error estimate.

12.4 INTERPOLATION ORDER

Finite element basis is quadratic.

12.5 TIME STEPPING

Both explicit and implicit methods have been presented in literature as viable methods of solving for nodes while moving forward in time. Explicit methods use known data to "explicitly" define each nodal value at an advanced time. Such explicit methods usually suffer in accuracy and stability unless the time step is small. Implicit methods solve "implicitly" for self-consistent values at the advanced time (i.e., the simultaneous finite element spatial equations are solved at the advanced

time). This improves the stability and accuracy for large time steps, at the cost of a simultaneous solution for all nodes in the mesh. Explicit methods can be more economical under the right circumstances.

The implicit generalized Gear (1971) method has been selected in SVOFICE as the most robust method for general application. The research literature supports this decision.

12.5.1 Time Integration

FlexPDE uses a selectable-order Backward Difference Formulation to advance variables in time. The default is second order, but you can select linear or cubic with the TORDER selector. Linear backward difference (torder=1) is equivalent to backward Euler integration. All the methods are Implicit. The analysis for default quadratic integration is as follows:

Assume that each variable can be approximated as a polynomial in time.

$$U(t) = p_0(t) \times u_0 + p_1(t) \times u_1 + p_2(t) \times u_2 \quad [179]$$

where:

$$\begin{aligned} U(t) &= \text{approximated function} \\ u_0, u_1 &= \text{known values at times } t_0 \text{ and } t_1 \\ u_2 &= \text{unknown value at time } t_2. \\ p_0, p_1 \text{ and } p_2 &= \text{Lagrange interpolation coefficients} \end{aligned}$$

The coefficients p_0 , p_1 , and p_2 are Lagrange interpolation coefficients,

$$\begin{aligned} p_0(t) &= \frac{(t-t_1)(t-t_2)}{(t_1-t_0)(t_2-t_0)} \\ p_1(t) &= \frac{-(t-t_0)(t-t_2)}{(t_1-t_0)(t_2-t_1)} \\ p_2(t) &= \frac{(t-t_0)(t-t_1)}{(t_2-t_0)(t_2-t_1)} \end{aligned} \quad [180]$$

With this interpolation, we can find the time derivative of $U(t)$,

$$U'(t) = p'_0 \times u_0 + p'_1 \times u_1 + p'_2 \times u_2 \quad [181]$$

where:

$$\begin{aligned} p'_0(t) &= \frac{(t-t_1) + (t-t_2)}{(t_1-t_0)(t_2-t_0)} \\ p'_1(t) &= \frac{-(t-t_0) - (t-t_2)}{(t_1-t_0)(t_2-t_1)} \\ p'_2(t) &= \frac{(t-t_0) + (t-t_1)}{(t_2-t_0)(t_2-t_1)} \end{aligned} \quad [182]$$

The time derivative at t_2 is then,

$$U'(t_2) = p'_0(t_2) \times u_0 + p'_1(t_2) \times u_1 + p'_2(t_2) \times u_2 \quad [183]$$

where:

$$\begin{aligned}
p'_0(t_2) &= \frac{(t_2 - t_1)}{(t_1 - t_0)(t_2 - t_0)} \\
p'_1(t_2) &= \frac{-(t_2 - t_0)}{(t_1 - t_0)(t_2 - t_1)} \\
p'_2(t_2) &= \frac{(2 \times t_2 - t_1 - t_0)}{(t_2 - t_0)(t_2 - t_1)}
\end{aligned} \tag{184}$$

Now, if we are given an equation

$$dt(U) = \mathbf{F}(U) \tag{185}$$

We can write:

$$\begin{aligned}
U'(t_2) &= \mathbf{F}(U(t_2)) \text{ as a fully implicit equation for } U_2, \text{ and} \\
U_2 &= \frac{\mathbf{F}(U_2) - p'_0(t_2) \times U_0 - p'_1(t_2) \times U_1}{p'_2(t_2)}
\end{aligned}$$

Solving this system requires either the solution of a linear system or a nonlinear system, depending on the form of $\mathbf{F}(U)$.

Notice that the core of this solution method is to find a value of U_2 such that the interpolated time derivative at the end of the step matches the specified driving term $\mathbf{F}(U)$ at the end of the time step. There is no time-centering issue involved with $\mathbf{F}(U)$: it is always at the end of the step.

12.5.2 Time Step Control

The approximation described above implies a constant curvature U'' over the interval (t_0, t_2) . When we later advance from t_2 to t_3 , we implicitly assume that U'' is constant over the interval (t_1, t_3) , but with a different U'' than the previous step. There has therefore been an inconsistent assumption about the value of U'' in the overlapped interval (t_1, t_2) .

The FlexPDE time step control, simply stated, is to measure how much difference the two estimates of U'' imply in U_3 , and to restrict this difference to the requested ERRLIM.

The curvature over (t_0, t_2) is,

$$U''_1 = \frac{2 \times U_0}{(t_1 - t_0)(t_2 - t_0)} - \frac{2 \times U_1}{(t_1 - t_0)(t_2 - t_1)} + \frac{2 \times U_2}{(t_1 - t_0)(t_2 - t_1)} \tag{186}$$

The curvature over (t_1, t_3) is,

$$U''_2 = \frac{2 \times U_1}{(t_2 - t_1)(t_3 - t_1)} - \frac{2 \times U_2}{(t_2 - t_1)(t_3 - t_2)} + \frac{2 \times U_3}{(t_2 - t_1)(t_3 - t_2)} \tag{187}$$

The difference is,

$$\begin{aligned}
E''_2 &= \frac{2 \times U_0}{(t_1 - t_0)(t_2 - t_0)} + \frac{2 \times (t_3 - t_0) \times U_1}{(t_1 - t_0)(t_2 - t_1)(t_3 - t_1)} \\
&\quad - \frac{2 \times (t_3 - t_0) \times U_2}{(t_2 - t_1)(t_3 - t_2)(t_2 - t_0)} + \frac{2 \times U_3}{(t_3 - t_2)(t_3 - t_1)}
\end{aligned} \tag{188}$$

Integrating over (t_2, t_3) produces an error,

$$E_3 = \frac{(t_3 - t_2)^2 \times U_0}{(t_1 - t_0)(t_2 - t_0)} + \frac{(t_3 - t_2)^2 (t_3 - t_0) \times U_1}{(t_1 - t_0)(t_2 - t_1)(t_3 - t_1)} - \frac{(t_3 - t_2)(t_3 - t_0) \times U_2}{(t_2 - t_1)(t_2 - t_0)} + \frac{(t_3 - t_2) \times U_3}{t_3 - t_1} \quad [189]$$

The N^{th} power of the nodal values of E is averaged, rooted and divided by the range of the variable U . N is controlled by TNORM in version 5 and ENORM in version 6. $N = 2^{\text{TNORM}}$. The range of U is the larger of the declared Threshold or the observed range of values.

$$E_{av} = \left[\text{SUM} \left(\left(E_3 / \text{Range}(U) \right)^N \right) \right]^{1/N} \quad \text{and}$$

$$\text{Deltat4} = \text{deltat3} \times \sqrt{\text{TERRLIM} / E_{av}}.$$

This process applies to variables U that are defined by an evolution equation $dt(U) = F(U)$. Steady equations are not assumed to be polynomial in time, and a different rule is applied to generate E_{av} for these variables.

In this case,

$$E_3 = \frac{U_3 - U_2}{\text{Changelim}}$$

Moving nodes adds another criterion, which is that the cell volume cannot change by more than a prescribed percentage on any cycle. The way this is controlled is different in V6 than in V5.

13 NUMERICAL IMPLEMENTATION - GT

SVFLUX makes use of a generic finite element solver called SVCORE. The following sections provide a brief overview of some of the more significant numerical methods used in the software.

Primary advantages of the SVCORE finite element solver are as follows:

- Fully implicit approach in the solver, which provides for a robust solution of difficult models with convergence issues,
- 2-noded line elements for 1D analysis, 3-noded triangle and 4-noded quadrilateral as elements for 2D analysis and 4-noded tetrahedron elements for 3D analysis,
- Automatic generation and control of time steps,
- The implicit integration scheme using the Weighted Residual Method,
- Newton-Raphson convergence iteration schemes, and
- Uses a high performance linear solver engine allowing solution of large models with more than million nodes.

13.1 INTERPOLATION ORDER

Finite element basis is linear. The selected interpolation equation will have an impact on the number of nodes on the resulting elements.

13.2 TIME STEPPING

Implicit method has been presented in literature as viable methods of solving for nodes while moving forward in time. Explicit methods use known data to "explicitly" define each nodal value at an advanced time. Such explicit methods usually suffer in accuracy and stability unless the time step is small. Implicit methods solve "implicitly" for self-consistent values at the advanced time (i.e., the simultaneous finite element spatial equations are solved at the advanced time). This improves the stability and accuracy for large time steps, at the cost of a simultaneous solution for all nodes in the mesh.

The implicit method has been selected in SVOFICE as the most robust method for general application. The research literature supports this decision.

13.2.1 Time Integration

The transient equations mentioned above can be spatially discretized and the Galerkin's principle of weighted residual method can be applied for the finite element formulations. The numerical integration of the partial differential equations results in a simpler expression of the equation:

$$\mathbf{M}\dot{\mathbf{h}} + \mathbf{K}\mathbf{h} = \mathbf{q} \quad [190]$$

where :

- \mathbf{M} = mass matrix,
- \mathbf{K} = stiffness matrix,
- \mathbf{q} = flux vector reflecting the boundary conditions,
- \mathbf{h} = unknown hydraulic head vector, and
- $\dot{\mathbf{h}}$ = time derivative of hydraulic heads at the nodal points = $\frac{\partial \mathbf{h}}{\partial t}$

The time derivative of Equation [190] can be approximated using a finite difference technique. The relationship between the nodal heads of an element at two successive time steps can be expressed using the backward difference approximation (implicit method):

$$\left(\mathbf{K} + \frac{\mathbf{M}}{\Delta t} \right) \mathbf{h}_{t+\Delta t} = \frac{\mathbf{M}}{\Delta t} \mathbf{h}_t + \mathbf{q} \quad [191]$$

The finite element flow equation (i.e., Equation [190]) can be written for each element and assembled to form a set of global flow equations. The set of global flow equations for the whole system is then solved using the sparse linear solver for the hydraulic heads at the nodal points, \mathbf{h} . However, Equation [190] is nonlinear because the coefficients of permeability are a function of matric suction in unsaturated seepage analysis, which is related to the hydraulic head at the nodal points.

The hydraulic heads are the unknown variables in Equation [190] or [191]. Therefore, Equation [191] must be solved using an iterative procedure that involves a series of successive approximations. In the first iteration, the coefficients of permeability are estimated based on the initial conditions of the hydraulic head or water table in order to calculate the first set of hydraulic heads at the nodal points. The computed hydraulic heads are used to calculate the average matrix suction in the element. The coefficient of permeability is adjusted in the subsequent iteration with the new set of matrix suctions. The adjusted set of coefficients of permeability is then used in the finite element formulations to calculate the new set of hydraulic heads. The above procedure is repeated until the difference in hydraulic heads at two successive iterations are smaller than a user specified tolerance.

13.2.2 Convergence Criteria

The convergence criterion used in SVFLUX GT is known as relative residual norm criterion. The solution is deemed to have converged when the following criterion is satisfied:

$$\frac{\|\mathbf{h}_{k+1} - \mathbf{h}_k\|}{\|\mathbf{h}_k\|} \leq tol \quad [192]$$

where \mathbf{h}_{k+1} is the solution of Equation [191] at $(k+1)$ th iteration for a particular time step and \mathbf{h}_k is the solution at k th iteration.

The tolerance (*tol*) is a user specified parameter, which can be set in the FEM Options dialog. Once a solution for a particular time step satisfies the criterion [192], the calculation for the time step concludes and moves forward for the next time step.

The convergence rate is highly dependent on the degree on nonlinearity of the permeability function of the materials and spatial discretization of the problem. A steep permeability function requires more iterations and a larger convergence tolerance. A finer discretization in both element size and time step will assist in obtaining convergence faster with a smaller tolerance (Fredlund and Rahardjo, 1993).

13.2.3 Time-Step Control

The staged analysis in SVFLUX GT is obtained by discretizing a stage into several small time-steps and using an incremental analysis. The time-step for each sub-step is controlled by the following:

- The time discretization set by the user in the Stage Settings dialog (minimum, maximum, and initial time increments)
- The time discretization set by the user for the outputs such as Contour plots and Graph plots or for any other printed output of the simulations results
- The time discretization of the applied boundary conditions
- The time discretization based on automatic adjustment of the time-step based on the global error in solution in each subsequent iteration

SVFLUX GT implements the adaptive time steps algorithm based on a slightly modified form of the error control algorithm proposed by Söderlind (2002). The solver adopts the next time-step considering above controls. If the solution failed to converge within the maximum iteration set by the user, the time-step is reduced based on the global error in the solution and re-try using a smaller time step. The above procedure repeats until the solution converges. If the time increment reaches to the "minimum" time increment set by the user in the Stage Settings dialog, the solution is deemed to have failed to converge. If such situation occurs, the user is advised to review the material properties if there are any materials with a sharp changes in coefficients of permeability. Similarly, the initial conditions, boundary conditions, and the mesh density can also be reviewed for problems with convergence issues.

14 REFERENCES

- Alvenas, G. and Jansson, P. E. (1997). Model for evaporation, moisture and temperature of bare soil: calibration and sensitivity analysis. *Agricultural and Forest Meteorology*, 88:47-56.
- Anderson, E.A. (1976). *A point energy and mass balance model of a snow cover*. Ph.D. Thesis, Department of Civil Engineering, Stanford University, Palo Alto, CA, USA.
- Barbour, S.L., Fredlund, D. G., Gan, J. K-M., and Wilson, G.W. (1991). Prediction of moisture movement in highway subgrade soils, *45th Canadian Geotechnical Conference*, Toronto, ON., Canada.
- Bathe, K.J. (1982). *Finite element procedures in engineering analysis*. Prentice-Hall.
- Bear, J. (1972). *Dynamics of fluids in porous Media*. American Elsevier Publishing Company, New York.
- Benson, C. H., Gunter, J. A., Boutwell, G. P., Trautwein, S. J., and Berzanskis, P. H. (1997). Comparison of four methods to assess hydraulic conductivity. *Journal of Geotechnical and Geoenvironmental Engineering*, 123(10), 929-937.
- Bowles, J.E., (1984). *Physical and geotechnical properties of soils*. 2nd ed. McGraw-Hill, New York.
- Brooks, R., and Corey, T. (1964). Hydraulic properties of porous media. *Hydrology Papers, Colorado State University*.
- Burdine, N. T. (1953). Relative permeability calculations from pore size distribution data. *Trans. Am. Inst. Min. Metall. Pet. Eng.*, 198, 71-78.
- Campbell, J. D. (1973). *Pore pressures and volume changes in unsaturated soils*. Ph.D. thesis, University of Illinois at Urbana-Champaign.
- Celia, M.A. and Bouloutas, E.T. (1990). A general mass-conservative numerical solution for the unsaturated flow equation. *Water Resources Research*, Vol. 26, No. 7, pp. 1483-1496, July.
- Chandrakant, S. Desai and John F. Abel, (1972). *Introduction to the Finite Element Method*. Van Nostrand Reinhold Company, New York, N.Y.
- Chapuis, Robert P., Chenaf, D., Bussiere, B., Aubertin, M., Crespo, R. (2001). A user's approach to assess numerical codes for saturated and unsaturated seepage conditions. *Canadian Geotechnical Journal*, 38: 1113-1126.
- Crespo, R., (1993). *Modelisation par elements finis des ecoulements a travers les ouvrages de retenue et de confinement des residus miniers*. M.Sc.A. thesis, Ecole Polytechnique de Montreal, Montreal.
- Dakshanamurthy, V., and Fredlund, D. G. (1981). A mathematical model for predicting moisture flow in an unsaturated soil under hydraulics and temperature gradient. *Water Resources*, vol. 17, No. 3, pp. 714-722.
- Dupuit, J., (1863). *Etudes theoriques et pratiques sur le mouvement des eaux dans les canaux decouverts et a travers les terrains permeables*. 2nd ed. Dunod, Paris.
- Ebrahimi-Biring, N.,Gitirana, Jr., G. F. N., Fredlund., D. G., Fredlund, M. D., and Samarasekera, L. (2004). A lower limit for the water permeability coefficient, *Proceedings of the fifty-seventh Canadian Geotechnical Conference*, Quebec, QC, Vol. 1, pp. 12-19.
- Edlefsen, N., and Anderson, A. (1943). Thermodynamics of soil moisture. *California Agriculture*, 15(2), 31-298.
- Fenton, G. A., and Vanmarcke, E. H. (1990). Simulation of random fields via local average subdivision. *Journal of Engineering Mechanics*, 116(8), 1733-1749.
- FlexPDE 6 (2007). *Reference Manual*, PDE Solutions Inc., Spokane Valley, WA 99206.
- FlexPDE 7 (2017). *Reference Manual*, PDE Solutions Inc., Spokane Valley, WA 99206.
- Fredlund, D. G. (1991). How negative can pore-water pressures get? *Geotechnical news*, 9(3), 44-46.
- Fredlund, D. G., and Rahardjo, H. (1993). *Soil Mechanics for unsaturated soils*. John Wiley & Sons, Inc.
- Fredlund, D. G., and Xing, A. (1994). Equations for the soil-water characteristic curve. *Canadian Geotechnical Journal*, 31(4), 521-532.
- Fredlund, D. G., Xing, A., and Huang, S. (1994). Predicting the permeability function for unsaturated soils using the soil-water characteristic curve. *Canadian Geotechnical Journal*, 31(4), 533-546.

- Fredlund M.D. (1996). *Design of a Knowledge-Based System for Unsaturated Soil Properties*. M.Sc. Thesis, University of Saskatchewan, Saskatoon, Saskatchewan, Canada.
- Fredlund, M. D., Fredlund, D. G., and Wilson, G. W. (2000). An equation to represent grain-size distribution. *Canadian Geotechnical Journal*, 37(4), 817-827.
- Fredlund, D. G., and Gitirana, Jr., de F. N. G. (2005). Unsaturated soil mechanics as a series of partial differential equations. *In Proceedings of the International Conference on Problematic Soils*, Famagusta, Northern Cyprus, pp. 3-30.
- Fredlund, M. D., Tran, D., and Fredlund, D. G. (2016). Methodologies for the Calculation of Actual Evaporation in Geotechnical Engineering. *International Journal of Geomechanics*, 16(6), D4016014.
- Freeze, R. Allan and John A. Cherry, (1979). *Groundwater*. Prentice-Hall, Inc., Englewood Cliffs, New Jersey.
- Gardner, W. R. (1958). Some steady-state solutions of the unsaturated moisture flow equation with application to evaporation from a water table. *Soil science*, 85(4), 228-232.
- Gear C.W. (1971). *Numerical initial value problems in ordinary differential equations*. Prentice Hall.
- Granger, R. J. (1989). A complementary relationship approach for evaporation from nonsaturated surfaces. *Journal of Hydrology*, 111(1-4), 31-38.
- Gray, D. M., (1970). *Handbook on the principles of hydrology*. Canadian National Committee for the International Hydrological Decade.
- Gitirana, Gilson Jr. (2004). *Weather related geo-hazard assessment model for railway embankment stability*, PhD Thesis, University of Saskatchewan, Saskatoon, SK, Canada.
- Gustafsson, D., Stähli, M., and Jansson, P. E. (2001). The surface energy balance of a snow cover: comparing measurements to two different simulation models. *Theoretical and Applied Climatology*, 70(1), 81-96.
- Haverkamp, R., Vauclin, M., Touma, J., Wierenga, P. J., and Vachaud, G. (1977). A comparison of numerical simulation models for one-dimensional infiltration. *Soil Science Society of America Journal*, Vol. 41, No. 2.
- Huang, S., Barbour, S. L., & Fredlund, D. G. (1994, June). A history of the coefficient of permeability function. *In Sino-Canadian Symposium on Expansive Soils/Unsaturated Soils*, Chinese Institution for Soil Mechanics and Foundation Engineering, CEES (pp. 57-80).
- Hwang, C. T. (1976). Predictions and observations on the behaviour of a warm gas pipeline on permafrost. *Canadian Geotechnical Journal*, 13(4), 452-480.
- Jame, Y.W. (1977). *Heat and mass transfer in freezing soil*. Ph.D Thesis, University of Saskatchewan.
- Kimbal, B. A., Jackson, R. D., Reginato, R. J., Nakayama, F. S., and Idso, S. B. (1976). Comparison of field-measured and calculated soil-heat fluxes. *Soil Science Society of America Proceedings*, Vol. 40, No. 1, pp. 18-25.
- Kozeny, J. (1927). Über Kapillare Leitung Des Wassers in Boden. *Sitzungsber Akad. Wiss., Wien Math.Naturwiss.Kl., Abt.2a*, 136:271-306.
- Leong, E. C., and Rahardjo, H. (1997). Permeability functions for unsaturated soils. *Journal of Geotechnical and Geoenvironmental Engineering*, 123(12), 1118-1126.
- Lowe, P. R. (1977). An approximating polynomial for the computation of saturation vapor pressure. *Journal of Applied Meteorology*, 16(1), 100-103.
- Kunze, R. J., Uehara G. and Graham K. (1968): Factors important in the calculation of hydraulic conductivity. In *Proc. Soil Sci. Soc. Amer.*, 32, 760-765.
- Kuusisto, E. (1980). On the values and variability of degree-day melting factor in Finland. *Hydrology Research*, 11(5), 235-242.
- MEND (1993). *SoilCover user's manual for evaporative flux model*. University of Saskatchewan, Saskatoon, SK, Canada.
- Mualem, Y. (1976). A catalogue of the hydraulic properties of unsaturated soils. *Technion Research and Development Foundation*.
- Pentland, J. S., (2000). *Use of a general partial differential equation solver for solution of heat and mass transfer problems in soils*. University of Saskatchewan, Saskatoon, SK, Canada.

- Penman, H.L., (1948)., Natural evapotranspiration from open water, bare soil and grass. *Proc. R. Soc. London Ser. A.* 193: 120-145.
- Philip, J. R., and de Vries, D. A. (1957). Moisture movement in porous materials under temperature gradients. *Transactions, American Geophysical Union*, Vol. 38, No. 2, pp. 232.
- Priestley, C. H. B., and Taylor, R. J. (1972). On the assessment of surface heat flux and evaporation using large-scale parameters. *Monthly weather review*, 100(2), 81-92.
- Ritchie, J. T. (1972). Model for predicting evaporation from a row crop with incomplete cover. *Water resources research*, 8(5), 1204-1213.
- Saxton, K. E. (1982). Mathematical modelling of evapotranspiration on agricultural watersheds. In *Proceeding of Modeling Components of the Hydrologic Cycle*. 183-203.
- Söderlind, G. (2002). Automatic control and adaptive time-stepping. *Numerical Algorithms*, 31(1-4), 281-310.
- Tetens, V.O. (1930). Über einige meteorologische. *Begriffe, Zeitschrift für Geophysik*. 6:297-309.
- Todd, D. K. (1980). *Groundwater hydrology*. 2nd ed. John Wiley & Sons, New York.
- Thornthwaite, C. W. (1948). An approach toward a rational classification of climate. *Geographical review*, 38(1), 55-94.
- Tratch, D. J., (1995). A geotechnical engineering approach to plant transpiration and root water Uptake, University of Saskatchewan, Saskatoon, SK, Canada.
- Tratch, D. J., Wilson, G.W., and Fredlund, D.G. (1995). An introduction to analytical modeling of plant transpiration for geotechnical engineers. In *Proceedings of 48th Canadian Geotechnical Conference*, Vancouver, BC, Canada, Vol. 2, pp. 771-780.
- Van Genuchten, M. T. (1980). A closed-form equation for predicting the hydraulic conductivity of unsaturated soils. *Soil science society of America journal*, 44(5), 892-898.
- Vereecken H., J. Maes, J. Feyen, and P. Darius, (1989). Estimating the soil moisture retention characteristic from texture, bulk density, and carbon content. *Soil Science*, Volume 148, No. 6
- Wilson, W. G. (1990). *Soil evaporative fluxes for geotechnical engineering problems*. PhD Thesis, Department of Civil Engineering, University of Saskatchewan, Saskatoon, SK, Canada.
- Wilson, W. G., Fredlund, D. G., and Barbour, S. L. (1994). Coupled soil-atmosphere modelling for soil evaporation. *Canadian Geotechnical Journal*, 31(2), 151-161.
- Wilson, W. G., Fredlund, D. G. and Barbour, S. L. (1997). The effect of soil suction on evaporative fluxes from soil surfaces. *Canadian Geotechnical Journal*, 34(4): pp. 145-155.
- Wyllie, M. R. J. and Gardner, G. H. F. (1958). The generalized Kozeny-Carman equation II. A novel approach to problems of fluid flow. *World Oil Prod. Sect.* 210-228
- Zapata, C. E., Houston, W. N., Houston, S. L., and Walsh, K. D. (2000). Soil-water characteristic curve variability. *Advances in Unsaturated Geotechnics*, Denver, Colorado, August 5-8, pp. 84-123.